Title
Improving Measurement, Quantifying Variation, and Predicting Tree Carbon Mass in California Conifers

Author
Jones, Dryw

Publication Date
2016

Peer reviewed|Thesis/dissertation

Improving Measurement, Quantifying Variation, and Predicting Tree Carbon Mass in California Conifers

By

Dryw Aldwyn Jones

A dissertation submitted in partial satisfaction of the

requirements for the degree of

Doctor of Philosophy

in

Environmental Science, Policy, and Management

in the

Graduate Division

of the

University of California, Berkeley

Committee in charge:

Professor Kevin L. O'Hara, Chair
Professor Joe R. McBride
Professor David D. Ackerly
Doctor Richard B. Standiford

Fall 2016

Abstract

Improving Measurement, Quantifying Variation, and Predicting Tree Carbon Mass in California Conifers

By

Dryw Aldwyn Jones

Doctor of Philosophy in Environmental Science, Policy, and Management

University of California Berkeley

Professor Kevin L. O'Hara, Chair

Carbon sequestration and storage are important areas of scientific research. Despite this importance, the current approach to carbon mass estimates consists primarily of estimating wood volume, multiplying that volume by a species average wood density value to obtain biomass, then multiplying biomass by 0.5. Alternatively biomass may be estimated from allometric equations and then converted to carbon with the same 0.5 carbon conversion value. This approach is fundamentally inaccurate. This dissertation presents three improvements in carbon mass estimation that are critical to moving the science forward. In the first chapter I explore the importance of utilizing carbon fraction measurement methods that are capable of capturing the volatile component of tree tissues. I demonstrate a novel method that captures an additional 1.10% - 2.21% carbon mass in tree tissues. This increase is equivalent to "finding" an additional 16 Pg of carbon at a global scale. In the second chapter I explore the variation in measured carbon fractions, wood densities, and carbon densities within tree boles of seven major conifer species. I determine the importance of accounting for this variation, and discover negative correlations between wood density and carbon fractions within trees suggesting that the current approach of studying these characteristics as two independent properties is potentially biased. Applying the carbon fraction measurements at the whole tree level led to increases in carbon mass estimates of between 3.6% to 10.6% compared to carbon mass estimates that used a carbon fraction of 0.5. These values point to a systematic bias in current carbon mass estimation protocols. In the third chapter I develop carbon mass prediction models for five conifer species that capture some of the variation determined in chapter two. The models developed are the first vertically integrable conifer tree models to be based on accurately measured carbon fraction data paired with wood density measurements. The models are validated with an independent database and applied to the whole tree level demonstrate that accounting correctly for carbon leads to carbon mass estimates that are between 98.4% and 109% of the carbon mass estimated using standard approaches. The data presented makes a strong argument for the need of models that accurately account for variation in and correlation of carbon fraction, and wood density.

Table of Contents

Acknowledgements

This dissertation would not have been possible without the guidance and support of my advisor Kevin O'Hara. His approach to mentorship allowed me the space I needed to develop this dissertation, and his gentle reassurance gave me the encouragement I needed to push through when the going got tough. The helpful comments of my committee members during the construction of my study plan were invaluable and helped me narrow my topics down to what was achievable. The well thought out feedback of Joe McBride, Kevin O'Hara and David Ackerly significantly improved every chapter presented in this dissertation and helped me think about my work from a variety of viewpoints.

I would like to acknowledge the assistance of former Forestry Camp Manager Jim Schaber, Blodgett Forest manager Rob York, Southern California Edison forester Ryan Stewart, and JDSF Research and Demonstration Program Manager Lynn Webb for assistance with locating research plots and identifying suitable sites.

This work would have taken even longer without the dedicated work of several field and lab assistants, namely: Nico Alegria , Haley Kitchens, Michelle Chen, Elizabeth Ebert, Brita Rustad, and Kate Clyatt.

I want to thank my family for never letting me doubt my capabilities, always encouraging me to follow my dreams, and for putting up with my constant discussion of my work even when it didn't make any sense to them. You helped me become the person I am and I needed every bit of my stubborn persistence, my confidence, my sense of humor, and my sense of curiosity to finish this journey. My mother deserves special acknowledgement in this area: you are the reason I challenge what is "known" about a topic, because you never let me win an argument that ended with "because that's the way it is". Without that trait I never would have continued to pull on the string that led to challenging the established methods that this dissertation challenges.

I especially want to thank Kathryn McGown, you have made my life so much better in so many ways and I thank you for supporting me, editing my papers so that they made more sense, cooking for me when I didn't have time, helping me stay calm, and simply being there for me when I needed you.

1 The influence of preparation method on measured carbon fractions in tree tissues

Introduction

Forest carbon sequestration and storage are important tools in mitigating climate change (Hynynen et al. 2005, Neilson et al. 2006, Woodbury et al. 2007, Skog 2008, Fahey et al. 2009, Malmsheimer et al. 2011). Forests store large amounts of carbon in living biomass and managed forests are capable of producing long-lived timber products that store carbon for decades or longer (Skog 2008, Malmsheimer et al. 2011, McKinley et al. 2011). The distribution of carbon within trees, and within forest biomass, plays a critical role in forest ecosystem carbon cycling (Litton et al. 2007), and influences carbon estimation from the individual tree to global scales. The majority of studies that estimate forest carbon in trees typically multiply wood volume by a species-specific average wood density, and a carbon mass fraction of 50% (mass carbon / biomass) (e.g., Chave et al. 2009). Alternatively, studies may instead multiply measured biomass by the same 50% value (e.g. Houghton 2005). Bark, branch, root, and foliar carbon masses are usually calculated as proportions of bole carbon, or more commonly, calculated from bole volume estimates using biomass expansion factors (Brown 2002). These individual tree carbon estimates are then summed up to the stand, or forest scale depending on the analysis, and the available data. The resulting forest carbon estimates are known to have significant uncertainties related to underlying variation in tree volume estimates (Melson and Harmon 2011), wood densities (Chave et al. 2005), and carbon fractions (Jones and O'Hara 2012). Research into improving the accuracy of forest carbon estimation has focused primarily on improved estimation of wood volume in forests (Brown et al. 2002; Melson and Harmon 2011). In quantifying error in tree and forest carbon estimates few studies have focused on intra- and inter-specific variation in wood density (Chave et al. 2005), and even fewer have analyzed carbon fraction variation within and between trees (Lamlom and Savidge 2003, Bert and Danjon 2006, Jones and O'Hara 2012, Thomas and Martin 2012b).

Due to the large amounts of biomass stored in forests, small changes to forest carbon fractions can lead to large changes in forest carbon mass estimates (Jones and O'Hara 2012). For example, an increase in the global wood carbon fraction from 50% to 51% would lead to a global carbon storage estimate that is approximately 7 petagrams (Pg) higher than that estimated by Dixon et al. (1994). This amount of carbon is equivalent to approximately half of the carbon stored in all forested areas in the continental United States (Dixon et al. 1994). This sensitivity of forest carbon mass estimates to small changes in estimated carbon fractions requires that carbon fraction measurements be as accurate as possible in order to ensure accurate forest carbon estimates. Given the chemical complexity of tree tissues, carbon fraction measurements should be obtained for all tree tissue types to develop representative whole tree carbon mass estimates.

Tree tissues are a complex mix of chemical compounds such as cellulose, hemicellulose, lignin and a variety of nonstructural chemicals (Kaar and Brink 1991, Schweingruber et al. 2008). All of these chemical compounds contain different amounts of carbon by mass (Lamlom and Savidge 2006). Therefore variations in the proportions of these compounds at the cellular-, tissue-, tree- or species-level should lead to different carbon mass fractions. For example, cellulose is approximately 42% carbon, and lignin between 63-72% carbon by mass; it would

therefore be expected that trees with higher proportions of lignin, such as conifers, would have higher carbon fractions than angiosperms which have lower relative proportions of lignin (Savidge et al. 2000). This expectation has been confirmed by studies that found higher average carbon fractions in conifers compared to angiosperms (Lamlom and Savidge 2003, Thomas and Malczewski 2007, Thomas and Martin 2012b).

Significant differences in carbon fractions have also been measured between different tree species within the broader conifer and angiosperm groupings (Elias and Potvin 2003, Lamlom and Savidge 2003, 2006, Thomas and Malczewski 2007, Martin and Thomas 2011, Jones and O'Hara 2012, Martin et al. 2015). Some studies have found inter-specific variation in carbon fractions between tree tissues including bark, foliage, root, bole, branch, sapwood, and heartwood (Bert and Danjon 2006, Lamlom and Savidge 2006, Peri et al. 2010, de Aza et al. 2011, Jones and O'Hara 2012, Castaño-Santamaría and Bravo 2012, Martin et al. 2015). Environmental factors can also lead to differences in measured carbon fractions of tree tissues within a species (Elias and Potvin 2003, Lamlom and Savidge 2006). Taken together, these studies illustrate that carbon mass fractions of tree tissues are the result of complex biophysical processes resulting in highly varied carbon fractions between tree species, individual trees, and tree tissue types. This natural complexity argues for analyzing carbon fractions of every tree tissue type in order to derive representative whole tree carbon fractions.

Carbon can be lost from tree tissues through volatilization of carbon containing chemicals (e.g. alpha-pinene, methanol), or through metabolism within living plant cells. These potential pathways for carbon loss make the argument for a method of measuring carbon fractions in tree tissues that captures, to the greatest extent possible, the volatile and nonvolatile carbon fractions of living tree tissues. Based on the dataset from Thomas and Martin (2012b), the majority of carbon fraction measurements from existing studies were derived using an oven-dry method of sample preparation, heating samples between 50 to 105 ºC until weights stabilized. This method accounts for 71% of the total carbon fraction measurements in the dataset. The next most common method, comprising 18% of the dataset, was freeze-drying, and the final method, comprising 11% of the dataset, was vacuum desiccation at ambient temperatures. All of the studies in the dataset utilized samples that had been ground to a powder. Although Lamlom and Savidge (2003) found that grinding samples to a fine consistency was important for lowering deviations between sample replicates, there has been no analysis to determine if grinding samples results in the loss of carbon.

The oven-dry method is designed to remove water from tree tissues, and is most effective when performed at temperatures between 101 ºC and 105 ºC (Williamson and Wiemann 2010). Removing water from tree tissues allows for more consistent measurements of wood density, or biomass as the amount of water in tree tissues is highly variable. Oven-drying works well in deriving wood density values that are highly correlated to other key functional traits such as mechanical support and water transport (Chave et al. 2009). The majority of research into tree tissue biomass estimation uses oven-drying to remove moisture from sample tissues. In order to connect carbon fraction measurements to this larger body of biomass research, oven-dried samples must be used as a baseline method. However, the potential loss of carbon due to oven-drying should be measured before carbon fractions obtained with this method are used to estimate carbon mass in living trees.

Two alternative drying methods have been compared to oven-drying: freeze-drying, and vacuum desiccation. The few studies (Lamlom and Savidge 2003, 2006, Thomas and Malczewski 2007, Martin and Thomas 2011, Jones and O'Hara 2012) that used these alternative

methods for carbon fraction measurements found that oven-drying resulted in lower carbon fraction measurements than either freeze-drying or vacuum desiccation. The methods employed by these authors varied; Lamlom and Savidge (2003, 2006) utilized vacuum desiccation at ambient temperatures, Thomas and Malckewski (2007, 2011) utilized freeze-drying, and Jones and O'Hara (2012) utilized repeated measurements of paired samples that were vacuum desiccated, and then oven-dried. Estimated losses of volatile carbon ranged between 0.3% to 2.5% in vacuum desiccated samples (Lamlom and Savidge 2003), 0.2% and 4.7% for freeze-dried samples (Thomas and Martin 2012a), and between 1.23% and 1.47% for repeated measurements of paired samples of coast redwood (*Sequoia sempervirens* (D Don) Endl.) (Jones and O'Hara 2012). These studies also showed significant differences in volatile carbon fractions between species (Lamlom and Savidge 2003, Thomas and Malczewski 2007, Thomas and Martin 2012b). Volatile carbon is known to be sensitive to high temperatures and low pressures. These factors vary by drying method and may be responsible for the loss of volatile compounds during oven-drying (Thomas and Martin 2012b), and freeze-drying (Díaz et al. 2002, Abascal et al. 2005). To date no study has compared the performance of these alternative sample preparation methods to each other or across different tree tissue types. If volatile carbon is lost using the methods mentioned above then an alternative method that does not lose carbon via the same mechanisms is necessary for accurate tree carbon fraction measurements.

This paper compares measured carbon fractions of tree tissue samples from nine conifer species prepared using four methods: oven-drying, freeze-drying, vacuum desiccation, and a method designed to minimize the loss of carbon (MLC). I use linear mixed effects modeling to analyze differences in equivalent carbon fractions from paired samples across the tested tree species, tissue types, and preparation methods. To assess the potential loss of carbon due to grinding samples, I ran separate comparisons of freeze-dried powdered samples to freeze-dried samples cut with a razor. My objectives were to:

1. Determine if there were significant differences in carbon fractions between four preparation methods: oven-drying, freeze-drying, vacuum desiccation and the MLC method;
2. Determine if there was a significant loss of carbon due to grinding tree tissues versus cutting tissues into small pieces with a razor; and
3. Determine if differences in methods were consistent across tissue types and species.

Materials and methods

Plot locations

Nine conifer tree species were sampled: sugar pine (*Pinus lambertiana* Dougl.), ponderosa pine (*P. ponderosa* Lawson & C. Lawson), Jeffrey pine (*P. jeffreyi* Balf.), coast Douglas-fir (*Pseudotsuga menziesii* (Mirb.) Franco var. *menziesii*), white fir (*Abies concolor* (Gord. & Glend.) Lindl. ex Hildebr.), red fir (*A. magnifica* A. Murray), incense-cedar (*Calocedrus decurrens* (Torr.) Florin), giant sequoia (*Sequoiadendron giganteum* (Lindl.) Buchholz), and coast redwood (*Sequoia sempervirens* (D. Don) Endl.). Trees were sampled at the following locations: 1) Baker Forest (39.916 N, 121.063 W), 2) Blodgett Research Forest Station (38.910 N, 120.662 W), 3) Whitaker Forest (36.699 N, 118.939 W), 4) Teakettle Experimental Area (36.968 N, 119.036 W), outside of 5) Loyalton, CA (39.675 N, 120.165 W), 6) near Shaver Lake, CA (37.046 N, 119.211 W), and in 7) Jackson Demonstration State Forest (39.364 N,

123.708 W). Summary statistics for sample trees can be found in Table 1, along with locations each species was sampled in.

Tissue sample collection and processing

A total of 370 cores were extracted from randomly sampled trees within each site. The only requirement for selection of sample trees was that they could be safely climbed, or cut down and cored. Cores were taken at breast height (1.37 m), base of live crown (HLC), and every 4 m within the live crown for each tree sampled. Extraction was performed using a 400 mm long Haglöf three threaded increment borer with a measured aperture of 5.15 mm. Immediately after extraction, cores were placed in clear plastic straws, sealed using adhesive tape, labeled with tree number and extraction height, then placed in a white plastic tube to reduce exposure to sunlight. The borer was cleaned between sample trees using clean tissue paper and a silicon lubricant until tissue paper showed no signs of staining from either tree residues or the lubricant. Sapwood of the core was determined by holding the straw up to the sun and marking the end of the translucent section of the core on the outside of the straw with a permanent marker. Cores were then placed in a cooler with ice for transportation back to the lab, and then placed in the lab freezer, which was maintained between -24 and -18 ºC. A complete analysis of all cores was not possible due to limitations on time and funding, and so a randomized subsample of cores was used to avoid introducing bias into the analysis. This process led to the selection of 56 cores, from 45 trees and all nine species. These cores were separated into bark and stemwood for later carbon fraction analysis. The stemwood portions of these frozen cores were then cut with a razor into core segments of four, or eight tree rings, and the tissue type (heartwood or sapwood) recorded. The number of tree rings per segment depended on the average ring width, where very small average growth rings were segmented into eight ring segments and large average growth rings were segmented into four ring segments. This process ensured that enough mass was present in the segment for carbon analysis using multiple preparation methods.

Foliage was collected in the field from 375 randomly sampled tree branches within the crowns of climbed trees. Proportional foliage subsamples were collected from each needle age class from each branch and placed in a small plastic resealable bag. A minimum of 100 needles were placed in each sample bag. When fewer than 100 needles existed on a branch all needles were taken off the branch, and placed in a bag. Foliage sample bags were placed on ice in the field, and placed in a freezer once taken back to the lab. Twenty-one foliage samples were randomly selected for carbon fraction analysis from 12 different trees, representing six tree species.

Core segment preparation

Core segments from bark, sapwood, and heartwood of the selected cores had the outermost portion removed with a razor blade in order to remove oxidized tissue and any possible contaminants from the exterior of the core. In the case of bark samples, where removing the external tissue was more difficult, the central portion of the bark was cut out and used for carbon analysis. For bark samples there was typically less mass and so fewer methods could be applied to the bark sample material from a given core. This led to fewer overall bark samples compared to stemwood samples in the final analysis. Table 2 contains a summary of sample size data by various grouping categories.

Individual core segments were cut with a razor into pieces weighing approximately 1 mg or less, and that material was placed into a sealed plastic sample tube labeled with core, and

segment ring numbers then placed back in the freezer. Foliage samples from individual branches were cut into pieces weighing approximately 0.5 mg or less, and that material was placed into sealed sample tubes labeled with a unique branch ID number then placed back in the freezer. For comparisons of carbon fractions between cut and powdered freeze-dried samples the core segments were first cut in half. One half of the segment was then ground to a fine powder (particle size < 0.3 mm) while still frozen following the methods in Jones and O'Hara (2012), while the other half was cut with a razor into small pieces weighing approximately 1 mg or less. The resulting material was then placed into separate sample tubes and labeled with unique core segment, or branch sample number along with information on whether the material had been ground or cut. The average mass of material in each sample tube by method was: 71.5 (5.7) mg for oven-drying; 57.9 (6.0) mg for vacuum-desiccation; 162.1 (18.9) mg for freeze-drying; and 70.4 (6.6) mg for the MLC method.

Core segment material processing methods

The material contained within the sample tubes was then divided into subsample tubes, which were processed using one of the following methods: oven-drying, vacuum desiccation, freeze-drying or placed back in the freezer without additional drying (MLC method). Oven-drying consisted of taking subsample material and drying it in a forced-air oven at 105 ºC until weight stabilized, typically less than 48 hours.

Vacuum desiccation took place in an airtight vacuum chamber (Bel-Art Scienceware, model F42010) containing an indicator silica gel as desiccant. The chamber experienced a small vacuum pressure from the loss of water vapor, and once a day this pressure was released by opening the stop-cock. A small number of stemwood subsamples were taken from the chamber and weighed each day until weights stabilized using an Ohaus Analytical Plus balance model AP310, with a precision of 0.2 mg. Subsamples were found to reach stable weight within one week. This method is comparable to the method utilized by Lamlom and Savidge (2003, 2006) with the one exception that I did not apply any additional vacuum pressure to the system other than what naturally occurred due to the loss of water vapor.

Freeze-dried subsamples were placed in a Labconco FreeZone 12 Freeze Dry System for one week as this was deemed a long enough period of time to sufficiently dry such small samples. The MLC method samples were placed in a test tube, sealed, and placed back in the freezer for later carbon analysis. To ensure that all samples were exposed to similar environmental conditions, the dried sample materials were also placed into separate test tubes, sealed, and placed in the freezer after their respective drying treatments. The result of this process was identical parent material treated using the four methods described above, and a separate group of freeze-dried samples that were used to determine if there was any difference in carbon fractions between cut samples paired with ground samples.

Carbon analysis

For subsamples from all methods described above, 3-5 mg of material from each subsample tube was weighed into a clean, dry tin capsule using a Metler Toledo XPE26 micro-analytic balance with a calibrated precision of 0.004 mg. The tin capsules were crimped and placed into a Thermo Scientific MAS 200R autosampler attached to a CE Instruments Flash 2000 CHNS/O analyzer for measurement of sample carbon mass using a modified Dumas method of flash combustion. The CHNS/O analyzer was calibrated between sample runs using acetanilide as the standard. Each sample run had a calibration curve R^2 of 0.999, or higher. An

acetanilide standard weighing between 1-3 mg was run every tenth sample to insure that the accuracy of carbon fraction measurements. Immediately after removal of the 3-5 mg combustion samples from each of the subsample tubes, the weight of the remaining subsample material was recorded (M_{rem}). This remaining material was then placed in individual tins labeled with a unique sample ID, and dried in an oven at 105˚C until stable weight was achieved. This stable mass was then recorded as M_{OD}. Carbon fractions of the combustion samples (C_{rem}) were determined by dividing the mass of carbon in the combustion sample by the total mass of the combustion sample. All measured carbon fractions were converted to oven-dry biomass equivalent carbon fractions (C_c) using the following equation:

Eq. 1 $$C_c = C_{rem} * M_{rem} / M_{OD}$$

If there is no difference in the proportion of carbon lost due to the particular method used then the C_c of a given sample (core segment, foliage, or bark), would be the same for all methods. That is because the methods are applied to identical parent material. This design creates carbon fraction values that are on the same baseline moisture content and therefore directly comparable. This is a very similar approach to that used by Martin and Thomas (2011) in developing carbon conversion factors, however, my formulation is simpler and requires fewer calculations.

In summary the MLC method consisted of the following: 1) frozen sample material was cut into small 1 mg pieces; 2) sample material was then placed into a test tube, sealed, and placed back in the freezer; 3) a 3-5 mg subsample was taken from the test tube to determine the carbon fraction of the sample (C_{rem}); 4) the remaining material in the sample test tube was immediately weighed (M_{rem}) after removal of the combustion sample and placed back into the sample test tube; 5) the remaining material in the test tube was oven-dried, and weighed (M_{OD}); 6) C_{rem} was then multiplied by the ratio of M_{rem} to M_{OD} in order to derive carbon conversion values as shown in Eq. 1. All other methods only differ from the MLC method in that the sample material from the other methods was dried prior to carbon fraction analysis.

Adjusting carbon fraction for dissolved carbon

Tree sap is known to contain small amounts of dissolved CO_2, which could show up in carbon fraction mass measurements (Teskey et al. 2008), when moisture is retained in sample material. All of the dried samples contained some residual moisture, and material from the MLC method retained most of the original moisture content. The moisture content was determined for each combustion sample by assuming that the volatile mass fraction (VMF) in the remaining material was composed of water alone. Based on this assumption the moisture fraction of the combustion samples can be determined by the following:

$$VMF = 1 - (M_{OD} / M_{rem}).$$

The concentration of dissolved carbon in all tree tissues was then determined using the equations in McGuire and Teskey (2002), assuming a CO_2 concentration in the gas phase of 14%, a temperature of 25 ºC, and a sap pH of 7. The resulting concentration of CO_2 in tissue sap was then converted into a dissolved carbon mass estimate for each sample and subtracted from the respective sample C_c values calculated in Eq. 1. These assumptions more than likely led to an overestimate of the amount of dissolved carbon found in the samples making the treatment of all methods more conservative relative to the oven-drying method. This process led to slightly lower C_c values, however, to try to account for the maximum potential dissolved carbon these slightly

lower C_c values were used in all analyses. The MLC method C_c values were reduced the most by this process as those samples had higher moisture content values overall.

Statistical analysis

A linear mixed effects (LME) model (Eq. 2), was used to test for differences in carbon fractions (y_i) between the different methods, and account for the unbalanced nested structure of the dataset. The fixed effects for Eq. 2 included a categorical variable that represented a tissue type within a given species (S_{ti}), and a categorical variable representing the four preparation methods (M_j). The data structure was organized as sample ID (m), within core ID (l), within tree ID (k). For foliar samples, sample branch number was used in place of core ID. Random effects (ϕ_{klm}) were assigned to each level of the data structure using a compound symmetric correlation matrix. This model was used to estimate parameters for the method fixed effects (M_j) for the entire data set, after accounting for average values of the species level tissue types (S_{ti}).

Eq. 2
$$y_i = S_{ti} + M_j + \phi_{klm},$$
$$\phi_{klm} \sim N(0,\sigma_b^2)$$

For comparisons between M_j estimates within each tissue type, or within each species, the data was subset based on the specific tissue type (e.g. heartwood, foliage) or species (e.g. Douglas-fir, ponderosa pine, etc.) of interest. This subset of data was then fit using Eq. 2. This analysis required replacing S_{ti} in Eq. 2, with either a categorical variable representing tissue type (S_t) or species (S_i).

All analyses was performed using the NLME package (version 3.1-118) (Pinheiro et al. 2015), in the R statistical platform (R Development Core Team 2015). Different variance structures were tested until normality of residuals and random effects was achieved. Statistical significance of differences between fixed effect parameters were determined using the multicomp (version 1.3-8) library in R with the Tukey HSD method to account for multiple comparisons. Summaries of sample size data can be found in Table 1, and Table 2.

A separate analysis was performed for the comparison of cut and powdered samples using Eq. 2 with M_j representing the powdered and cut preparation methods only. Conditional (R_c^2) and marginal (R_m^2) values were calculated following the procedures in Nakagawa, and Schielzeth (2013). R_c^2 values represent the portion of variance explained by the entire model including random effects, while the R_m^2 values represent the proportion of variance explained by the modeled fixed effects only. Standard errors are presented in parenthesis following all mean values with the exception of Table 1, where standard deviations are shown in parenthesis.

Results

Comparison of preparation methods across tissue types and species

The fixed effect parameter estimates for the MLC method were significantly higher than the parameter estimates for the other three preparation methods (Table 3), indicating consistently higher carbon fraction (C_c) measurements using the MLC method compared to paired sample material prepared using other methods. The largest difference in method C_c, was 1.89 (0.14) between the MLC and oven-dry methods, and the smallest difference was 0.27 (0.19) between the freeze-drying and vacuum desiccation methods. The differences between fixed effect

parameter estimates for freeze-drying versus vacuum desiccation were not significant. Parameter estimates for freeze-drying and vacuum desiccation were significantly higher than parameter estimates for oven-drying indicating higher C_c fractions measured in samples of both of these methods relative to paired oven-dry samples. Significant differences in fixed effect parameter estimates were found between powdered and cut samples (Table 3), with cut samples having higher average carbon fractions than the powdered samples by 0.32 (0.15). The R_m^2 for the final LME model, fit to all data, was 0.74, while the conditional R_c^2 was 0.77. The small difference in R_c^2 and R_m^2 values indicates only moderate improvement in overall model fit when accounting for random effects. A power of variance structure was determined to best model the heterogeneity of the data, with separate variances for each tissue type. All carbon fractions in Figure 1 are reported as percentages of oven-dry mass (C_c) after adjusting for maximum potential dissolved carbon. The R_c^2 and R_m^2 values in Figure 1 are for the fit of the predicted values to the observed values within each tissue type.

Comparison of preparation methods within tissue type

There were significant differences between fixed effect parameter estimates for methods within all tissue types (Table 4). Parameter estimates for the MLC method were higher than all other methods within each tissue type tested, and significantly higher than all other methods within sapwood, and heartwood. Higher parameter estimates reflect higher average carbon fractions for the MLC method compared to the other methods within each tissue type. The order of methods from lowest average C_c to highest was oven-drying, vacuum desiccation, freeze-drying, and MLC. The significance of these differences varied by tissue type. For example, average C_c values for freeze-drying was significantly higher than vacuum desiccation within sapwood but not within heartwood, and MLC values were significantly higher than all other methods within heartwood and sapwood but not within bark.

Comparison of preparation methods within species

Differences between fixed effect parameter estimates for a given method compared to the oven-drying method are shown in Table 5. The values in this table are equivalent to average volatile carbon mass fraction of the different methods adjusted to oven-dry mass weights. The MLC method parameter estimates are significantly higher than estimates for the oven-drying method for all species, and higher than both the freeze-drying and vacuum desiccation methods for all species. Differences ranged from 1.01 (0.13), to 1.86 (1.04) for MLC; 0.11 (0.08), to 1.25 (.46) for freeze-drying; and -0.30 (0.49), to 1.20 (0.28) for vacuum desiccation. Parameter estimates for the freeze-drying method were higher than the oven-drying method for all species and significantly higher for all species except Jeffrey pine, incense-cedar, and red fir. Parameter estimates for the vacuum desiccation method were lower than for oven-drying for sugar pine though not significantly different. For all other species, parameter estimates for the vacuum desiccation method were higher than estimates for the oven-drying method, and significantly higher for incense-cedar, Jeffrey pine, ponderosa pine, and red fir. The overall trend is for higher volatile carbon fractions to be measured by the MLC method, followed by the freeze-drying method, then the vacuum desiccation method and finally the oven-drying method.

Mean carbon fraction

Mean carbon fraction values for the methods by tissue type (bottom row of Figure 1) tended to follow the results of the fixed effects testing with higher mean values for the MLC method and

lower mean values for the oven-drying method within tissue types. The upper row of Figure 1 shows that mean bark carbon fraction values were higher than heartwood and foliage, which are approximately equal, while sapwood showed the lowest carbon fractions. Of the four tissue types, bark had the largest 95% confidence intervals, indicated by the larger size of the shaded area around the mean value in the bottom row of Figure 1. This larger confidence interval for bark is due to high variability in bark samples, as indicated by the greater vertical spread between observations shown in the upper row of Figure 1. Mean values for species C_c (Table 6) ranged from a low of 49.58 (0.33) for oven dried white fir tissues, to a high of 54.42 (0.38) for giant sequoia processed by the MLC method. Standard errors were generally largest for the MLC and vacuum desiccated samples and lowest for oven-dried samples. For every species, the order of average C_c values from lowest to highest was: oven-drying, vacuum desiccation, freeze-drying, and MLC.

Discussion

Differences between methods

The significant differences between the tested methods are extremely important for the growing field of tree carbon analysis and its extension to tree, forest, landscape, regional, and global scale carbon mass estimation. My findings demonstrate that the MLC method more accurately represents carbon fraction in tree tissues in comparison to all other methods tested, and that carbon fractions in tree tissues are sensitive to a range of factors in addition to the effects of high heat from oven-drying determined by Lamlom and Savidge (2003). Given the varying results in species mean level C_c values in my study (Table 6), and in the literature (Lamlom and Savidge 2003, Thomas and Martin 2012b), it is possible that analyzing a different set of tree species could have led to different results. However, the findings of this study leave little doubt that there is a significant potential to underestimate carbon fractions using the most common preparation methods, including freeze-drying, and vacuum desiccation.

Vacuum desiccation method

Vacuum desiccated tree tissue samples have been shown to retain higher amounts of carbon compared to oven-dried samples (Lamlom and Savidge 2003, Jones and O'Hara 2012). My study confirms this finding, however, I found somewhat lower average volatile carbon fractions (Table 5) than these two studies using the vacuum desiccation method in similar, or identical, tree species. Lamlom and Savidge (2003) found an average volatile fraction of about 1% in eastern white pine (*Pinus strobus* L.), while this study found an average of approximately 0.4% in the three pine species analyzed. The lower volatile fraction detected in my vacuum desiccated samples is most likely due to inherent differences in volatile chemical composition of the species measured, and, to a lesser extent, utilizing cut samples instead of powdered samples. I found that cut samples retained higher amounts of carbon compared to powdered samples, so my cut oven-dried samples may have retained higher amounts of volatile carbon compared to the powdered oven-dried samples used by Lamlom and Savidge (2003).

The difference in volatile carbon measured by Jones and O'Hara (2012) for coast redwood compared to values from this study are also likely due, in part, to utilizing cut samples instead of powdered. It is also possible there is an interaction between grinding samples and oven-drying that led to a greater loss of carbon in oven-dried samples from the Jones and O'Hara

(2012) study than occurred in my study. This interaction effect was not directly tested in this study, as I only used freeze-dried samples for my cut versus powdered comparison, and the exact interaction effect is not known. The redwood cores used by Jones and O'Hara (2012) were also tested after only a week in the freezer, while my cores where in the freezer for up to a month, and it is possible some carbon loss occurred in frozen cores over time, thereby reducing the measurable carbon present in the samples for this study. Some of the difference could also be due to the adjustment made to account for the maximum potential dissolved carbon that might have been present in the samples.

The consistently poorer performance of vacuum desiccation compared to the MLC method is most easily attributable to the vacuum pressures the samples were exposed to, along with the samples being exposed to room temperature versus below freezing temperatures. Vacuum pressure applied to tree tissue samples at ambient temperatures may result in the loss of some carbon, though the amount of carbon loss would depend on the vapor pressures of the chemical constituents present in the material, the length of time the vacuum was applied, and the vacuum pressure applied.

Freeze-drying method

Freeze-drying performed better in recovering carbon than either oven-drying or vacuum desiccation (Table 3), and resulted in higher overall mean species C_c values (Table 6). There is ample evidence that freeze-drying retains more of the carbon contained in wood samples than does oven-drying, although most of that evidence comes from only two papers (Thomas and Malczewski 2007, Martin and Thomas 2011). The samples from both of these papers were compared to samples that were oven-dried at temperatures above 100 ºC for 48 hours, ensuring no residual moisture, though specific tests of residual moisture content were not performed prior to carbon analysis in either paper. The combination of similar drying temperatures and times makes their findings comparable to my findings in comparing the oven-drying to freeze-drying methods, though Thomas and Malczewski (2007) did not adjust their freeze-dry carbon fractions to an oven-dry basis as the Martin and Thomas (2011) paper did. The average difference in carbon fractions between freeze-drying and oven-drying found in the referenced papers was about 2%. The difference between freeze-drying and oven-drying found in my study was about 0.8% (Table 3). The disparity between my findings and those of the referenced studies can be partially explained by the 0.32% difference in carbon fractions between cut samples and powdered samples (Table 3). The remaining difference is most likely related to the different species measured between studies, as species are known to have different volatile carbon fractions (Thomas and Martin 2012b), and within my study volatile carbon (Table 5) and mean carbon (Table 6) by species ranged significantly.

Additionally, the studies that utilized freeze-dried samples only tested sapwood tissues (Thomas and Malczewski 2007, Martin and Thomas 2011). My analysis shows that sapwood displayed a higher potential loss of carbon than either bark or heartwood (Table 4), as measured by differences between the MLC method and the oven-drying method. My findings may therefore be more representative of the average volatile carbon fraction for conifer tissues than the findings of Thomas and Malczewski (2007) or Thomas and Martin (2011). My paired sample analysis of methods demonstrates that freeze-drying may not be suitable for all tree species or tissues types if the desired goal is to accurately measure the carbon fractions of fresh tree tissues. Freeze-drying has been shown to result in the loss of volatile carbon in tree foliage (Díaz et al.

2002), and this effect would likely impact all other tree tissues containing volatile carbon compounds (Abascal et al. 2005).

MLC method

The MLC method significantly outperformed all other methods (Table 3). The MLC method captured an additional carbon fraction of 1.10% compared to the next best method: freeze-drying. Compared to oven-drying, the most widely used preparation method, the MLC method captured an additional carbon fraction of 1.89% (Table 3). Given that cut samples also showed improvements in carbon fraction measurements of 0.32% (Table 3), the net improvement in the MLC method versus the most commonly used method, oven-drying of powdered samples, is 2.21%. This is a very important difference as it represents a potential systematic bias in the majority of available data on carbon fractions. This improvement in carbon fraction estimation is equivalent to "finding" an additional 16 Pg of carbon within forest vegetation at a global scale, assuming an estimate of global carbon of 359 Pg using a carbon fraction of 50% (Dixon et al. 1994). As a note of caution, however, it is not advisable to take the fixed effect parameter estimates from my analysis and use them to adjust existing carbon fraction measurements, as this would ignore the significant variability in volatile carbon fractions that exist within different tree species and tissue types, and the highly variable methods used in the literature to date. Instead my findings make a strong argument for developing a standardized method for carbon fraction analysis within tree tissues along the lines of the MLC method, which could be incorporated into standardized methods of trait collection (Pérez-Harguindeguy et al. 2013). It should also be noted that the MLC method requires less equipment than freeze-drying or vacuum desiccation, which could reduce overall costs of carbon fraction analysis significantly compared to freeze-drying and vacuum desiccation.

Cutting vs. grinding

Grinding samples to a powder has been the primary method of preparing tree tissue samples for carbon fraction analysis. Every study in the Thomas and Martin (2012b) review that described how samples were prepared used powdered samples. The primary purpose for grinding samples into a fine powder was to reduce the observed variation between repeated measurements for some species (Lamlom and Savidge 2003). Grinding tissue samples to a well-mixed powder should result in material with equal proportions of chemical constituents (lignin/cellulose etc.) as the source material. Cut core pieces that have representative proportions of early and latewood, and contain complete ring segments, should also contain equal proportions of chemical constituents as the source material. Cut core pieces can therefore be as effective at capturing representative proportions of tree chemical compounds as powdered samples if careful attention is paid to the dissection process. Cut samples are also much easier and faster to obtain than putting samples through a ball mill, or other grinding equipment.

Loss of volatile carbon is significantly influenced by the surface area of the volatile material in question (Guo and Murray 2000). This relationship between volatilization and surface area is the likely explanation for my finding that powdered samples have significantly lower carbon conversion fractions than cut samples, as the surface area of sample material is much greater when that material is ground to a powder than when left in larger pieces. The comparison of cut versus powdered samples used freeze-drying only in preparing the sample material, had I used the MLC method for the comparison it is possible that the difference detected would have been larger, as the samples would have had a greater amount of carbon present in them to begin

with. Interactions between sample particle size, drying method and carbon losses should be considered when designing carbon fraction measurement methodologies in order to ensure that this potential source of carbon loss is accounted for.

Tissue carbon fractions

Measuring carbon fractions of different tree tissues is necessary for identifying the sources of variation in carbon fraction within trees. This variability is apparent in the carbon fractions shown in Figure 1, and in the variability of volatile carbon fractions shown in Table 4. Comparing the MLC method to the oven-drying method indicates that there was a greater amount of volatile carbon present in sapwood than in heartwood or bark (Table 4). Given that the majority of volatile carbon fraction data comes from one study that looked at freeze-dried sapwood samples (Martin and Thomas 2011), further investigation is needed to more fully describe the volatile component of whole tree carbon fractions.

My data demonstrated different mean carbon fractions between tissue types (Figure 1), with higher average carbon fractions in bark tissue, followed by heartwood and foliage, and then sapwood. This is not the general trend reported in Thomas and Martin (2012b), which found a one-to-one relationship between bark and stem carbon fractions in their meta-analysis of tree carbon data. The reported one-to-one relationship is likely due to pooling data from angiosperms and conifers, and using simple linear regressions on the resulting pooled data. Interestingly, some of the studies in the Thomas and Martin (2012b) review reported higher carbon fractions for bark than stem wood within a species (Laiho and Laine 1997, Tolunay 2009), demonstrating the importance of using paired samples when analyzing the relationship between tree tissue type carbon fractions within a species. In a more recent study, Martin et al. (2015), also found significant differences between tissues within a species. Given that bark tissue has a higher lignin content than stem wood (Harkin and Rowe 1971), and lignin has a higher carbon fraction than cellulose (Lamlom and Savidge 2003), my findings that bark has higher average carbon fractions than stemwood are not surprising, though this higher carbon fraction in bark is not generalizable based on the findings of Martin et al. (2015). I believe that many tree species will demonstrate differences in carbon fractions between tissue types when analyzed directly rather than the utilizing the type of pooled data meta-analysis performed by Thomas and Martin (2012b).

Species and tissue level volatile carbon fractions

The species sampled in this study showed a large amount of variability in their volatile carbon fractions (Table 5), and in their mean carbon fractions as measured by a particular method (Table 6). The analysis reflected in these numbers is somewhat different than the analysis performed on the entire dataset (Table 3) as samples within a species are more likely to be unbalanced with respect to tree tissue types, than was the analysis for the entire dataset. Given the variability in volatile carbon fraction between tissue types this imbalance in data could lead to average volatile carbon fraction estimates that are more representative of the balance of tissue types represented in the samples, than of a species level average. The species data does demonstrate the general trend of higher levels of carbon fractions measured by the MLC method than all other methods, and the variability in volatile carbon fractions between species.

The variety of methods utilized to measure carbon fractions in the literature result in different estimates of species-specific carbon fractions between studies that are not necessarily comparable. For example, there are two reported carbon fraction values reported for Manchurian walnut (*Juglans mandshurica* Maxim.) (Thomas and Malczewski 2007, Zhang et al. 2009).

Thomas and Malczewski (2007) reported a carbon fraction of 48.36% from sapwood samples that were freeze-dried, while Zhang et al. (2009) reported 52.8% from stemwood that was oven-dried at 70 ºC without specifying the proportion of sapwood and heartwood. Without knowing what effect the different methods have on carbon fractions, or what tissue types are represented in the carbon fraction samples, there is no way to tell if the discrepancy between these studies is due to the balance of tissue types, regional differences in population genetics, or simply due to the different methods employed.

Applying carbon fractions to existing biomass data

Adjusting carbon fractions to oven-dry weights allows for easy conversion of oven-dry wood density to carbon density (mass C per unit volume) inclusive of the volatile carbon fraction retained by a particular method (freeze-dry, MLC etc.). Carbon density can be used to easily convert wood volume to carbon mass. To ensure that the correct carbon density is calculated, wood density data must be derived from material that has been oven-dried at the same temperature and for the same duration as the material used to calculate the carbon fraction conversion (C_c) values. Unfortunately, there is a great deal of variability in the temperatures and drying times used to oven-dry material for carbon fraction and wood density analysis. Most studies have used oven-drying temperatures of either 70º C or 105º C for carbon fraction analysis (Thomas and Martin 2012a), and various temperatures for wood density analysis (Williamson and Wiemann 2010). One approach that could be used to obtain carbon fraction values that are compatible with existing wood density data, would be to use my MLC method to obtain carbon fraction measurements, then record the stable mass of the residual wood tissue sample after oven-drying at 70º C, then continue to dry the sample at 105º C and record the new stable mass. The oven-dried mass results could then be used in Eq. 1 to obtain the appropriate C_c values for an oven-dry mass basis of 70º C, or 105º C. These temperatures represent the plurality of temperatures used to obtain carbon fraction values from the oven-drying method in the literature (70º C), and the suggested drying temperature for wood density samples (105º C) (Williamson and Wiemann 2010). This approach could be used to place carbon fractions from different studies on the same baseline moisture content and allow for more meaningful comparisons of carbon fractions between studies.

Method improvements

An ideal sampling method for tree tissue carbon fraction analysis would leave little room for volatilization of carbon compounds, similar to the MLC method employed in this study. Minimizing the loss of volatile carbon likely requires cooling samples as soon as they are collected, ensuring that they are not exposed to vacuum pressures, and cutting samples rather than grinding them to a fine powder. Where low temperature storage is not quickly available, a pressurized pre-chilled chamber could be utilized to store tree cores and foliage until they can be placed in a freezer. Although it may be impossible to completely prevent the loss of volatile carbon, it is important to attempt to reduce losses in order to capture the greatest amount of carbon stored in living tree tissues. Any future study designed to improve the accuracy of carbon fraction estimates in tree tissues must ensure that the methodology captures the greatest amount of carbon possible.

Conclusion

The primary methods that have been used to measure tree carbon fractions have likely underestimated the total carbon present in tree tissues. Failure to account for inherent problems with existing methods could result in systematically underestimating tree carbon fractions by 1.1% (0.15) to 1.89% (0.14), equivalent to a coefficient of variation of 2.2% to 3.78% respectively for the commonly used global carbon fraction of 0.5. I found a great deal of variability in volatile carbon fractions between species, between tissue types within species, and between methods used, leading to the conclusion that studies into carbon fractions must account for these sources of variation in order for meaningful comparisons of carbon fractions.

Figures and Tables

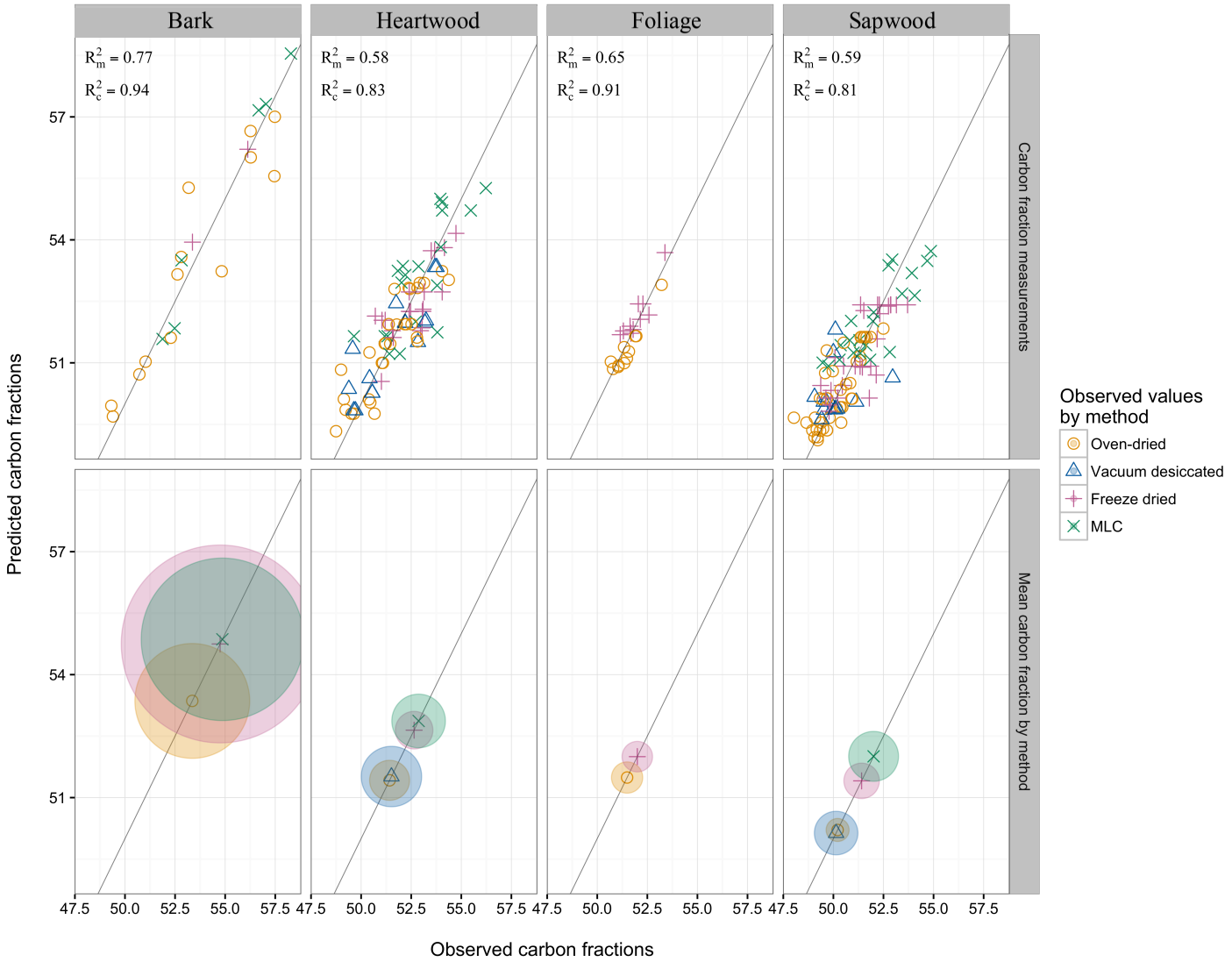

Figure 1. Predicted vs observed carbon fractions are shown on the top row of the figure along with the marginal R_m^2 and conditional R_c^2 values for the regression of the relationship shown in each facet of the graph. Mean values for each method within tissue type are shown on the bottom row with the 95% confidence interval of each mean shown by the shaded region around it. Carbon fractions are C_c values derived using Eq. (1), and adjusted to an oven-dry basis for each method used, then adjusted to account for dissolved carbon.

Table 1. Summary statistics for sample trees used in carbon fraction analysis. Standard deviations shown in parenthesis following the average value for each metric listed.

Species	DBH (cm)	HT (m)	HLC (m)	# of trees	# of C samples
Douglas-fir	67.1 (41.7)	34.8 (11.6)	13.4 (5.2)	4	24
Giant sequoia	338.2 (130.1)	72.1 (14.0)	20.9 (5.4)	5	22
Incense-cedar	39.7 (30.1)	20.9 (8.3)	10.3 (2.7)	6	21
Jeffrey pine	25.5 (13.6)	10.3 (4.2)	2.0 (1.0)	4	11
Ponderosa pine	74.6 (40.4)	35.5 (14.3)	11.9 (5.9)	8	52
Red fir	9.3 (9.5)	5.2 (6.6)	1.2 (0.8)	3	17
Redwood	68.4 (15.0)	38.2 (4.3)	22.9 (3.3)	5	19
Sugar pine	162.3 (84.2)	43.9 (12.3)	19.9 (9.8)	3	36
White fir	81.8 (44.8)	37.7 (13.5)	13.5 (6.2)	9	26

Table 2. Summary sample information by grouping category.

	Grouping factor	number of samples
Sampling level	Tree	45
	Core	56
	Core segment	111
Method used	MLC	46
	Freeze-drying	58
	Vacuum desiccation	27
	Oven-drying	97
	Cut	10
	Powdered	10
Tissue type	Foliage	21
	Bark	21
	Sapwood	102
	Heartwood	84

Table 3. Differences between fixed effect parameter estimates between methods for all tissue types.

Fixed effects compared	Difference between fixed effects	Standard error	*P*-value
Vacuum desiccation vs. oven-drying	0.51	0.17	0.02
Freeze-drying vs. oven-drying	0.79	0.11	<0.01
MLC vs. oven-drying	1.89	0.14	< 0.01
Freeze-drying vs. vacuum desiccation	0.28	0.19	0.48
MLC vs. vacuum desiccation	1.38	0.19	< 0.01
MLC vs. freeze-drying	1.10	0.15	< 0.01
Powdered vs. cut	-0.32	0.15	0.03

Differences are determined only for paired samples measured by each method being compared. Positive differences indicate significantly ($p < 0.05$) higher carbon fractions for the method on the left hand side of the comparison. Fixed effects parameters estimated by fitting Eq. 2 to all carbon fraction data. Significance of differences determined by a Tukey HSD multiple comparisons test.

Table 4. Differences between fixed effects parameter estimates for compared methods within tissue types. Significant differences indicate that the parameter estimates of the compared methods within tissue types are not equal. Positive values for differences indicate higher carbon fractions for the method on the left hand side of the comparison. Fixed effect parameters estimated by fitting Eq. 2 to data for each tissue type listed.

Tissue type	Comparison made	Difference in parameter estimates	Standard error	*P*-value
Bark	MLC vs. freeze-drying	1.664	1.071	0.26
	MLC vs. oven-drying	1.940	0.668	0.01
	Freeze-drying vs. oven-drying	0.275	1.021	0.96
Heartwood	MLC vs. freeze-drying	0.695	0.256	0.03
	MLC vs. oven-drying	1.860	0.233	< 0.01
	MLC vs. vacuum desiccation	1.148	0.261	< 0.01
	Freeze-drying vs. oven-drying	1.165	0.223	< 0.01
	Freeze-drying vs. vacuum desiccation	0.453	0.272	0.34
	Vacuum desiccation vs. oven-drying	0.712	0.245	0.02
Sapwood	MLC vs. freeze-drying	1.280	0.060	< 0.01
	MLC vs. oven-drying	2.286	0.049	< 0.01
	MLC vs. vacuum desiccation	1.839	0.121	< 0.01
	Freeze-drying vs. oven-drying	1.006	0.051	< 0.01
	Freeze-drying vs. vacuum desiccation	0.559	0.121	< 0.01
	Vacuum desiccation vs. oven-drying	0.447	0.113	< 0.01
Foliage	Freeze-drying vs. oven-drying	0.457	0.122	< 0.01

Table 5. Difference in fixed effect parameter estimates between listed method and oven-drying method. * Indicates significant differences between oven-dried sample carbon fractions and a given method. Standard errors for differences are shown in parenthesis. Positive values indicate higher carbon fractions for the listed method compared to the oven-drying method. Fixed effect parameters estimated by fitting Eq. 2 to data for each species listed.

Species	Freeze-drying	Vacuum desiccation	MLC
Douglas-fir	0.53 (0.19)*	0.35 (0.17)	1.05 (0.17)*
Giant sequoia	0.98 (0.02)*	NA	2.24 (0.03)*
Incense-cedar	0.11 (0.08)	0.87 (0.01)*	2.66 (0.01)*
Jeffrey pine	0.17 (0.21)	0.40 (0.14)*	2.23 (0.12)*
Ponderosa pine	1.11 (0.18)*	1.20 (0.28)*	1.66 (0.23)*
Red fir	0.06 (0.14)	0.65 (0.21)*	2.83 (1.04)*
Redwood	1.25 (0.46)*	0.44 (1.05)	2.38 (0.56)*
Sugar pine	1.16 (0.22)*	-0.30 (0.45)	2.63 (0.34)*
White fir	0.28 (0.10)*	0.32 (0.50)	1.80 (0.38)*

Table 6. Mean carbon fraction values for each species as measured by a particular method.

Species	Oven-drying	Freeze-drying	Vacuum desiccation	MLC
Douglas-fir	49.93 (0.35)	50.94 (0.37)	50.48 (0.39)	51.95 (0.38)
Giant sequoia	52.40 (0.35)	53.41 (0.37)	52.95 (0.39)	54.42 (0.38)
Incense-cedar	51.86 (0.34)	52.87 (0.36)	52.40 (0.38)	53.88 (0.37)
Jeffrey pine	50.67 (0.51)	51.68 (0.53)	51.22 (0.54)	52.69 (0.53)
Ponderosa pine	50.51 (0.24)	51.52 (0.27)	51.05 (0.29)	52.53 (0.28)
Red fir	49.97 (0.42)	50.97 (0.44)	50.51 (0.45)	51.98 (0.45)
Redwood	50.64 (0.37)	51.65 (0.39)	51.18 (0.40)	52.66 (0.39)
Sugar pine	51.56 (0.26)	52.57 (0.29)	52.11 (0.31)	53.58 (0.30)
White fir	49.58 (0.33)	50.59 (0.35)	50.12 (0.37)	51.60 (0.36)

Mean carbon fractions are the parameters of the model derived from fitting carbon fraction data for each species to Eq. 2. Standard errors for the parameters are shown in parenthesis. Mean carbon values include all tissue types.

2 Variation in carbon fraction, tissue density, and carbon density within conifer trees

Introduction

Understanding where carbon is stored within a forest is an essential component of accurately estimating forest carbon stocks. Accurate estimates of carbon stocks can inform climate change mitigation efforts at global scales (Brown 2002), and at smaller scales are critical to understanding nutrient cycling as plant tissues release carbon due to disparate decay rates (Fogel and Cromack 1977, Johansson et al. 1995). This type of information could also inform land managers of the carbon consequences of particular forest management activities as treatments affect different components of a stand. In order to understand how carbon mass is allocated within a stand we need to first know how carbon mass is allocated within individual trees and if that allocation varies predictably from tree to tree.

Forest carbon stock estimates typically utilize some version of the following approach. A species average wood density (dry mass wood / green volume wood) is used to convert tree bole volume into bole biomass (Dixon et al. 1994; Goodale et al. 2002). Tree bole biomass is then converted into total tree biomass using conversion factors based on ratios of tree component biomass (e.g. Goodale et al. 2002). Alternatively allometric models may be based on whole tree biomass measures and then related to diameter, or height and diameter (e.g. Jenkins et al. 2003; Chojnacky et al. 2014). However tree biomasses are calculated, stand, forest, or ecosystem level biomass is obtained by summing individual tree biomasses across the scale of interest. Total biomass values are then converted into carbon mass estimates using a carbon fraction of 0.5. This "standard" approach to estimating carbon mass is widely used in forest carbon research throughout the world (Karchesy and Koch 1979, Harmon et al. 1990, Dewar and Cannell 1992, Hollinger et al. 1993, Matthews 1993, Thuille et al. 2000, Pacala et al. 2001, Brown 2002, Goodale et al. 2002, Chave et al. 2005, Woodbury et al. 2007, Fahey et al. 2009, Van Deusen and Roesch 2011).

This approach to carbon mass estimation implies three assumptions: (1) intraspecific variation in wood density is insignificant; (2) intraspecific variation in carbon fraction is nonexistent or negligible; and (3) interspecific variation in carbon fraction is nonexistent or negligible. Using a species-level average wood density implies that a unit of wood volume from a given species has the same biomass regardless of the size, age, or location of the tree it came from. This assumption ignores known variation in wood density related to tree height and diameter (Chave et al. 2005, 2009, Nogueira et al. 2008), regional intraspecific variation in wood density (Nogueira et al. 2007), and variation related to radial position in the bole (Wiemann and Williamson 1989, Woodcock and Shier 2002). Failing to integrate known sources of variation in wood density may lead to inaccurate biomass estimates where the regional variation in wood density is significant, or where wood density varies significantly with tree size or other measurable features.

The second assumption of this standard approach is that carbon fractions are constant for all species. This assumption is not supported by the literature, which shows significant interspecific variation in carbon fractions (Lamlom and Savidge 2003; Lamlom and Savidge 2006; Martin and Thomas 2011; Jones and O'Hara 2012; Thomas and Martin 2012). Significant

differences between angiosperms and conifers were found in a literature review of available carbon fraction data by Thomas and Martin (2012), with conifers demonstrating higher carbon fractions as a group. Within the angiosperm and conifer groups significant differences in carbon fractions also exist, with a coefficient of variation greater than 20% of the mean 50% value between species within the same provenance (Thomas and Martin, 2012). Significant differences in carbon fraction estimates were also found across biomes (Thomas and Martin, 2012). Carbon fractions should be measured for each species of interest in order to come up with the most accurate carbon mass estimates. Failure to do so risks over- or under-estimating the mass of carbon contained within forests.

In evaluating the third assumption listed above, Jones and O'Hara (2012), found significant differences in carbon fraction between heartwood and sapwood within individual coast redwood (*Sequoia sempervirens* (Lamb. ex Don D) Endl.) trees. Their results are similar to those found by Lamlom & Savidge (2006) in giant sequoia (*Sequoiadendron giganteum* (Lindl.) J. Buchholz), and by Bert and Danjon (2006) in maritime pine (*Pinus pinaster* Ait.). In all three cases heartwood contained significantly higher carbon fractions than sapwood. This finding was reversed for sugar maple (*Acer saccharum* Marshall) (Lamlom and Savidge 2006) where carbon fraction increased with distance from pith. There is currently insufficient data to determine if these findings hold true for other tree species; therefore, more research into intraspecific variation in carbon fraction is necessary in order to determine if carbon fraction varies predictably between wood types within trees. Differences between carbon fraction in heartwood and sapwood could also lead to significant differences in carbon mass estimates across tree sizes, as larger trees tend to have higher proportions of heartwood than smaller trees.

Depending on the tree species and growth history, wood density can be higher or lower in heartwood than sapwood (Woodcock and Shier 2002). When present, these different tissue densities can lead to higher or lower carbon densities (mass carbon/green wood volume) in heartwood compared to sapwood. Jones and O'Hara (2012) showed that in multiaged coast redwood stands, higher tissue densities in heartwood, combined with higher carbon fractions, resulted in higher stand carbon densities as stand-level heartwood proportions increased over time. Alternatively, if sapwood has a higher average carbon density than heartwood, lower stand average carbon densities would be expected over time. Despite demonstrated differences in wood types, most studies of stemwood density estimate stemwood average densities, and these averages ignore the potentially nonlinear relationships between tree size and sapwood to heartwood ratios (Jones et al. 2015).

Tree bark density and carbon fraction are not well studied, though bark can be a significant portion of total tree biomass, and in some cases has much higher carbon fractions than stemwood (Correia et al. 2010, de Aza et al. 2011). This difference in carbon fraction between bark and stemwood suggests that bark carbon mass would be more accurately estimated directly rather than as a proportion of bole mass. Bark has also been shown to be strongly correlated with wood characteristics, such as wood density (Poorter et al. 2014) suggesting that tree species with similar bark characteristics may have similar tissue properties. The physical characteristics of bark, such as color, and texture are derived from the chemical constituents that comprise it. It would, therefore, be logical to conclude that the physical aspects of bark could be related to underlying tree properties such as carbon fraction, wood density, and carbon density. As bark descriptions are widely available for many species, bark groups would be a logical method of categorizing species. In addition to the potential improvement in carbon fraction modeling by

bark group, accounting for species-specific averages and sources of variation in bark carbon fraction, and bark tissue density should significantly improve carbon mass estimation models.

Analyzing relationships between the species-specific tree tissue properties of carbon fraction, density, and carbon density is a necessary first step in improving the accuracy of carbon mass estimates. Additionally, quantifying the relationships, if any, between these species-specific tree tissue averages and measurable tree characteristics related to tree size, or stand conditions could significantly improve my understanding of forest carbon storage and sequestration.

While tissue density has been studied across many species, including both conifer and angiosperm groups, the majority of carbon fraction studies have looked at angiosperms with data for only 37 conifer species reported in Thomas and Martin (2012a). This means that little information exists on variation in carbon fraction between conifer species, or between tissue types within conifers. Increasing the number of conifer species, and studying individual tissue types within conifers therefore would be an important part of improving overall understanding of carbon dynamics in forest stands.

Using data from nine conifer species across a range of sizes, elevations, bark characteristics, and latitudes, I approach these issues with the following objectives:

1. Determine if accounting for tissue type leads to a significant improvement in estimates of carbon fraction, density, and carbon density over species level, and tree group averages alone;
2. Determine what the differences in tree bole carbon mass estimates are due to using the typical 0.5 carbon fraction, versus measured tissue type carbon fractions; and
3. Determine if carbon fractions, tissue densities, and carbon densities vary predictably from species-tissue type averages based on measureable tree characteristics and sample location within trees.

Materials and Methods

Plot locations and sampled species

Nine conifer species were sampled: coast Douglas-fir (*Pseudotsuga menziesii* (Mirb.) Franco var. *menziesii*), coast redwood, giant sequoia, incense-cedar (*Calocedrus decurrens* (Torr.) Florin), Jeffrey pine (*Pinus jeffreyi* Balf.), ponderosa pine (*P. ponderosa* Lawson & C. Lawson), red fir (*Abies magnifica* A. Murray), sugar pine (*P. lambertiana* Dougl.), and white fir (*A. concolor* (Gord. & Glend.) Lindl. ex Hildebr.). Study plots were located in the following locations: Jackson Demonstration State Forest (39.364 N, 123.708 W), Baker Forest (39.916 N, 121.063 W), Blodgett Forest Research Station (38.910 N, 120.662 W), Whitaker Forest (36.699 N, 118.939 W), Teakettle Experimental Area (36.968 N, 119.036 W), outside of Loyalton, CA (39.675 N, 120.165 W), and near Shaver Lake, CA (37.046 N, 119.211 W). Not all species were present in all locations. The nine species were placed into three tree groups, based on bark characteristics to determine if any significant improvement in model fit of the three tree properties (carbon fraction, tissue density, and carbon density) existed between these easily identified groups. The tree groups were: trees with furrowed bark, included Douglas-fir, white fir, and red fir; trees with fibrous bark, included redwood, giant sequoia, and incense-cedar; and trees with scaly bark, included ponderosa pine, sugar pine, and Jeffrey pine.

Core extraction and handling

Summary statistics for the sampled trees are shown in Table 7. Tree cores were extracted from breast height (1.37 m), midway between breast height and base of live crown, and every 4 m within the live crown from randomly sampled trees within study plots. A 40.6 cm long increment borer with an aperture of 5.15 mm was used to extract all cores from sample trees. To prevent contamination, the increment borer was cleaned between each sample tree with a silicon-based lubricant and clean paper tissues. After extraction, cores were placed in plastic straws, sealed using adhesive tape, and placed in a white plastic tube to reduce exposure to sunlight. The sapwood component of each core was determined either by color, or by holding the core up to the sun and marking the translucent portion of the cores on the outside of the straw where sharp color differences were not obvious. Cores were then placed in a cooler with ice for transportation back to a lab freezer.

Core processing

In the lab, frozen cores were cut into segments that included 4 or 8 tree rings depending on the ring widths. It was necessary to use variable number of ring widths per segment to ensure that enough mass was present in the core segment sample for carbon and density analysis. A total of 42 tree cores were used for carbon fraction analysis. The cores were randomly selected from the 370 cores collected in the field. Core segments were taken from within the bark, sapwood, and heartwood sections of the selected tree cores. All core segments that were analyzed had the outermost portion removed with a razor blade in order to remove oxidized tissue and remove any possible contaminants from the exterior of the core. A razor was used to cut core segments into pieces less than 1 mg in mass. This material was separated into 2-4 vials and the material in each vial was prepared for carbon mass measurement using one or more of the following, common sample preparation methods: vacuum desiccation, freeze-drying, oven-drying, or left un-dried. After processing, all vials were placed back into the freezer.

Carbon fraction analysis

Tree tissue carbon fraction and density sample size data can be found in Table 8. For carbon fraction determination, weighed subsamples of 0.3 - 0.5 mg from each prepared vial were placed into tin capsules and then into a CE Instruments Flash 2000 CHNS/O analyzer (Rodano, Milano, Italy) for sample carbon fraction (CF_R) determination using combustion and mass chromatography. The CN analyzer was calibrated between sample runs using acetilinide as a standard to develop a calibration curve. The calibration curve had a R^2 of 0.999 or higher for all sample runs. After removing the subsample, the sample material remaining in each vial was weighed and this weight was recorded as M_R. This material was then placed in an individual tin labeled with sample ID and dried at 105˚C until stable mass was achieved. This stable oven-dry mass was recorded as M_{OD}. The final carbon fractions (CF_C) were calculated using:

Eq. 3 $$CF_C = CF_R * M_R / M_{OD}.$$

This calculation was performed so that all carbon fractions used the same baseline tissue moisture content and could therefore be compared in a sensible way. A more complete description of the carbon fraction data can be found in Jones & O'Hara (2016).

Tissue density and carbon density analysis

Paired tissue density and carbon fraction core segments were used to match carbon fraction with tissue density measurements from the same tree heights and ring ages within a given tree. The tissue density of each core segment was determined by dividing the green volume (cm^3) of the core segment by the oven dry mass (g) of the core segment. The green volume of the segment was determined by multiplying the segment length (cm) by the internal area of the increment borer aperture (0.208 cm^2). With one tissue density value per segment sample, the total number of density samples was 90. Carbon density was determined by multiplying the corresponding tissue density and carbon fraction measurement for all preparation methods used on a given sample, resulting in 203 carbon density values.

Difference between 0.5 value and measured carbon fractions for species-tissue types

The average carbon fraction values for each species-tissue type were used to make comparisons of carbon mass for 1000 kg example trees for each of the 9 species. For consistency in biomass estimation, the BIOPAK equations (Means et al. 1994) were used to derive bark and bole masses. The total biomass of each example tree within each species was held constant to demonstrate the impact of measuring carbon fractions versus using the 0.5 value. Using the standard approach, the estimated biomass for each tree tissue component (bark or bole) was multiplied by 0.5 to obtain carbon mass estimates.

To calculate bark carbon mass using measured carbon fractions, the mass of estimated bark was multiplied by the corresponding bark carbon fraction. For carbon mass of sapwood and heartwood, a sample tree for each species was selected from the database that most closely matched the DBH and height used to derive the 1000 kg example tree. Bole cross sectional sapwood and heartwood areas were determined for the cores from each sample tree. The cross sectional area represented by each tissue type within each core, was multiplied by the species average tissue type density. The results of these calculations were then summed across each core within a sample tree. The ratio of total heartwood core mass to total core mass was used to estimate heartwood biomass proportion in the 1000 kg example tree boles. Sapwood bole mass was determined by subtracting heartwood mass from total bole mass. The bole mass for each tissue type was then multiplied by the respective species-tissue type carbon fraction to derive total carbon mass for bark, sapwood and heartwood.

Statistical analysis

Linear mixed effects (LME) analysis was used to account for the nested structure of the data and to account for random effects related to sampling procedures. For carbon fraction and carbon density analyses the nested data structure was organized as sample ID (m) nested within core (n), nested within tree (o), nested within plot (p). For tissue density analysis, the nested data structure was organized as core nested within tree, nested within plot. Random effects (ϕ) were assigned to each level of the data structures mentioned above and a compound symmetric correlation matrix was used to model relationships between observations. The equations for the most complex levels of analysis for each tree property were:

Eq. 4

$$y_i = CF_{ijk} + B_l X_l + \phi_{mnop},$$
$$\phi_{mnop} \sim N(0,\sigma_b^2)$$

Eq. 5 $$y_i = D_{ijk} + B_l X_l + \phi_{nop},$$
$$\phi_{nop} \sim N(0,\sigma_b^2)$$

Eq. 6 $$y_i = CD_{ijk} + B_l X_l + \phi_{mnop},$$
$$\phi_{mnop} \sim N(0,\sigma_b^2)$$

In Eq. 4 - 6, fixed effects were assigned to the mean values for the combination of species (i), tissue type (j), and a given preparation method (k), resulting in the notation CF_{ijk}, for carbon fraction analysis, D_{ijk} for tissue density analysis, and CD_{ijk} for carbon density analysis. In the case of D_{ijk} only one preparation method, oven-drying, was used but for consistency with the other two properties the notation was kept. Models with species level averages (CF_{ik}, D_{ik}, CD_{ik}) and models with species level averages with additional fixed effects related to other tree characteristics in the form of a covariate matrix ($B_l X_l$), were tested against each other to determine if the covariate matrix improved the overall model fit. Models with tree group level (t) averages (CF_{tk}, D_{tk}, CD_{tk}), were tested against method level models to determine if grouping by bark characteristics significantly improved the model fit. These simpler models had the same random effects structure as the models in Eq. 4 - 6. This modeling approach effectively centers the data on the average of a given grouping level. Accounting for grouping level averages allows for modeling the deviations from the respective means as functions of measurable tree characteristics, or location of samples within trees. This approach reduces the influence that any one grouping level (species, tissue type, tree group, method) has on the modeled relationships. Parameters (B_l) were estimated for several potential covariates and their interactions (X_l) using LME modeling. LME models for all three tree properties were limited to a maximum of five potential covariates and/or their interactions selected from a larger pool of covariates using the glmulti package v. 1.07 (Calcagno 2013) in the R programing language (R Development Core Team 2015). The glmulti package was used to fit the best combination of covariates and their interactions to the data using multiple linear regression. LME modeling was performed using the NLME package v. 3.1-118 (Pinheiro et al. 2015) in the R statistical platform.

For the three tree properties of interest (CF, D, CD), the significance of accounting for grouping level, and additional covariates was determined by performing an ANOVA on nested LME models of increasing complexity: 1) a model with means for the given method used (CF_k, D_k, and CD_k), 2) models fit to means for the three tree groups (t) and method (CF_{ik}, D_{ik}, and CD_{ik}), 3) models for species level averages (CF_{ik}, D_{ik}, and CD_{ik}); 4) models with species level averages and additional covariates $CF_{ik} + B_l X_l$, $D_{ik} + B_l X_l$, and $CD_{ik} + B_l X_l$; 5) models with average values for species-tissue types, CF_{ijk}, D_{ijk}, and CD_{ijk}; and 6) models of the forms found in Eq. 4-6. Maximum log-likelihood (ML) was used during model covariate selection so that models with different fixed effects could be compared. Maximum log-likelihood ratios were also used to determine if nested models were significantly different from each other. The final reported LME models for a given tree property were fit using reduced maximum log-likelihood (REML) methods as this approach produces less biased parameter estimates (Pinheiro and Bates 2000). This means that Akaike information criterion (AIC) (Akaike 1974) would be different between the final LME models and the models used to determine the importance of tissue type and additional covariates. Marginal r-squared (R_m^2), and conditional r-squared (R_c^2) values were calculated for the final LME model fits by tree group. These two values are most easily interpreted as the proportion of variation explained by the fixed effects alone (R_m^2), and the proportion of variation explained by fixed and random effects (R_c^2) (Nakagawa and Schielzeth

2013).

Carbon fraction data was summarized by species-tissue type, along with the relative standard deviation of a given measurement from the widely used 0.5 average. These relative deviations were calculated as percentages of the mean value of 0.5 or CV_{50}.

Results

Symbols, descriptions, and units for covariates used in the final LME models are shown in Table 9. Table 9 shows that the most common type of covariate to be included in the final models were related to height of sample in tree, crown length, or metrics related to height and crown length. Radial distance from pith and tissue density also significantly contributed to final models, though they were not as consistent as covariates related to vertical position within the tree.

ANOVA results for comparisons of the nested models show that carbon fraction models were significantly improved with each increase in model complexity (Table 10). Accounting for tree group, or tissue type alone did not significantly improve model performance for either density or carbon density. For density, and carbon density models, significant improvements begin at the species level with additional covariates added. Models with tissue type and additional covariates (Table 10, model # 6, #12, and #18) performed significantly better than all simpler model forms for all three tree properties.

The final models for each tree property included covariates representing location of samples within trees (RH, R, HAR), and tree crown metrics (LCR, NLCR, FHLC, HLC), but not covariates related to tree size such as diameter at breast height, or tree height though these covariates were tested (Table 11). The carbon fraction model was significantly improved with the addition of an interaction term for tissue density and relative height (p:RH), while the density and carbon density models were both significantly improved with the addition of an interaction term including radius from pith (RH:R).

The potential influence of each term on a given model is demonstrated by the fraction of variation (FV) values in the FV-upper and FV-lower columns in Table 11. The upper fraction of variation was calculated by multiplying the given parameter estimate by the mean value of the term plus one standard deviation. The FV-lower values were determined my multiplying the parameter estimates by the mean value minus one standard deviation, then dividing by the mean tissue property value of CF_{ijk}, D_{ijk}, or CD_{ijk}. For terms that included RH in them, the RH portion of the term was held at one. The FV values range from -0.8709 to 0.5361, with the largest FV values found in the density and carbon density models. The FV values for the CF_{ijk} model recalculated relative to the widely used 0.5 carbon fraction are the CV_{50} values for each term. The p:RH CV_{50} values range from -0.0279 to -0.0259; HLC:FHLC CV_{50} values range from 0.0001 to 0.0106; and the HAR:HLC CV_{50} values range from -.0018 to 0.

Carbon fraction data is shown in Table 12. Measured mean tree tissue carbon fractions (CF_{ij}) and standard deviations, shown in parenthesis, ranged from 0.507 (0.009) for white fir sapwood, to 0.588 (0.009) for Douglas-fir bark (Table 12). Corresponding CV_{50} values were 0.014 (0.018), to 0.176 (0.018). A comparison of carbon mass estimates for each species tissue type within 1000 kg example trees is shown in Figure 2. Carbon mass by bark (C_{bm}), sapwood (C_{sm}), and heartwood (C_{hm}) are calculated using a carbon fraction of 0.5, and using the CF_{ij} values from Table 12. Each tree was set at 1000 kg mass, including bark so that the only

difference in carbon mass estimate is due to using measured carbon fraction values rather than the widely used 0.5 value. Total carbon masses for the trees estimated with a 0.5 fraction are 500 kg. For the trees estimated using the CF_{ij} values from Table 12 the total carbon masses for each species are as follows: Douglas-fir, 519 kg; giant sequoia, 544 kg; incense cedar, 553 kg; Jeffrey pine, 529 kg; ponderosa pine, 518 kg; red fir, 522 kg; coast redwood, 532 kg; sugar pine, 541 kg; and white fir, 518 kg. The difference in these masses as a percentage of the trees estimated with a carbon fraction of 0.5 are: Douglas-fir, 3.8%; giant sequoia, 8.9%; incense cedar, 10.6%; Jeffrey pine, 5.8%; ponderosa pine, 3.6%; red fir, 4.4%; coast redwood, 6.4%; sugar pine, 8.2%; and white fir, 3.6%.

Bark carbon fraction values ranged from a low of 0.515 (0.005) for Jeffrey pine, to a high of 0.588 (0.009) for Douglas-fir (Table 12). Heartwood values ranged from a low of 0.513 (0.010) for Douglas-fir, to a high of 0.551 (0.010) for giant sequoia. Sapwood values ranged from a low of 0.507 (0.009) for white fir, to a high of 0.541 (0.008) for incense-cedar. Carbon fractions were generally lower for sapwood than heartwood, though bark did not show a consistent trend. The CV_{50} values ranged from a low of 0.014 (0.018) for white fir sapwood, to a high of 0.176 (0.018) for Douglas-fir bark.

LOESS regressions indicate vertical trends in each tree property (CF, D, CD) by tree group (Figure 3). The values on the x-axis are expressed as percentages of species tissue type values to center the data. This allows for a more meaningful comparison of deviations from average for each tree group. Density and carbon density showed the greatest range in deviations from the species-tissue type means ranging from approximately 0.8 to 1.4, while carbon fractions stayed relatively close to their respective means ranging from 0.96 to 1.04. Density and carbon fraction showed negative correlations in their trends with significant variation between tree groups. The fibrous bark group displayed the greatest range in deviations from the mean, followed by the furrowed bark group, with the scaly bark group displaying less variation.

The shaded regions of the LME model predicted data versus observed data (Figure 4), represent the 95% confidence intervals for each tissue type within a given tree group – tree property. The lack of overlapping confidence intervals between the heartwood samples of the three tree groups, along with the lack of overlapping confidence intervals for the sapwood portion of the furrowed bark group and the other two groups indicates significant differences between those means across the tree groups. The wide confidence intervals for the bark portions of the graphs are mostly related to the high variation found in the bark samples, but is also a function of the smaller sample sizes of bark tissues. The R_c^2 values for the model fits range from 0.64 to 0.95, while the R_m^2 values range from 0.34 to 0.91. The difference in these two values indicates the variation in the model that is explained by the random effects related to individual trees, and individual cores taken from those trees. Differences between the R_m^2 and R_c^2 are most pronounced in the density properties of the furrowed bark trees, with smaller differences displayed by carbon density compared to the tissue density.

Discussion

Measured carbon fractions versus 0.5

The differences between carbon mass estimates derived from measured CF_{ij} values, versus the values derived from assuming a carbon fraction of 0.5 (Figure 2, Table 12), demonstrate the importance of correctly accounting for variation in carbon fractions within trees, and between

tree species. The increase in estimated carbon mass related to using CF_{ij} values ranged from 3.6% to 10.6%, indicating the error caused by treating wood biomass from all species the same (i.e. using 0.5). Given that measured carbon fraction values for angiosperms average lower carbon fractions than 0.5 (Thomas and Martin 2012b), conifers almost certainly play a more important role in global carbon cycles than global estimates based on the 0.5 value currently suggest.

The difference in carbon mass estimates of tissue types are equally important as different tissues store carbon for variable amounts of time (van Geffen et al. 2010). These different tissue decay rates mean different rates of carbon dioxide release from the separate tissue carbon pools. Correctly estimating these pools is an obvious first step in improving overall understanding of carbon decay dynamics in forests. These differences are also important in tracking carbon mass in timber products.

Comparisons between model complexity levels

The improvement in AIC and the significant difference determined through log-likelihood ratios shown between model 1 and model 2, demonstrates the potential to partially explain the variation in carbon fraction values with easily observed bark characteristics (Table 10). Interestingly, this improvement does not seem to apply to bark carbon, though this is more likely due to smaller sample sizes and high internal variation in bark samples within tree groups (Figure 4). There is no improvement in model performance for either tissue density or carbon density. This is partially due to the high variation found in these two properties between individuals within a species, and within individual trees as shown by the difference in R_c^2 and R_m^2 values in Figure 4.

The lower AIC for the species average carbon density model (CD_{ik}) compared to the species-tissue type model (CD_{ijk}) (Table 10) provides interesting insights into carbon fractions in different tissue types. Tissue types can have different average carbon fractions (Bert and Danjon 2006; Jones and O'Hara 2012), and different average densities (Miles and Smith 2009), so accounting for these known differences in any carbon density model should improve the predictive power of the model. The lack of improvement in AIC is most likely accounted for by the negative interaction between tissue density and carbon fraction demonstrated in Figure 2, along with the greater number of parameters necessary to estimate species-tissue type averages versus species level averages alone.

Carbon fraction modeling

Carbon mass estimates using a value of 0.5 have also assumed that no error is associated with this value. Measured CV_{50} values as high as 17.6% (Table 12) suggest that this assumption is incorrect for whole tree carbon mass, and certainly incorrect as it pertains to tree tissue carbon mass. There is a strong indication that conifer carbon fractions are generally higher than 0.5, and that angiosperms are generally lower than 0.5 (Thomas and Martin 2012b). My data supports this trend as all conifer tissues measured in my study had carbon fractions higher than 0.5. This supports the contention from Jones & O'Hara (2016) that all tissue types should be studied for carbon fraction in order to develop representative biomass weighted tree and forest-level carbon fractions. Failure to do so will result in biased carbon mass estimates for areas that are dominated by either conifers, or angiosperms.

The improvement in carbon fraction estimation by accounting for bark features (Table 10) could be beneficial for carbon estimation in other forest types. In species rich tropical forests

where measuring every species would be impractical, grouping species by easily recorded metrics, such as bark characteristics, could simplify the process of developing improved carbon estimates. Though this study did not measure angiosperms, my findings of significant differences between tissue types is consistent with the findings of studies that have specifically looked at carbon fractions in different angiosperm tissue types (Lamlom and Savidge 2006, Peri et al. 2010, Castaño-Santamaría and Bravo 2012). The majority of carbon fraction studies, however, have not studied tissue types as potential sources of variation (Jones and O'Hara 2016). This is especially true for angiosperm species where sapwood has been the primary tissue type studied (Thomas and Martin 2012b). Given the potential for significantly different carbon fractions between tissue types, it is advisable that both heartwood, and sapwood be studied in developing tree stem carbon fraction values. Doing so could have major consequences for global carbon storage estimates.

The improvement in model fit with increasing carbon fraction model complexity shown in Table 10, demonstrates that accounting only for species average values does not accurately estimate the fractions found within trees, though species-level averages are clearly superior to using a constant value of 0.5. This finding is consistent with other studies that have documented significant variation between sapwood, heartwood, and bark within conifers (Correia et al. 2010; de Aza et al. 2011; Jones and O'Hara 2012). In a review of existing carbon fraction studies, Thomas and Martin (2012b) found only six studies that measured different bole tree tissue carbon fractions and none of those studies looked at carbon fractions as measured by all of the common methodologies. By including multiple carbon fraction methods, my results are more broadly applicable to carbon fraction research as a whole.

The significant improvement in model performance with the addition of the parameter covariate matrix B_lX_l (Table 10, model #4 & #6) indicates the potential to more accurately predict carbon fraction utilizing measureable tree characteristics. My best-fit carbon fraction model (Table 10, model #6), which included the B_lX_l matrix, demonstrates that in addition to tissue type, other tree characteristics contribute to more accurate estimation of carbon fractions. Model #4 did not outperform the more complex models and suggests that significant physiological differences between tissue types are driving the relationship and that these differences are not easily modeled with linear combinations of covariates alone (Table 10).

The negative relationship between CF_{ijk} and the p:RH interaction term (Table 11) has not been identified in previous studies. This term has the potential to shift the mean model estimate by -2.7% to -2.5%, which indicates significant differences in carbon fractions between the top and bottom of the tree. Bert and Danjon (2006) found a quadratic relationship between carbon fraction and relative tree height, but did not use paired carbon fraction and tissue density measures in their analysis. The negative relationship found in my study suggests a reduction in carbon fraction within tissue types with increasing tree height. This negative relationship with height is enhanced for denser tissue samples within a given species-tissue type. Tissue density is often lower above the live crown (Chave et al. 2009), which would lead to a decrease in the negative impact from the p:RH term at heights above the live crown, and an increase in the effect below live crown. The negative correlation between carbon fraction and tissue density is most easily seen in the fibrous, and furrowed bark tree groups in Figure 2, as the carbon and density curves for those groups are nearly mirror images of each other. It is possible that, in isolation, the effect of the p:RH term would be very similar to the quadratic relationship found by Bert and Danjon (2006), as the highest density is found at intermediate RH values for the scaly and furrowed bark tree groups, with relative reductions in density at higher RH values (Figure 2).

The same cannot be said for the fibrous bark group as that group demonstrates the lowest densities at intermediate RH values. The significant improvement in carbon fraction estimation between model #1 and #2 in Table 10, and the lack of overlap in confidence intervals between mean tissue type values in Figure 4, indicates that grouping these trees by bark characteristics could be a reasonable first step in improving carbon fraction estimates.

The negative relationship between tissue density and carbon fraction is an important finding as it suggests a more complex relationship between biomass and carbon mass within conifers than implied by utilization of a constant carbon fraction of 0.5. Two other studies that looked at the interaction between tissue density and carbon fraction found positive relationships in angiosperms (Elias and Potvin 2003, Becker et al. 2012). My finding of the opposite relationship is possibly due to my focus on conifers, though my inclusion of bark samples could also partially explain this relationship. Regardless of the cause, my results indicate that intraspecific carbon fraction and tissue density relationships are far more complex than a static carbon fraction value such as 0.5 would imply. This argument is bolstered by the species-level trends found by Thomas and Malczewski (2007), which showed a positive relationship between wood density and carbon fraction for angiosperms, while conifers displayed the opposite trend. The results of their analysis, however, were not statistically significant.

The positive parameter estimate for the HLC:FHLC term indicates an increased carbon fraction for trees with high HLC values (Table 11). This term has the potential to shift the mean model estimate from 0.02% to 1.4%, depending on the size of the tree and the position relative to the live crown. This increase in carbon fraction is greater for tree tissues located in the live crown. Given this relationship, tall trees with high height to live crowns would be expected to have higher overall average carbon fraction values than short trees with small live crowns. This relationship could indicate the potential for canopy class to influence carbon fractions. Although both suppressed and dominant trees could have similar HLC values in a given stand, only the dominant trees would be expected to have longer live crowns, resulting in higher maximum FHLC values for dominant trees and therefore a larger positive effect of the HLC:FHLC term. The inclusion of this term also partially balances the negative terms in the model.

The negative parameter estimate for the HAR:HLC term indicates a reduction of carbon fraction at the top of the tree, with a rapid weakening of this relationship with increasing distance from the tree top (Table 11). This term has the smallest potential impact ranging between -0.47% to 0%. This is because the HAR term decreases at a faster rate than does distance from the tree top. A rapidly decreasing HAR term and a constant HLC term within a tree results in a stronger negative relationship near the top of trees than exists further down, though with an overall strengthening of the relationship with increasing HLC values. This negative trend toward the top of trees is primarily displayed by the fibrous bark group from an RH value of 0.4 to the tree top, and may act to bring predicted carbon values back toward the mean species-tissue type value (Figure 2).

The mean species-tissue type carbon fraction parameter estimate (CF_{ijk}) of 1.002 (0.002), suggests that observed carbon fractions are evenly distributed around the mean species-tissue type carbon fraction values (Table 11). If the parameter estimate were not equal to one, it could indicate that the variance might be better explained by additional covariates or that the variance was not equally distributed around the mean value.

The modeled relationships were not improved much by accounting for random effects, as shown by the small differences between R_c^2 and R_m^2 values in Figure 4. This indicates that the fixed effects portions of the models, specifically the species-specific tissue type averages, and

the covariate matrix, are accounting for the majority of the variation in the data. This is critical to understanding carbon fractions, because it indicates most of the variation in carbon fraction in conifers can be accounted for simply by calculating species-tissue type averages. This approach may be infeasible in areas with high species diversity, however, in those cases grouping trees by bark characteristics could lead to some improvements in carbon fraction estimation similar to the improvement found between model #1 and #2 (Table 10).

Tissue density

Wood density has been studied for varying purposes for over a century (Stamm 1928, Chave et al. 2005). Appropriate application of this historical data to carbon mass estimation requires understanding the underlying relationships between carbon fraction and tissue density. The lack of improvement in AIC in comparing model #7 with models #8 through #11 (Table 10), indicates that partitioning tree density in species-level, and tissue type-level categories alone does not significantly improve model estimates. However, modeling tissue type averages and additional covariates, model #12, significantly improves model performance over all other models. This means that accounting for changes in tissue density in addition to tissue type averages not only results in a significant difference in log-likelihood ratios, but also improves overall model AIC relative to a means only model.

In this study, the final density model (Table 11) estimates a negative parameter associated with RH, a phenomena that is common among conifers. Interestingly, the model suggests that the higher the average species-tissue type density (D_{ijk}), the more negative the relationship will be. This interaction between RH and D_{ijk} is likely driven by the tree species in the furrowed bark group which show the largest reduction in density with increasing RH values (Figure 2). The potential for this term to influence the mean model estimate is very large, ranging from between -52.4% to -36.5%. This indicates the potential improvement in model fit that could be obtained by accounting for position within the tree.

The reduction in predicted density is partially balanced by the positive parameter estimate for the NLCR:RH interaction term (Table 11). The impact from this term ranges from 32.1% to 53.6%, nearly equal to the negative range of values from the D_{ijk}:RH term. The NLCR:RH term indicates that trees with higher NLCR values demonstrate an increase in density with increasing RH values. This could indicate the more suppressed trees with high NLCR values have higher density near the tree tops than dominant trees. This may be due to slower growth rates altering the percentage of early wood contained within tree rings, which is known to impact wood density (Ikonen et al. 2008), or it could be related to a smaller portion of crown wood found in trees with smaller live crown ratios.

The negative parameter estimate for the RH:R term indicates a reduction in density within a species-tissue type with increasing distance from the pith. This is opposite of the trend observed by Ikonen et al. (2008) in Scots pine (*Pinus sylvestris* L.). The value of this parameter is low, however, the dataset included trees with radii over 230 cm, so some significant reductions in tissue density could occur in much larger trees, such as giant sequoia. Overall the potential impact on the mean model estimate ranges from -23.2% to 0%, which is a smaller range than the other two terms though still significant. The interaction of these positive and negative relationships with RH most likely corresponds to the trends in density values shown in Figure 2.

As with the carbon fraction model the term representing the species-tissue type average values (D_{ijk}) had a parameter estimate statistically indistinguishable from 1 (Table 11). This indicates that the data was fairly evenly distributed around the mean values. The overall fit of the

model to the data was significantly improved with the inclusion of random effects related to individual trees, and cores (Figure 4). This is a result of the large inter- and intra-tree variability in tissue density. Although the addition of the parameter matrix improved the model, the vast improvement in the model fit due to inclusion of random effects clearly demonstrates that the fixed effects are not describing the majority of the variability. This could be remedied by adding variables that account for ring width, proportion of earlywood to latewood, and other tree ring specific variables as those have been shown to be closely correlated with wood density (Peng and Stewart 2013). These ring specific variables are not easily measured, and therefore not very useful in estimating overall tree biomass, or carbon mass without time consuming sampling procedures.

Carbon density

This study is the first to utilize paired density and carbon fraction samples in order to directly analyze the relationship between these two tree properties. The product of these values is carbon density, and, as can be seen in Figure 2, tissue density dominates the resulting relationship. The trend lines in the carbon density graph are somewhat less extreme versions of the corresponding tissue density curves with each carbon density curve remaining closer to the mean species-tissue type value at a given RH value, than either the carbon fraction or tissue density curves. This limited spread around the mean values is due to the negative relationships between carbon fraction and tissue density. The trend in carbon density has the same shape as the density curves and this is due to the much larger variation within density samples compared to the carbon fraction samples. When two values are multiplied together the property with the highest variability should drive the resulting trend.

The positive FHLC term for carbon density appears to be tracking the increase in observed carbon density samples above RH values of approximately 0.55 (Table 11, Figure 2). The potential impact of this term on the mean model value ranges from 1.2% to 38.9%. This term indicates that trees with lower HLC values and long live crowns should have higher carbon density near the top of the tree. This likely reflects the trends in the fibrous and scaly bark tree groups as the furrowed bark group trends toward lower carbon densities near tree tops. This increase is entirely driven by the trends in tissue density values as the carbon fraction values are trending back toward the species-tissue type averages near the tree tops (Figure 2).

The negative parameter estimate for the CD_{ijk}:RH term likely represents the strongly negative trend in the carbon density data for the furrowed bark group with increasing RH values (Table 11). The other tree groups do not demonstrate as consistent a negative trend with increasing RH values. Given that the furrowed bark species tend to have higher tissue density values, the effect of the interaction term is to increase the negative trend with RH for that group relative to the other two groups with lower density values. The potential influence of this term on the overall model mean estimate is between -87.1% to -61.0%, much higher than the comparable term found in the density model.

The LCR:NLCR term, with a simple substitution of (1-LCR) for the NLCR term, is equal to $LCR\text{-}LCR^2$. This term is maximized when LCR is equal to 0.5, with symmetric reductions in value moving away from 0.5. This indicates the importance of live crown in determining overall carbon density, though it, like many of the terms in the carbon density model, appears to be primarily driven by changes in tissue density rather than carbon fraction. The potential impact of this term on mean model estimates is between 22.6% to 30.1%.

The negative parameter for the FHLC:R term indicates a reduction in the effect of positive FHLC term related to samples further from the pith. This reduction is more significant for large diameter trees and would be applicable to each species-tissue type. This effect could partially be driven by the inclusion of large old-growth trees in the study such as giant sequoia and some individual pines. The FHLC:R term is very similar in effect to the RH:R term in the density model and it is this trend in density that is driving the trend in carbon density as the carbon fraction model suggests no significant effect related to distance from pith. The potential impact of this term on the overall mean model estimate is between -21.9% to 0%.

Carbon density is the only modeled tree property with a parameter estimate not equal to one for the species-tissue type average covariate (CD_{ijk}) (Table 11). Both carbon fraction and tissue density have species-tissue type average covariates equal to one, suggesting that the negative correlation between these two values is the likely reason for a parameter estimate different than one for carbon density. Alternatively the model may be skewed by the strong negative relationship between density and relative height found in the upper part of the tree stems. There is a higher concentration of observed values near the base of the tree than at any other point on the tree. This data concentration near the tree base could increase the average values for the species-tissue types, and therefore a reduction in the parameter for the species-tissue type (CD_{ijk}) would be necessary to more closely track the observed values throughout the tree.

The best-fit models for carbon density are less influenced by the addition of random effects than the tissue density models, but more than the carbon fraction models (Figure 4). As carbon density is a combination of tissue density and carbon fraction, it is logical that the high variability displayed by the density samples would be somewhat reduced by the lower residual variance found in the carbon fraction values. It is also likely that the negative correlation between carbon fraction and tissue density are partially responsible for reducing the residual error allocated to the random effects. This finding is promising as the high variability in tissue density creates high variability in any final biomass or carbon mass estimate; however, if that variability can be partially offset by correctly accounting for carbon fraction values then the overall carbon mass estimate would display reduced error relative to biomass estimates. Biomass studies that rely on species average tissue density values rarely ascribe any error to the species tissue density values used. This is problematic as it artificially reduces the true error in the underlying biomass estimate. A similar approach is used in dealing with underlying errors in the carbon fraction value of 0.5, which is assumed to be errorless. The data in my study, and in all other studies of tree tissue carbon fractions have clearly demonstrated that the 0.5 value is far from errorless. Given the importance of forest carbon, it is extremely important that all values involved in deriving carbon mass estimates are correctly assigned any underlying, otherwise statistically meaningful comparisons of mean values cannot be made.

Conclusion

My study demonstrated significant differences in measured carbon fraction values from the widely used value of 0.5, with CV_{50} values as high as 17.6%. These differences in carbon fraction alone resulted in whole tree bole carbon mass estimate increases of up to 10.6% over carbon mass estimates that use 0.5. My study determined that significant improvements in carbon mass estimation in conifer trees are possible by directly accounting for tissue type carbon fraction, and density, as well as measureable tree characteristics related to live crown and

position within the bole. Some improvement in carbon fraction modeling occurred by grouping tree species by visible bark characteristics. The negative relationship between tissue density and carbon fraction determined in this study had not been noted before and is very important in demonstrating why simple approaches to converting biomass into carbon are flawed. It is likely that this relationship would have gone unnoticed with an approach that only analyzed average values of carbon and density rather than paired samples as the variation in density is quite high relative to the variation in carbon, making significant trends between means more difficult to determine. Additionally this relationship suggests that these two key tree properties should be modeled separately in order to improve carbon mass estimates, rather than attempting to directly model the combined property of carbon density.

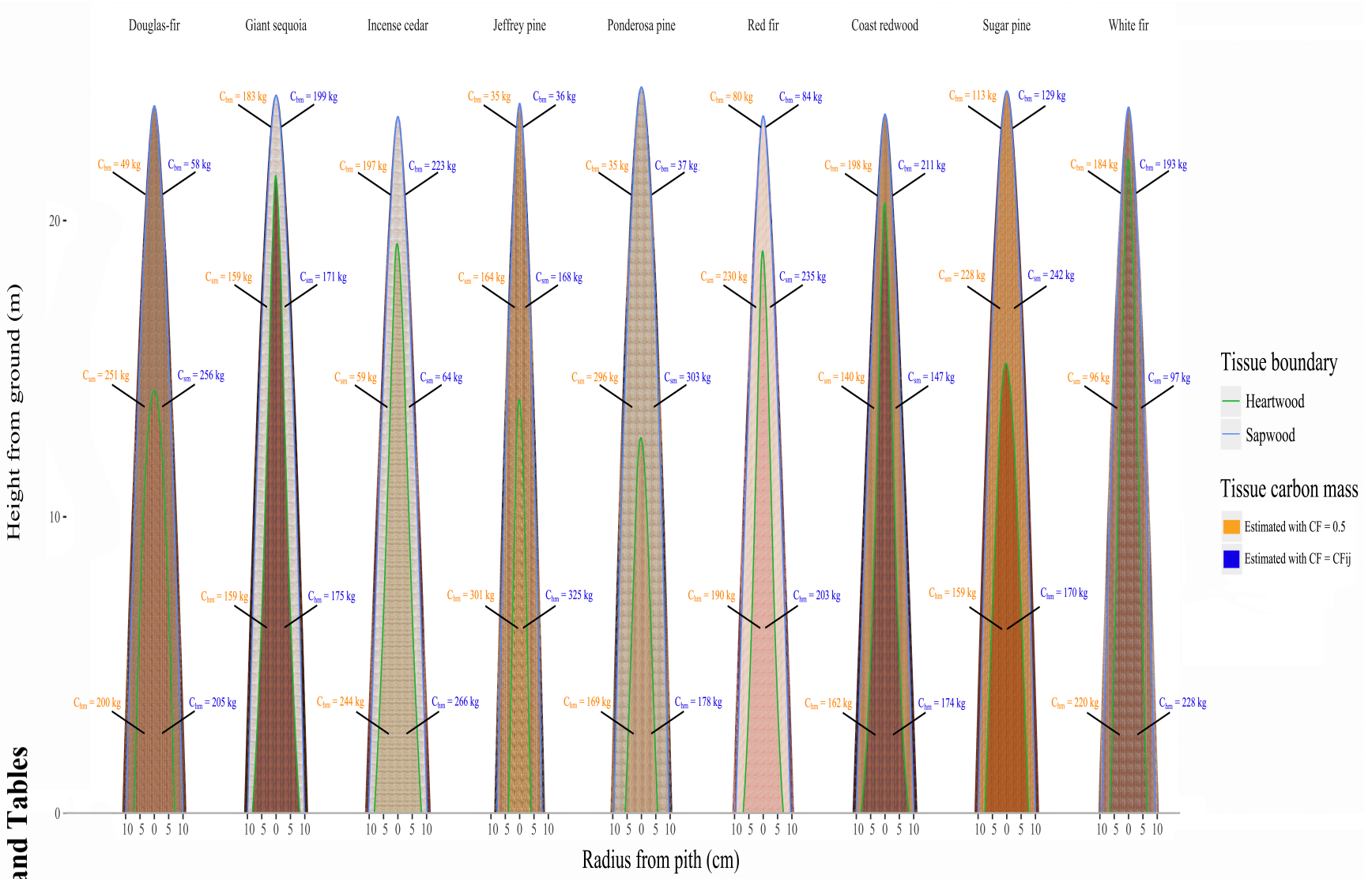

Figure 2. Tissue carbon mass estimates for nine conifer species. Carbon mass estimates using a value of 0.5 are shown in orange, while carbon mass estimates using measured carbon fractions for each species tissue type are shown in blue. Carbon mass for each tissue type is indicated with the following: C_{bm} (bark), C_{sm} (sapwood), C_{hm} (heartwood). Each tree has a total biomass of 1000 kg, including bark. Bole biomass proportions were determined using area weighted biomass proportions of sapwood and heartwood from tree cores.

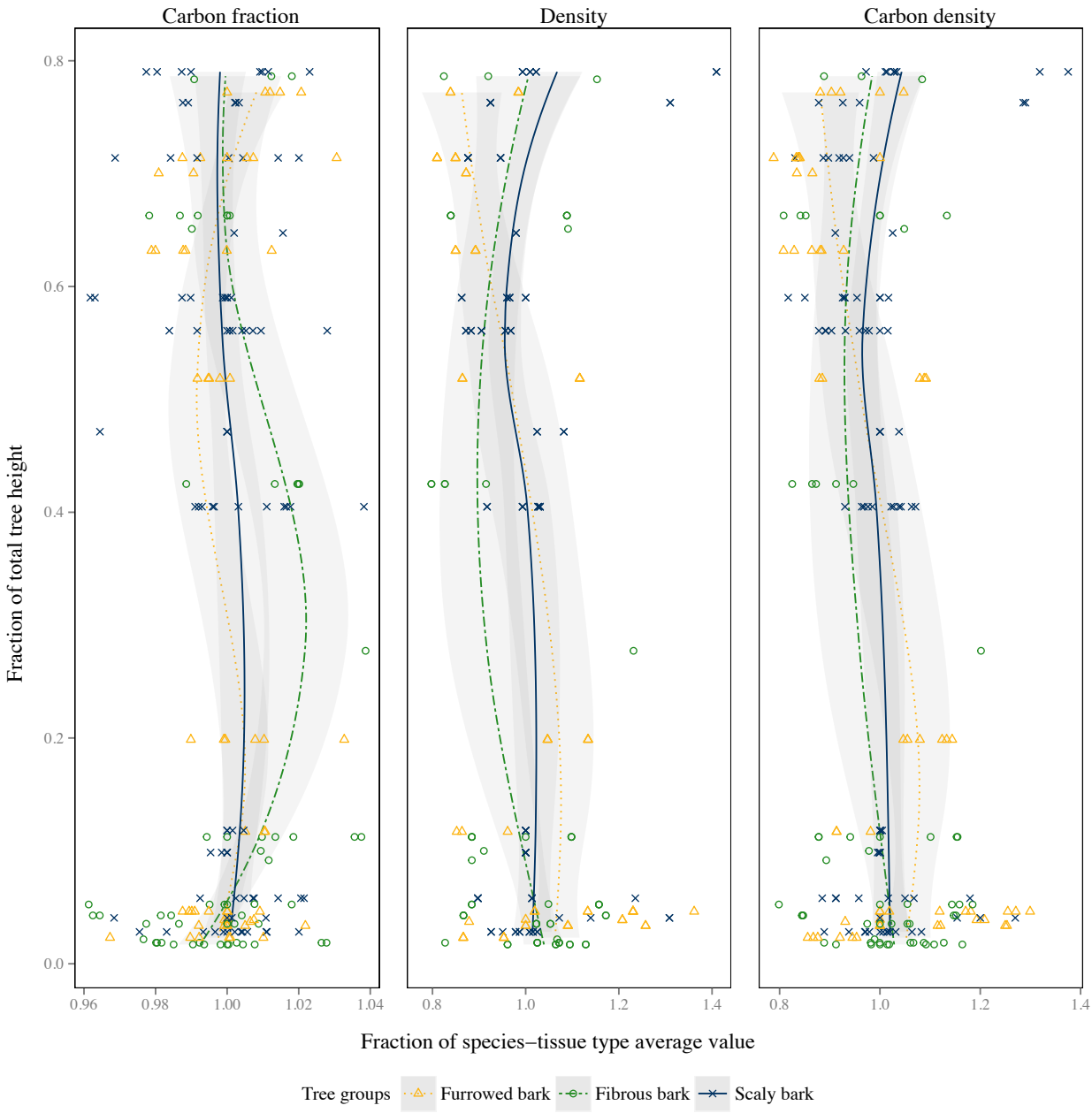

Figure 3. Fractions of species-tissue type averages across relative heights are shown. Species values are grouped into three tree groups based on bark characteristics: fibrous, scaly, and furrowed. LOESS regressions are shown for each tree group to demonstrate the moving average change in tree property throughout the tree bole.

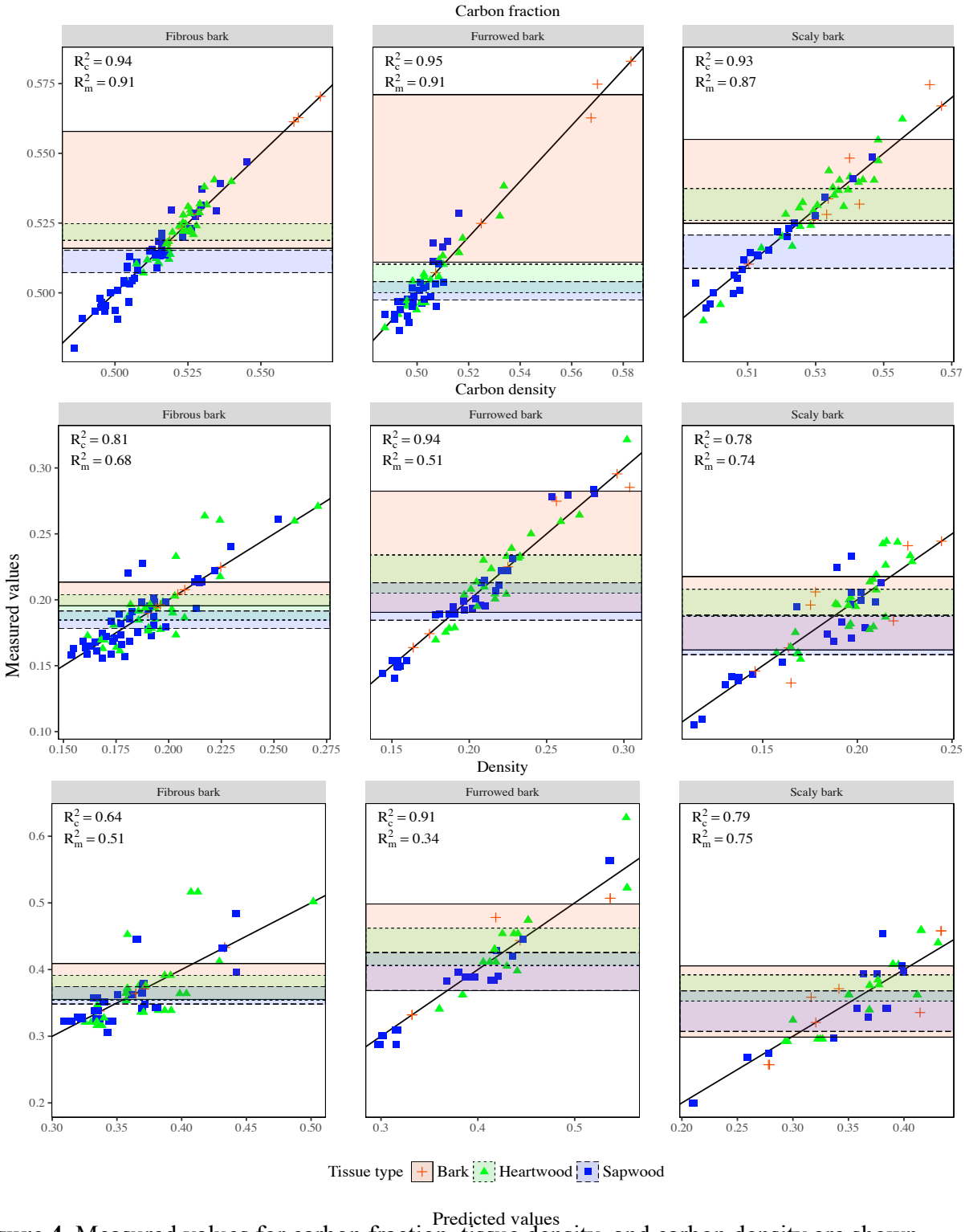

Figure 4. Measured values for carbon fraction, tissue density, and carbon density are shown relative to predicted values. R_c^2 values correspond to the proportion of variance explained by the fixed and random effects in the model, while R_m^2 values correspond to variance explained by the fixed effects alone. Shaded regions represent the 95% confidence interval in measured values for a given tissue type within a particular tree group.

Table 7 Summary statistics for trees used in paired carbon fraction, tissue density, and carbon density analysis. Standard deviations are shown in parenthesis after mean values.

Species	DBH (cm)	HT (m)	HLC (m)	*n*
Douglas-fir	67.1 (41.7)	34.8 (11.6)	13.4 (5.2)	4
Giant sequoia	338.2 (130.1)	72.1 (14.0)	20.9 (5.4)	5
Incense-cedar	39.7 (30.1)	20.9 (8.3)	10.3 (2.7)	6
Jeffrey pine	25.5 (13.6)	10.3 (4.2)	2.0 (1.0)	4
Ponderosa pine	74.6 (40.4)	35.5 (14.3)	11.9 (5.9)	8
Red fir	9.3 (9.5)	5.2 (6.6)	1.2 (0.8)	3
Redwood	68.4 (15.0)	38.2 (4.3)	22.9 (3.3)	5
Sugar pine	162.3 (84.2)	43.9 (12.3)	19.9 (9.8)	3
White fir	81.8 (44.8)	37.7 (13.5)	13.5 (6.2)	9

Table 8 Carbon fraction and density sample number summary by tissue types.

Tissue type	*n* - carbon	*n* - density
Bark	24	14
Sapwood	94	36
Heartwood	85	40

Table 9 Symbols, descriptions, and summary statistics of covariates found in final LME models. Mean values are followed by corresponding standard deviations in parentheses.

Symbol	Covariate descriptions	Mean	Units
CF_{ijk}	Average carbon fraction value for a given species tissue type and method	0.5167 (0.0191)	-
D_{ijk}	Average oven dry tissue density value for a given species tissue type	0.3778 (0.0675)	g/cm^3
CD_{ijk}	Average carbon density value for a given species tissue type and method	0.1950 (0.0348)	g/cm^3
p	Segment dry mass divided by segment green volume	0.378 (0.068)	g/cm^3
RH	Height to core divided by total tree height	0.318 (0.294)	-
HLC	Height to live crown	14.2 (6.6)	m
FHLC	Height to core divided by HLC	0.813 (0.766)	-
HAR	Height to core divided by bole cross sectional area at core height	0.013 (0.016)	m/cm^2
LCR	Length of live crown divided by tree height	0.398 (0.151)	-
NLCR	One minus LCR	0.602 (0.151)	-
R	Radius to center of segment from pith	36.5 (51.0)	cm

Table 10 ANOVA results for comparisons of nested tree property models. All models were regressed using maximum log-likelihood methods. Test column shows model numbers that were compared. *P*-values result from log-likelihood ratio tests for listed comparison.

Covariates	DF	AIC	Model #	Test	*p*-value
CFk	7	-1100.5	1	-	-
CFtk	15	-1106.0	2	1 vs. 2	0.006
CF_{ik}	35	-1111.5	3	2 vs. 3	0.0009
$CF_{ik} + B_lX_l$	38	-1114.7	4	3 vs. 4	0.0269
CF_{ijk}	82	-1284.6	5	4 vs. 5	<.0001
$CF_{ijk}+B_lX_l$	84	-1305.6	6	5 vs. 6	<.0001
Dk	7	-630.3	7	-	-
Dtk	15	-622.6	8	7 vs. 8	0.4089
D_{ik}	35	-608.1	9	8 vs. 9	0.1814
$D_{ik} + B_lX_l$	38	-626.0	10	9 vs. 10	<.0001
D_{ijk}	81	-627.1	11	10 vs. 11	0.0001
$D_{ijk} + B_lX_l$	85	-683.8	12	11 vs. 12	<.0001
CDk	7	-888.3	13	-	-
CDtk	15	-877.9	14	13 vs. 14	0.6874
CD_{ik}	35	-865.5	15	14 vs. 15	0.1204
$CD_{ik} + B_lX_l$	39	-892.6	16	15 vs. 16	<.0001
CD_{ijk}	81	-903.3	17	16 vs. 17	<.0001
$CD_{ijk} + B_lX_l$	85	-935.9	18	17 vs. 18	<.0001

Table 11 Summary of LME model parameter fits from Eq. 4-6. X_l symbol descriptions can be found in Table 9. B_l is the matrix of parameter estimates for the given covariate matrix X_l. *P*-values less than 0.05 indicate that the specified parameter estimate is significantly greater than zero. The upper and lower columns give the result of evaluating a given term at the mean covariate value from Table 9 plus one standard deviation (upper), and minus one standard deviation (lower).

Tissue Property	X_l	B_l	s.e.	*p*-value	FV - upper	FV - lower
Carbon fraction	CF_{ijk}	1.002	0.002	<0.01	-	-
	p:RH	-0.026	0.011	0.02	-0.0270	-0.0250
	HLC:FHLC	2.20E-04	9.52E-05	0.02	0.0140	0.0002
	HAR:HLC	-0.004	0.002	0.04	-0.0047	0
Density	D_{ijk}	1.015	0.016	<0.01	-	-
	D_{ijk}:RH	-0.444	0.109	<0.01	-0.5233	-0.3647
	RH:NLCR	0.269	0.073	<0.01	0.5361	0.3211
	RH:R	-0.001	0	<0.01	-0.2316	0
Carbon density	CD_{ijk}	0.787	0.03	<0.01	-	-
	FHLC	0.048	0.005	<0.01	0.3887	0.0116
	CD_{ijk}:RH	-0.739	0.061	<0.01	-0.8709	-0.6071
	LCR:NLCR	0.237	0.029	<0.01	0.3009	0.2261
	FHLC:R	-3.09E-04	8.84E-05	<0.01	-0.2189	0

Table 12 Mean carbon fraction values, and coefficients of variation relative to an assumed carbon fraction of 0.5, for tissue types within nine conifer species. Standard deviations are shown in parenthesis after the mean carbon fraction, and coefficient of variation values.

Species	Bark CF	Bark - CV_{50}	Heartwood CF	Heartwood - CV_{50}	Sapwood CF	Sapwood - CV_{50}
Douglas-fir	0.588 (0.009)	0.176 (0.018)	0.513 (0.010)	0.026 (0.02)	0.510 (0.009)	0.02 (0.018)
Giant Sequoia	0.544 (0.004)	0.088 (0.008)	0.551 (0.010)	0.102 (0.02)	0.538 (0.010)	0.076 (0.02)
Incense-cedar	0.567 (0.015)	0.134 (0.03)	0.545 (0.009)	0.09 (0.018)	0.541 (0.008)	0.082 (0.016)
Jeffrey pine	0.515 (0.005)	0.03 (0.01)	0.539 (0.004)	0.078 (0.008)	0.513 (0.003)	0.026 (0.006)
Ponderosa pine	0.528 (0.008)	0.056 (0.016)	0.527 (0.008)	0.054 (0.016)	0.512 (0.005)	0.024 (0.01)
Red fir	0.528 (0.011)	0.056 (0.022)	0.533 (0.008)	0.066 (0.016)	0.511 (0.006)	0.022 (0.012)
Redwood	0.531 (0.013)	0.062 (0.026)	0.538 (0.012)	0.076 (0.024)	0.527 (0.007)	0.054 (0.014)
Sugar pine	0.570 (0.010)	0.14 (0.02)	0.534 (0.005)	0.068 (0.01)	0.532 (0.009)	0.064 (0.018)
White fir	0.525 (0.010)	0.05 (0.02)	0.517 (0.004)	0.034 (0.008)	0.507 (0.009)	0.014 (0.018)

3 Biomass and carbon mass prediction models for five conifer species: Integrable biomass and carbon mass prediction models for whole trees and tree portions

Introduction

Accurate forest carbon estimates are an increasingly important part of forest management, and are critical to understanding carbon dynamics within forests. Understanding how carbon is allocated within a forest is important to understanding carbon flux as forest carbon pools have different decay rates (Cousins et al. 2015). Accurate estimates of carbon storage, and fluxes, are critical to the success of forest management plans designed to store and sequester carbon. The total carbon flux from management activities, or natural disturbances, will be directly related to the total carbon stored on a given site, and directly influenced by how that carbon is distributed within the area (Hoover and Stout 2007). Accurate estimates of carbon emissions, or net sequestration rates require accurate estimates of the total amount of carbon stored in the carbon pools present within a given forest.

Current carbon mass estimation protocols utilized in forest management rely primarily on approaches that convert volume estimates to biomass using species average wood density estimates, and a universal carbon fraction conversion ratio of 0.5 (e.g. Woodall et al. 2010). The 0.5 value is likely taken from research devoted to global estimates of carbon mass which suggest a global average around 0.5, though there is no clear indication that this value was ever validated, even at a global scale (Lamlom and Savidge 2003). This 0.5 carbon conversion factor, or carbon fraction, is commonly used in studies that estimate total forest carbon at smaller scales as well (Cohen et al. 1996, Goodale et al. 2002, Chave et al. 2005, Woodbury et al. 2007, Fahey et al. 2009). Carbon fractions have been shown to vary significantly between tree species, and within individual trees (Lamlom and Savidge 2003, 2006, Jones and O'Hara 2012, 2016, Thomas and Martin 2012b). Accounting for these known sources of variation would therefore significantly improve the accuracy of carbon mass estimates of trees and forests.

In addition to improving carbon mass estimates by accounting for variation in tissue carbon fractions, there can be significant improvements in living carbon mass estimates by using the correct methods. The majority of measured carbon fractions likely underestimate the carbon fractions of living tissues by failing to capture some of the volatile carbon present (Jones and O'Hara 2016). The high variability in volatile carbon fractions within tree tissues suggests that accurate carbon mass estimates for the whole tree, and for separate tree tissue types, requires correctly measuring living carbon fractions, and applying those fractions to their respective tissue type biomasses.

Biomass models using species average wood density values are used for several species across many regions (Woodall et al. 2010). The application of these models is most accurate for biomass estimates across an entire species range, or over an entire region, as local wood density averages vary significantly from species wide averages (Chave et al. 2009, Jones and O'Hara 2012). Wood density is also known to vary within tree boles (Rueda and Williamson 1992, Woodcock and Shier 2002, Ver Planck and MacFarlane 2014), across tree ring ages and growth rates (Langum et al. 2009), and therefore biomass estimates would be expected to be more accurate when this variation is accounted for in a given biomass model.

The significant deviations in wood density from the species average, and carbon fractions from the 0.5 value, can result in underestimates of carbon mass of as much as 16% in coast redwood (*Sequoia sempervirens* (D Don) Endl.) tree boles, and likely result in similar inaccuracies in other tree species (Jones and O'Hara 2012). These inaccuracies could be addressed by accounting for changes in wood density and carbon fraction related to easily measured tree characteristics (Jones and O'Hara 2012, 2016). Developing carbon prediction models that account for variation in wood density and carbon fraction utilizing tree characteristics commonly collected for forest inventories would be a significant step in improving carbon mass estimates.

Although whole tree biomass equations have been developed for several species (Chojnacky et al. 2014), there are no carbon mass prediction equations that have been developed to accurately capture the known variation in carbon fraction within trees, and between tree components. In order to improve carbon mass estimation in forests it is therefore necessary to develop a model that accurately accounts for the variation in wood density and carbon fraction that occurs between tree species and within individual trees. Converting existing biomass models to carbon models with an appropriately weighted carbon fraction could achieve this result; however, this approach risks ignoring potential covariance between carbon fraction and wood density that could best be addressed by analyzing carbon mass variation directly.

Biomass models exist that can predict biomass distributions (Parresol and Thomas 1989, Jordan et al. 2006, Zakrzewski and Duchesne 2012), and whole tree biomass (Ver Planck and MacFarlane 2014). These models have the advantage of allowing biomass estimates for standing trees and harvested logs, which could result in more accurate biomass accounting than is possible with whole tree biomass models alone. Although carbon is often assumed to be a fixed portion of biomass, the variation in carbon fraction between tree tissues suggests that a better approach to carbon mass estimates would be a biomass weighted carbon fraction that accounts for these known sources of variation. A model that accounts for this variation, and allows for easier tracking of carbon mass between harvests would be a valuable tool in the complex field of carbon accounting.

Branch and bark biomass have not been studied to the same degree as bole biomass, but are strongly correlated with bole biomass (Chojnacky et al. 2014). Bark and branch carbon masses are probably correlated with bole carbon masses; however, accounting for carbon fraction of tissues is necessary to determine exactly what that correlation might be (Elias and Potvin 2003, de Aza et al. 2011, Jones and O'Hara 2016).

This paper addresses these issues by developing integrable biomass and carbon mass models that directly account for variation in carbon fraction and wood density throughout sampled conifer trees. I present biomass, live carbon, and oven-dry carbon mass prediction models that can be used to determine the mass of above ground carbon contained in a forest stand, individual trees, whole logs, foliage, branches, and bark.

Specifically I set out these objectives:

1. Develop biomass, and carbon mass area density (g/cm^2) prediction models from tree bole core segments taken from multiple locations along tree boles;
2. Develop an integrable linear density (g/cm) taper function using the values from integrated biomass and carbon mass area density models;
3. Validate the predictions from the integrated linear density models with data from oven-dried tree discs taken from independent sample trees;

4. Analyze bark and bole relationships among the tree discs to determine bark mass fraction relative to bole mass;
5. Develop leaf mass, and leaf carbon mass prediction models for individual branches, and for the entire tree;
6. Develop branch mass, and carbon mass, prediction models for individual branches, and for the entire tree; and
7. Determine the deviation in mass proportions, and total masses between prediction models developed in this study, and estimates from commonly used "standard" approaches.

Methods and materials

Plot locations

Five conifer tree species were sampled: sugar pine (*Pinus lambertiana* Dougl.), ponderosa pine (*P. ponderosa* Lawson & C. Lawson), coast Douglas-fir (*Pseudotsuga menziesii* (Mirb.) Franco var. *menziesii*), white fir (*Abies concolor* (Gord. & Glend.) Lindl. ex Hildebr.), and incense-cedar (*Calocedrus decurrens* (Torr.) Florin). Trees were sampled at the following locations: 1) Baker Forest (39.916 N, 121.063 W), 2) Blodgett Research Forest Station (38.910 N, 120.662 W), and 3) near Shaver Lake, CA (37.046 N, 119.211 W). Table 13 shows summary statistics for sample trees, along with sample locations for each species.

Tissue sample collection and processing

Sample cores were taken from different heights within randomly sampled trees from each site listed in Table 13. At each core extraction point, height of extraction, tree bole diameter and bark thickness were recorded. Sample trees were selected only if they could be safely climbed, or cut down and cored. Cores were taken at breast height (1.37 m), base of live crown (HLC), and every 4 m within the live crown for each tree sampled. A 400 mm long Haglöf increment borer, with an aperture of 5.15 mm, was used to extract all cores. After extraction cores were placed in clear plastic straws, sealed using adhesive tape, labeled, and placed in a white plastic tube. Core sapwood was determined by holding the straw up to the sun and marking translucent section of the core on the outside of the straw. Cores were placed in a cooler with ice and transported back to the lab. In the lab, cores were placed in the freezer, which was maintained between -24 and -18 ºC. A total of 276 cores, from 86 trees were processed for wood density data. Wood density cores were separated into the bark portion of the core, and core segments containing 4 growth rings until the entire core was processed. In some cases the innermost core segment contained fewer than 4 growth rings, in these cases the segments lengths were measured and the number of rings recorded. A total of 41 cores were processed for carbon fractions. These cores were separated into tissue types for carbon fraction analysis. A more complete description of this process can be found in Jones and O'Hara (2016).

Branch and foliage sampling

Within each sample tree crown, two branches were randomly selected from each third of the crown, for a total of 6 branches per sample tree. Branch diameter was measured above the branch collar using calipers with a precision of 0.5 mm on the major and minor axis, along with height of branch from the ground to the nearest cm. Foliage was separated from the branch in the field and branches were cut up and placed in bags for processing back in the lab. In the lab branches

were placed in paper bags, labeled and oven dried at 103 ºC until weights stabilized, at which point their weights were recorded. Branch carbon mass was determined by multiplying total branch biomass by the biomass weighted average bole plus bark carbon fractions.

Proportional foliage subsamples were collected from each needle age class on sample branches and placed in a small plastic resealable bag and labeled with tree ID and sample branch number. Foliage sample bags were placed on ice in the field, and placed in a freezer once taken back to the lab. Foliage was weighed in the lab after drying in a force air oven at 101 ºC for 24 hours. A more detailed review of the leaf sampling can be found in Jones et al. (2015). Twelve foliage samples were randomly selected for carbon fraction analysis from 8 different trees, representing five tree species.

Core segment density and carbon density

Wood density core segments were measured for length using digital calipers with a precision of 0.001 cm. The volume of each segment was calculated by multiplying segment length by the area of the increment borer aperture (0.832 cm^2). Wood density segments were then wrapped in aluminum foil labeled with unique core ID, segment ring numbers, and oven-dried at 103 ºC until weights stabilized. Stable mass of the density segments was recorded and divided by the core segment volume resulting in core segment density (D) values in g/cm^3.

This study uses carbon fractions (CF) measured by oven-dry methods and the MLC method described by Jones and O'Hara (2016). Mean carbon fraction values are given for each species tissue type in Table 14. Carbon mass for each carbon sample was determined using a CE Instruments Flash 2000 CHNS/O analyzer, which was calibrated between runs of 40 samples using acetanilide as the standard. Standards were also placed every tenth sample to insure calibration accuracy. Carbon mass was divided by oven dry sample mass to adjust all carbon fractions to the same baseline moisture content. This process resulted in carbon fractions for living tissues and oven-dry tissues as shown in Table 14. Carbon fractions, for each species wood type, were multiplied by individual segment densities to yield carbon densities (CD) in units of grams carbon/cm^3 for each segment.

Area density

Area density in this study is an estimate of mass per unit area in g/cm^2. Modeling area density is advantageous in that the model can capture the density variation between core segments. This area density model can be integrated to yield the average mass per unit tree height represented by each tree core. This approach allows for filling in data for missing portions of tree cores. Representative area density (g/cm^2), and area carbon density (g carbon/cm^2) values were calculated by multiplying the segment density, or carbon density value, by the representative circumference at the midpoint of each segment. Representative radii were calculated when the measured core length, minus the bark portion, was greater than the measured inside bark radius of the bole at the point of core extraction. Measured segment lengths were multiplied by the inside bark bole radius and divided by the measured core length. These converted segment lengths were then used to determine representative radii, which were the distance from tree center to the center of the segment's converted length. In cases where the measured core length was less than half the measured inside bark diameter, there were no adjustments made on the measured lengths of core segment as these cases were due to the increment borer not reaching the center of the bole. Core segment area density is equivalent to the mass of a wooden ring that is 1 cm tall, 1 cm thick, with a radius equal to the radius from the pith to the center of the core

segment, and a density equal to the core segment density. Effectively this means that area density is composed of a deterministic geometric component ($2*\pi*r$) and a highly variable core segment density component. To differentiate between the explanatory power of the geometric and density components, a model of the form $\alpha*2*\pi*r$, where α is a species average density, was fit to the area density data. This model is equivalent to accounting only for the geometry of the relationship and allowing the model to choose an average density value for each species. If species level variation in density were negligible this geometry driven model would perform as well as models that allow density to vary between core segments.

Linear density (g/cm) for the intact portion of the cores was calculated as the sum of core segment area densities. Representative segment areas were determined as the difference between the bole area represented by the outside of the core segment minus the bole area represented by the inside of the core segment. This linear density is best understood as representing the mass of a tree bole disc that is 1 cm high with a density equal to the area weighted densities of the tree core segments. To differentiate between the explanatory power of the geometric and density components, a model of the form $\alpha*\pi*IBR^2$, where IBR is inside bark bole radius and α is a species average density, was fit to the linear density data. This is equivalent to the cross sectional area of the tree bole at a given height times a species average density. If species level variation in density were negligible, the geometry driven model would be expected to perform as well as models that allow density to vary.

Disc biomass and carbon mass

Table 13 shows the summary statistics for trees that were used to validate the predictive models developed from core data. Each tree had discs removed from 0.3 m, 1.37 m, halfway between 1.37 m and live crown, live crown, and every two meters within the live crown. A chainsaw was used to cut the tree discs from the tree bole. Each disc was labeled with a unique tree ID, and disc height. Discs were placed in labeled paper bags with bark attached, and sealed with adhesive tape. In the lab, discs were measured for disc thickness using digital calipers at four locations on the disc, starting with the tallest portion of the disc, and every 90 º around the disc until four measurements had been taken. Average disc thickness was calculated as the average of these measurements. Average disc thickness was used to determine the height of the bottom and top of the tree disk from the ground prior to the tree being cut down. Once measured, discs with bark still attached were placed back into labeled paper bags and placed in an oven set to 103 ºC, and dried until weight stabilized. Total disc masses were recorded using an Ohaus Analytical Plus balance (model AP310), with bark masses determined by subtracting the mass of the disk with bark removed from the total disc mass.

Tree discs were photographed in the field with a ruler placed on them for size reference. These photographs were used to determine the ratio of heartwood to sapwood present in the tree discs. Disc carbon mass was calculated by multiplying disc biomass by the weighted carbon fraction determined by the ratio of heartwood to sapwood area. This calculation was performed for both living carbon and oven-dry carbon estimates.

Statistical analysis

All analyses were performed using the NLME package (version 3.1-118) (Pinheiro et al. 2015), in the R statistical platform (R Development Core Team 2015). Where necessary, different variance structures were tested until normality of residuals and random effects was achieved. As part of the NLME modeling process additional covariates were added to model parameters to test

for improved model fit. All covariates that are used in the final models, along with their descriptions can be found in Table 15.

Core area density and area carbon density were modeled using non-linear mixed effects (LME) models (Pinheiro et al. 2015). Table 16 shows the model forms that were evaluated for fit to area density. The overall best model was determined by log-likelihood ratio testing of models fit using maximum log-likelihood approaches (Pinheiro et al. 2015). Final model parameters were estimated using reduced log-likelihood regression. Random effects were assigned to cores nested within trees for models 19-24 in Table 16. For models 28 and 31 random effects were assigned at the individual tree level. For all mixed effects models additional covariates were tested in order to see if their inclusion explained a significant portion of the random effects associated with each parameter. If random effects for any parameter were not significantly different from zero they were dropped. Random effects were assigned to each level of the data structure using a compound symmetric correlation matrix.

To estimate the missing portion of linear density in cores that did not reach the pith, the best-fit model for area density was integrated from zero to the radius of the missing portion of the core. This value was added to the sum of representative linear densities for the rest of the core resulting in total core linear density.

Linear density was modeled throughout the tree bole using a taper function, that was originally developed for radial taper of the species in this study (Biging 1984). The model form has logical assumptions that apply equally well to linear density as they do to tree radial profiles. Those assumptions are that the taper at the base of a tree may be different than it is at the top of a tree, that the base of the tree has the largest value and values are progressively lower at every point above the base, and that any values above the top of the tree should be equal to zero. The model form was fit to the linear density data without the addition of any other covariates so as to insure logical consistency across the three modeled tree characteristics. This was also done to create a simpler integrated model form that would more easily be incorporate into existing estimation procedures for whole tree bole biomass, and carbon mass.

Bark mass was modeled as a fraction of inside bark disc mass using linear regression and data from tree discs. Foliar mass and branch mass were modeled at the individual branch level by fitting the respective models in Table 16 to the data. These individual branch models were then applied to trees in which all branches had been measured for branch height along bole, and branch diameter. The resulting branch and foliage masses were summed for the whole tree. These whole tree masses were used to model whole tree foliage and branch masses by fitting the appropriate models from Table 16 to the whole tree data.

For the best fit model of area density, individual branch, and foliage branch mass, conditional (R_c^2) and marginal (R_m^2) values were calculated following the procedures in Nakagawa and Schielzeth (2013). R_c^2 values represent the portion of variance explained by the entire model including random effects, while the R_m^2 values represent the proportion of variance explained by the modeled fixed effects only. Standard errors are presented in parenthesis following all mean values with the exception of Table 13 and 14, where standard deviations are shown in parenthesis.

Biomass and carbon mass estimation comparisons

To demonstrate differences in mass proportions, and total tissue masses, the final biomass models for foliage, branch, bark, and bole tissues were compared to models using a “standard” approach to biomass and carbon mass estimation (Woodall et al. 2010). It was assumed that

biomass estimates would differ from the models developed in this study when compared to models developed for entire species ranges, therefore, all example trees were set to a total biomass of 1000 kg. For the "standard" estimation approach branch, bole, and bark models from (Woodall et al. 2010) were used as these models are well established in carbon accounting protocols, and can predict most of the tissue types presented in this paper. Foliar mass was calculated separately using models from Chojnacky et al. (2014). To ensure representative tree dimensions, the average height:diameter ratio for the trees in this study was used to confine example tree heights to a proportion of a given diameter. Tree diameter was then set for each species so that the total estimated mass of the each example tree was equal to 1000 kg. To obtain heartwood and sapwood mass values the average heartwood to inside bark area density ratio was determined from tree cores, and applied to the total bole wood mass estimate. Sapwood mass was determined by subtracting heartwood mass from bole mass.

Results

Area density

Goodness of fit metrics for models with no additional covariates added, and goodness of fit metrics for the final best-fit model with additional covariates are shown in Table 17. Model 23 performed better than all of the other models measured by AIC, BIC and log-liklihood. R^2 values were better for all other models with the exception of the geometry driven model which had a lower R^2 value than all other models. The final parameter estimates for model 23, including any associated additional covariates, are listed in Table 18 for each species and each type of area density. Live crown ratio (LCR), and height to live crown divided by diameter at breast height (HLDR), both significantly improved the overall model fits as demonstrated by the significant improvement in model AIC (Table 18). Different covariates were tested for biomass and carbon mass area densities. Variation in covariates used across area density models led to illogical predictions of average core carbon fractions so all models were set to the same model form based on the best-fit biomass area density model. Random effects for parameter α were significant at the core within tree level, while parameter β and θ had no significant random effects. The random effects had a mean of 0 with the standard deviations listed in Table 18.

Figure 5 shows the fit of the observed versus predicted area density values for biomass, oven-dry carbon mass, and living carbon mass models. Models with random effects included performed very well with R^2_c values equal to or very close to 1 for the biomass, oven-dry carbon, and living carbon area density models. The closeness of the data points around the one to one line indicates that the chosen model form captured the radial variation in area density. The even distribution around the one to one line in Figure 5 indicates that the models account for radial and horizontal variation throughout a wide range of area density values.

Linear density

The mass taper model (model 26) performed better than the geometry driven model by all metrics listed in Table 17. The integrated form of model 23 with respect to representative core radius was used to predict the missing portion of core linear density in cases where the increment borer could not reach the pith. Random effects estimates for individual tree and cores were included in this prediction model to get values that were fit to each core and tree. As all other covariates in model 23 are constant relative to core radius, the integrated form of model 23 is

obtained by replacing the r covariate with ½ r^2, where r is the representative radius to a point in the core. The constant of integration was set to zero as there cannot be any linear density when the radius is equal to zero. The parameter estimates remain unchanged for the integrated form of the model. The mean and standard deviation for the percent of linear density in the missing portion of all cores was 3.7 (7.9)%. Given the importance of including large trees in the data set it was deemed necessary to estimate the missing portion of linear density even though it made up a small portion of the overall dataset.

Disc mass predictions

The parameter estimates for model 26 fit to the linear density data from cores are shown in Table 19. Figure 6 shows the predictions from fitting model 26 to the linear density data derived from cores versus observed values. The overall fit of the model was very good with measured R^2 values in the range of 0.94 to 0.99. The fit of the model was impressive given the range of area densities, and tree sizes covered by the core data. The majority of species demonstrated an even spread around the one to one line in Figure 6 indicating the models account for the variation in the data across the range of predicted values. There does appear to be a slight deviation from the one to one line in the incense-cedar data near the middle of the data range. This slight deviation could potentially have been addressed by the addition of covariates in either the α or β parameter. This deviation, however, does not appear to impact the predicted disc mass values shown in Figure 7.

The predicted disc mass estimates were derived through numerical integration of model 26, using parameters from Table 19. The integration range was from the height above the ground from the bottom of the individual tree discs, to the top of the discs. The fit of the data shown in Figure 7 is very good, with the lowest R^2 value being 0.98. There is divergence from a one to one relationship with slopes between 1.02 to 1.32, indicating that the inside bark mass predictions based on core data tend to underestimate the mass of the tree discs. This underestimate appears to be systematic as a simple adjustment in slope is all that is necessary to create a smooth fit of the data around the regression line.

Bark mass as a function of inside disc mass relationships for biomass, oven-dry carbon, and living carbon are shown in Figure 8. The data appears to be well-modeled using a linear fit of bark mass against inside bark mass of the individual tree discs. There is no apparent departure from the linear relationship along the spread of the data. The lowest R^2 was 0.96. The slope of this relationship can be used to turn inside bark mass estimates into total mass estimates by adding the slope value to 1 and multiplying the resulting value by the corresponding inside bark mass estimates. As the relationship appears to hold for a range of masses this process should work for whole tree bole mass estimates as well.

Branch and foliage mass

Parameter estimates for the individual, and tree total branch mass data fit to models 28 and 29 are shown in Table 20. Branch mass predictions versus measurements are shown in Figure 9, and total branch mass predictions versus total tree branch mass estimates are shown in Figure 10. The random effects significantly improved the model fit for the individual branch mass models indicating that individual trees demonstrate significant differences in the modeled branch mass relationships. For tree total branch mass modeling, shown in Figure 10, the random effects did not improve the fit of the models as demonstrated by the R_m^2 and R_c^2 values being equal.

The addition of relative height (RH) to the parameters in the individual branch models improved the overall fit, indicating that branch position influences mass predictions in addition to branch cross sectional area. The influence of these additional covariates was significantly different between species. The RH parameter estimates significantly varied by species (Table 20). Total tree branch mass models were significantly improved with the addition of live crown ratio (LCR), and height to the base of live crown (HLC) to the model parameters as reported in Table 20. The model fits were improved by allowing parameter estimates for the HLC covariate to vary for each species, while leaving all other parameters fixed within a given mass type estimate.

Individual branch and total tree foliage mass model parameters are given in Table 21. The R_c^2 values are higher than the R_m^2 values for individual branch foliage models indicating an improvement in model fit with random effects included (Figure 11). The tree total foliage mass models were not improved by including random effects as shown by the equal R_c^2 and R_m^2 values in Figure 12.

The addition of RH, and RDC covariates to the individual branch foliage mass models significantly improved model fit. Allowing some parameter estimates to vary across species significantly improved the model fit. For tree total foliage mass estimates only the addition of LCR to the β parameter significantly improved model performance. Allowing the estimates for the intercepts of the β, and θ parameters to vary across species significantly improved the model fit.

Biomass and carbon mass estimation comparisons

Mass proportions, total tissue masses, and tree total masses for example trees representing each of the mixed conifer species are presented in Figure 13. The left half of the tree represents masses estimated for each tissue type using standard approaches, which includes using a carbon fraction of 0.5 for all tissue types, while the right half of the trees represent mass estimates based on the models and values from this study. Areas in the trees are proportional to the mass of the tissue type represented. Total tissue type mass is shown in the box next to each tissue type. For all species the standard approaches resulted in a greater proportion of mass allocated to branches, this can be seen by comparing the areas for branch mass between the left and right sides of each tree. Foliar mass estimates were fairly similar between the two approaches, while a greater proportion of mass was found in the boles of the example trees for this study. Bark mass estimates were the most variable between estimation approaches, with the standard approach sometimes predicting a higher mass proportion and sometimes a lower mass proportion for bark.

Tree carbon mass estimates for all of the standard approach trees are 500 kg, due to the application of a carbon fraction of 0.5. Oven-dried carbon tree masses ranged from 492 kg to 529 kg, while living carbon tree masses ranged from 514 kg to 545 kg (Figure 13).

Discussion

Area density

The distribution of area density values around the one to one line indicates that the high variability in wood, and carbon densities is well modeled. The random effects at the core within tree-level improved the fit of the data, and allowed for adjustments to the model fit for each core. This makes the predictive power of the model very high for each core. This approach would not

be advisable if the predictions were to be applied outside of the dataset, but this approach is excellent for predicting missing portions of cores within the dataset. The capture of variation in density is demonstrated by the significantly better AIC value in model 23 compared to the geometry driven model. Interestingly the R^2 metric points in the other direction, though this more likely indicates that the larger data points are over represented in the geometry driven model, while AIC is less biased toward large data values. A similar approach to modeling wood density variation within boles was used by Ver Planck and MacFarlane (2014), except they used tree discs to develop average density values and then multiplied these values by a taper model with an assumed bole shape. My study does not rely on any assumptions about the tree bole shape, instead I fit the model directly to the linear density data. This approach allows the model to account for any correlation that might exist between linear density and bole geometry. If density and bole geometry are modeled separately then any potential correlation might not be accounted for. An additional advantage to my approach is that it is possible to directly model heartwood mass, and sapwood mass as separate tree components. Without measuring those tissue types separately that would not be possible, and when entire tree disks are used there is no clear way to separate those two tissue components.

Linear density

The superior performance of model 26 compared to the geometry driven model 27 (Table 17) demonstrates the significant improvement in model performance due to accounting for variation in density. By fitting model 26 to the linear density data, I have developed the first set of vertically integrable tree bole biomass and carbon mass prediction equations. Though other integrable biomass functions exist (Zakrzewski and Duchesne 2012, Ver Planck and MacFarlane 2014), there are no carbon prediction models that account for the variation in carbon mass due to the proportion of wood types, integrable or otherwise. Accounting for the differences in carbon fraction shown in Table 14, is critical to creating accurate carbon mass predictions.

The models developed here produce carbon mass predictions that account for the biomass proportions of sapwood, and heartwood in tree boles and bole portions. Predicting carbon mass in portions of trees is required to correctly account for carbon flow out of tree stands during timber harvesting operations, where portions of trees such as branches and tree tops may be left on site. Using the models presented here, tracking carbon in the living stand, and in the portions of the stand that are removed could be done with stand inventory and harvested data alone; this cannot be said for biomass and carbon mass models that only predict entire tree, or bole masses.

Similar approaches have been used for biomass models, but no model has been specifically designed to account for the balance of wood types, or to incorporate accurately measured carbon fraction values. The mass models presented here are also easily modified to include bark carbon mass. Bark inclusive linear density is obtained through multiplying the linear density estimates by one plus the respective slope parameters shown in Figure 8. This allows for tracking biomass and carbon mass for each portion of the bole. Given that different bole tissue types decay at different rates (Cousins et al. 2015), it would be advantageous to be able to accurately estimate the portions of the bole in the main stem and bark that are left behind after site disturbances.

My models predict three types of mass: biomass, oven-dry carbon mass, and living carbon mass. This is a unique contribution of this work as the most commonly measured tree tissue oven-dry carbon fractions are not representative of living carbon, due to the loss of volatile carbon compounds during oven-drying (Jones and O'Hara 2016). This makes my carbon models

more accurate for two reasons: 1) they explicitly account for variation in carbon fractions between species, and 2) they further account for variation in carbon fraction between tissue types. The majority of carbon fraction estimation methods rely on simplified conversions of biomass to carbon mass utilizing a carbon fraction of 0.5 for all tree species and tissue types. My study directly accounts for both of these sources of carbon fraction variation. Using the models presented here it is a simple matter to derive whole tree, biomass weighted carbon fractions by dividing either of the carbon mass models for a particular tree tissue by the respective biomass model, for a given tree. The resulting biomass carbon fractions could then be used to convert biomass estimates derived from existing biomass models for the respective species to carbon mass estimates that are more accurate than using a value of 0.5.

Disc mass predictions

There are several sources of potential error in my approach to developing the linear density estimates from cores. The primary concern is that cores are not necessarily representative of the density measured in discs (Williamson and Wiemann 2010). That is why calibrating the model with data from tree discs taken along the tree bole is necessary. From the slopes shown in Figure 7, which range from 1.02 to 1.32, it is clear that the predictions from cores consistently underestimated the disc mass values. This implies that the core samples expanded radially after extraction from the tree. There may have been compression of the cores perpendicularly to the core length, but this would not have made a difference as my density estimates used the measured aperture for the increment borer rather than relying on direct measurements of the core diameter.

The quality of the adjusted prediction values demonstrates the viability of this approach in developing accurate prediction models. Additionally, by calibrating my models this way, I have demonstrated that the models I developed can accurately represent the variation contained within trees. There was no increase or decrease in model predictive power along the range of disc masses, indicating that the models worked well for the entire tree bole. I included stump height discs in the prediction calibration to make sure the models were correctly accounting for the rapid increase in linear density that is expected to occur at the base of trees. From the fit of the data, the models are accounting for the rapid increase in linear density at the stump, indicating that these models most likely are capable of estimating stump biomass in addition to the rest of the bole.

Branch and foliage mass

The tree total branch mass, and foliage mass models were the least accurate with respect to the tree total mass predictive value. This is somewhat expected as tree crowns can be highly variable, and my random sampling approach allowed for the possibility of small internode branches being measured throughout the crown. The predictions are still reasonably good with the lowest R^2 of 0.60 (Figure 10), and an R^2 of 0.88 (Figure 12) for ponderosa pine branch and foliage mass estimates respectively. Given that these two tree features tend to be smaller percentages of the total tree biomass, higher inaccuracies in these models do not necessarily lead to a significant impact on total tree biomass and carbon mass estimates.

Tree total branch biomass has not been studied as thoroughly as bole biomass. Studies that modeled branch biomass have used a similar model form as model 29 (Jenkins et al. 2003, Chojnacky et al. 2014). My study allowed for modifications of this base model with the addition of covariates to the model parameters. For the species studied here, the addition of height to base

of live crown (HLC) to the exponential component of the model improved overall model fit. This intuitively makes sense as total branch biomass should increase with tree size, and larger trees tend to have higher HLC values. The improvement in model fit with the addition of live crown ratio (LCR) also makes sense as trees with high LCR ratios, and high HLC values would have long live crowns. The improvement in model fit with the addition of LCR could also imply variable responses to wind force on crowns as high LCR is expected to increase wind stress on a tree.

Variations in mass proportion and total mass

There are considerable deviations in biomass proportions between my models and estimates from more standard approaches (Figure 13). This can be seen by comparing the two sides of each example tree, and keeping in mind that each half represents a tree with total mass of 1000 kg. My study found higher proportions of bole wood mass and smaller proportions of branch mass compared to the standard approach. It is generally understood that trees produce a given amount of carbon each year that must be allocated to the various tissue types necessary for growth, as well as cellular respiration. Understanding how that carbon is allocated has important implications for timber production as well as carbon cycling.

The largest differences shown in Figure 13 are between the standard carbon mass estimates and the estimates using carbon fraction data from this study. Because all of the example trees were 1000 kg, these differences are due only to the proportion of biomass in a given tissue type, and the difference between using the 0.5 value and measured carbon fractions. At the whole tree carbon mass level, the differences are effectively the impact of using biomass-weighted carbon fractions for the individual tree components. In the oven-dried carbon row of Figure 13, white fir carbon mass is actually lower than the standard estimate due to the lower than 0.5 carbon fraction measured for oven-dried white fir tissue. Compare this to the living carbon mass estimates presented in the third row of the diagram and notice a "gain" in mass of 22 kg. This mass gain represents the impact of accounting for volatile organic compounds that are lost due to oven-drying of tree tissues. Similar increases in carbon mass are demonstrated between the oven-dried carbon mass estimates and the living carbon estimates of the other species. These percent increase in carbon mass range from about 2.2% to 4.5% of the respective oven-dried carbon mass estimates. Those are important differences and those values are directly related to the impact of measuring all carbon present in living tissue, including the volatile portion.

Compared to the standard approach, incense cedar living carbon mass is 9% higher. White fir showed the smallest increase in carbon mass at about 2.8% above the standard estimate. Though small, this increase in mass is important as it applies to all white fir biomass throughout the species range. The significance of a 2.8% to 9% increase in carbon mass estimates due only to accounting for carbon fractions correctly cannot be understated.

Conclusion

This study presents the first vertically integrable bole carbon mass model, along with branch and foliage prediction models, for five mixed conifer species in the Sierra Nevada. These models can be used to predict biomass, oven-dry carbon mass, and living carbon mass for whole trees, and tree portions. My models are the only models to directly account for known sources of variation in carbon fraction, and can be used to estimate biomass weighted carbon fractions for the species studied. Comparisons between my models and more standard approaches demonstrate significant

differences in carbon mass estimates, as well as overall biomass proportion estimates. I present relationships between bark mass and bole mass to allow for separate predictions of tree bark carbon, or for whole tree carbon mass.

Figures and Tables

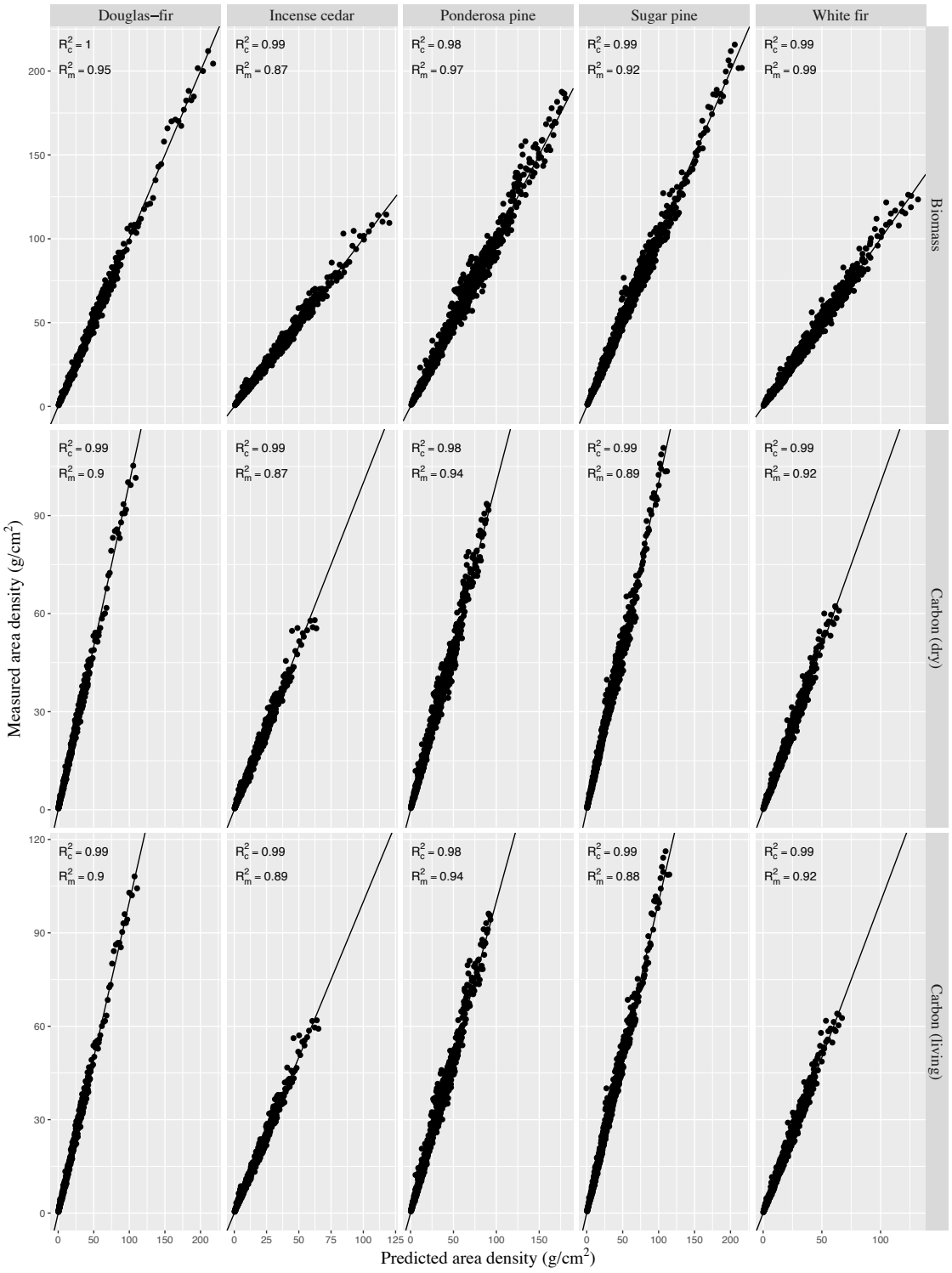

Figure 5. Predicted area density vs. measured area density values. The solid line represents a one to one relationship. R_m^2 is the proportion of variance in the data explained by the fixed effects of the model alone, while R_c^2 is the proportion of variance explained by the fixed and random effects of the model.

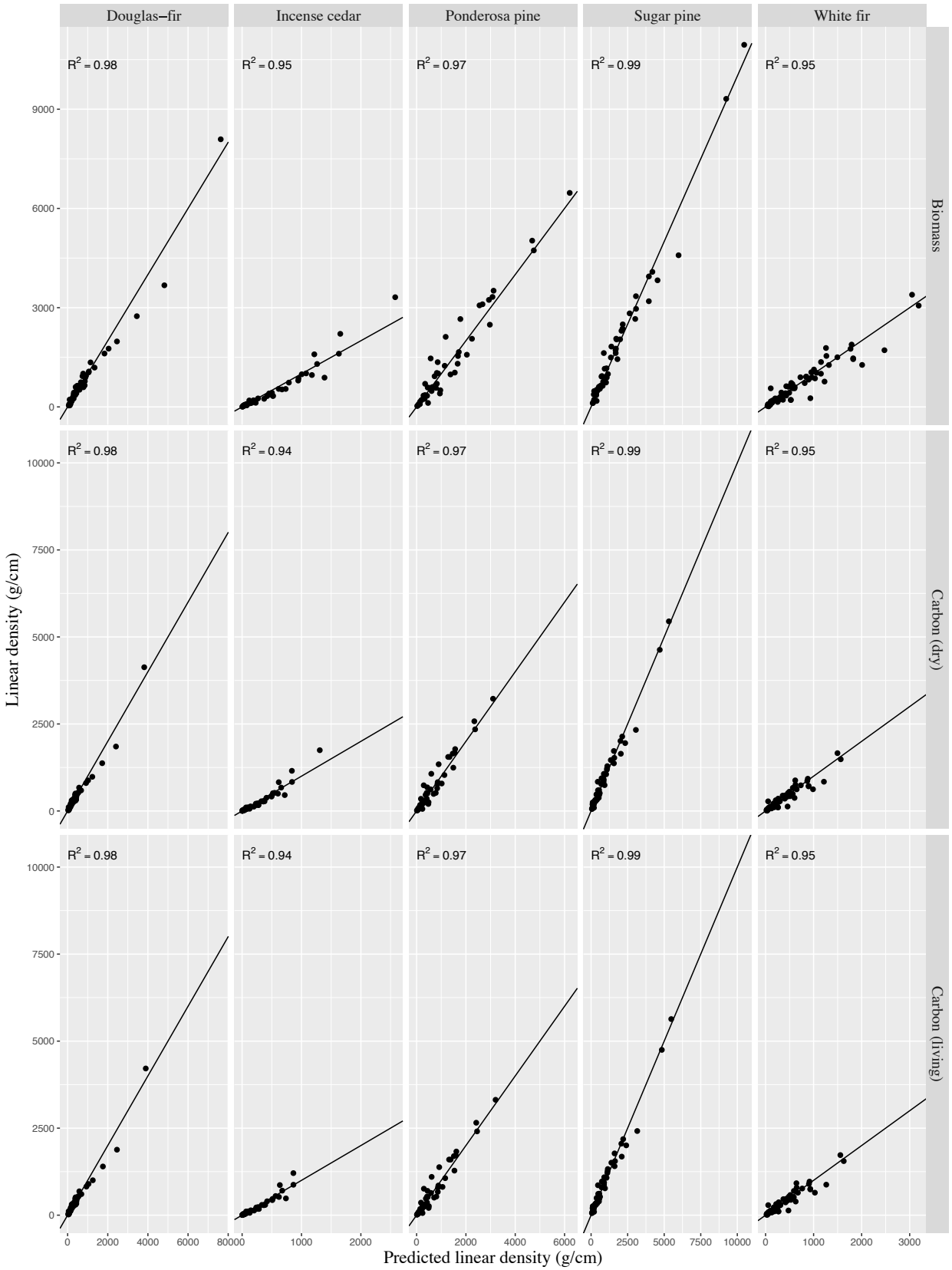

Figure 6. Predicted linear density vs. measured linear density values. The solid line represents a one to one relationship. R^2 values represent the proportion of variance in the data explained by the respective model.

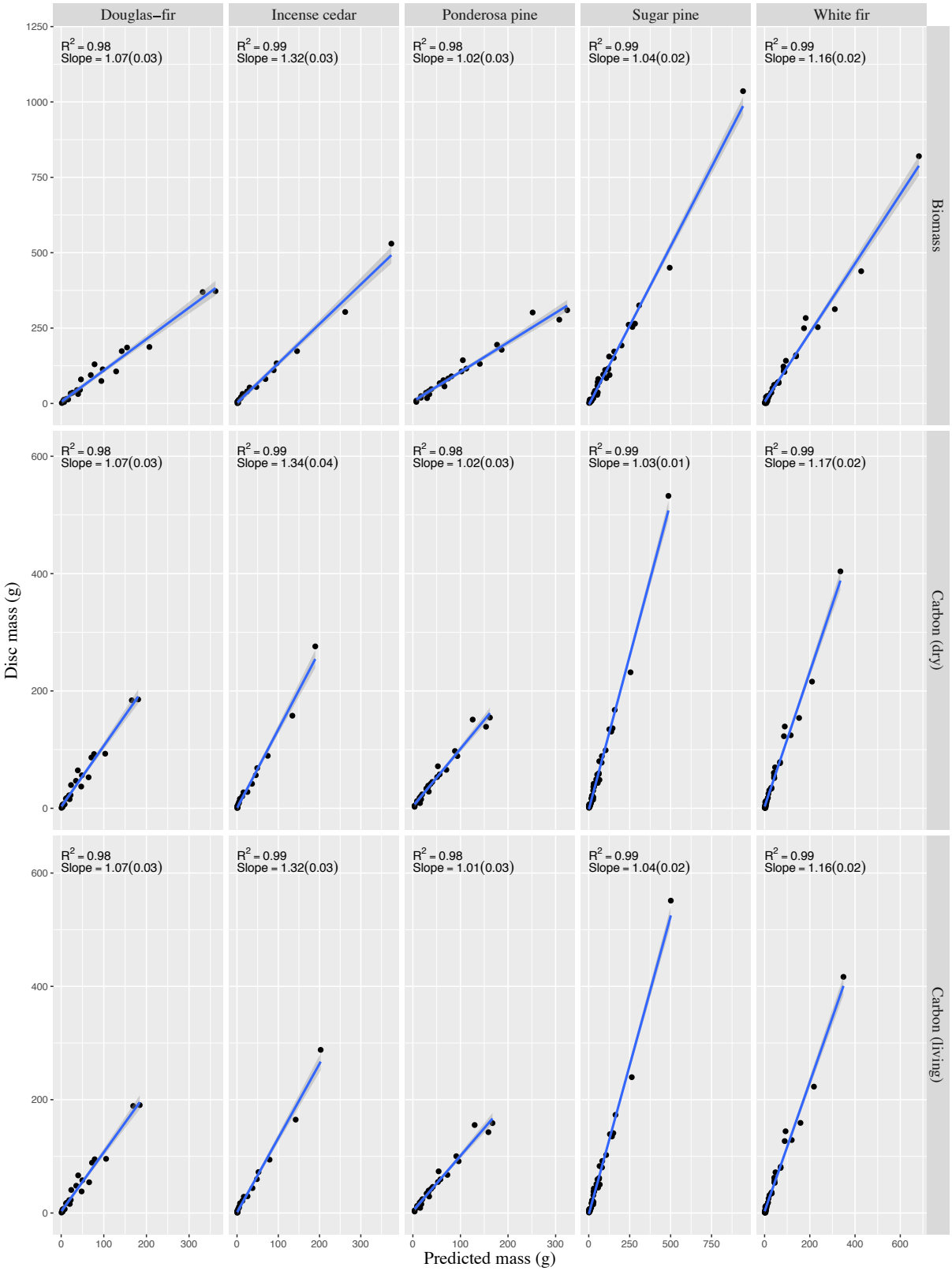

Figure 7. Disc mass values vs. values from numerical integration of the linear density models. Slope estimates and the standard errors of the slope estimates in parenthesis are shown. R^2 and slopes are given for the linear regression of the disk data on the predicted data.

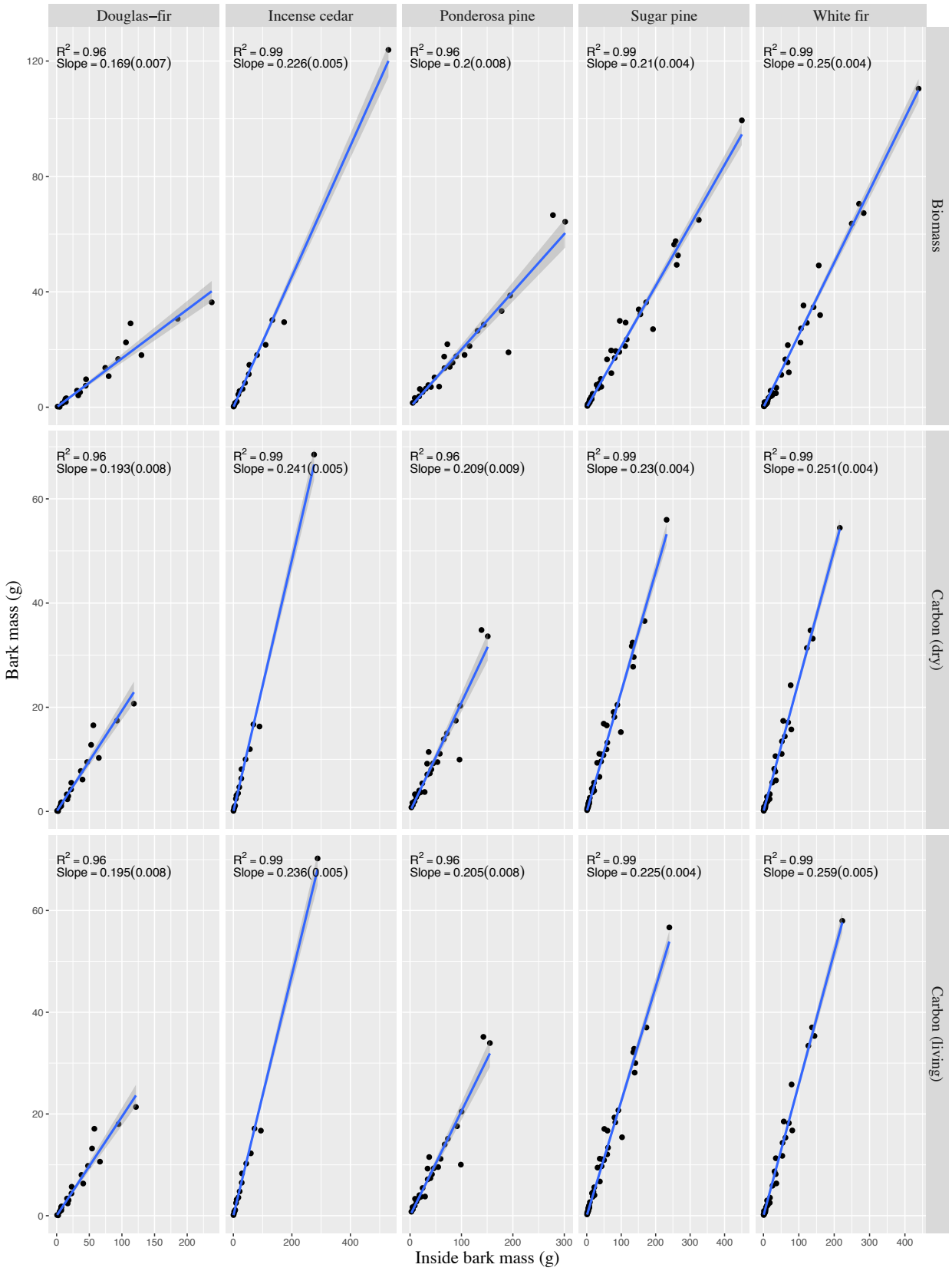

Figure 8. Bark mass vs. inside bark mass is shown. Slope estimates and the standard errors in parentheses are shown. R^2 represent the proportion of variance in the data explained by the bark mass model.

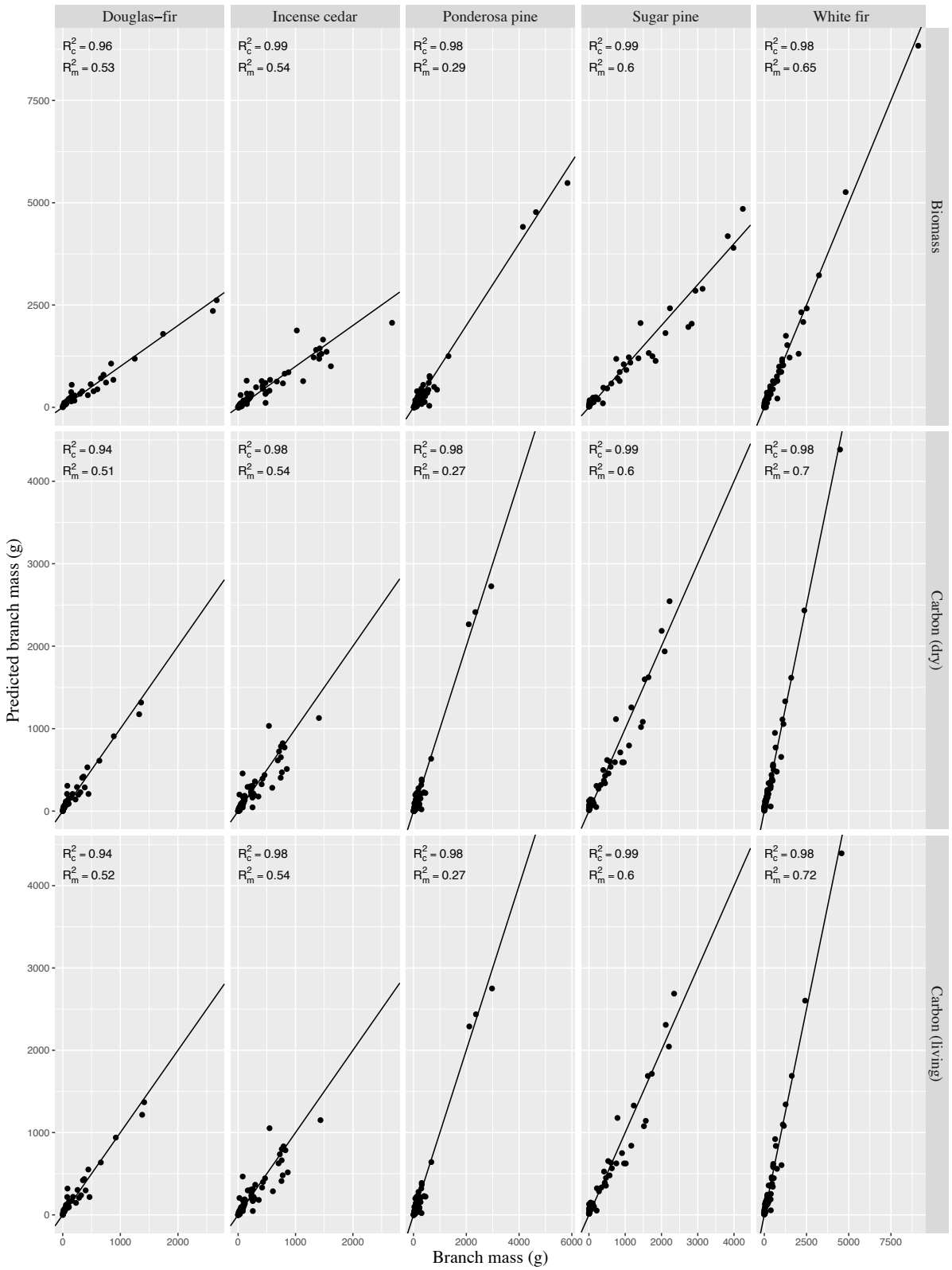

Figure 9. Predicted individual branch masses vs. observed. The solid line represents a one to one relationship between the values. R_m^2 is the proportion of variance in the data explained by the fixed effects of the model, while R_c^2 is the proportion of variance explained by the entire model.

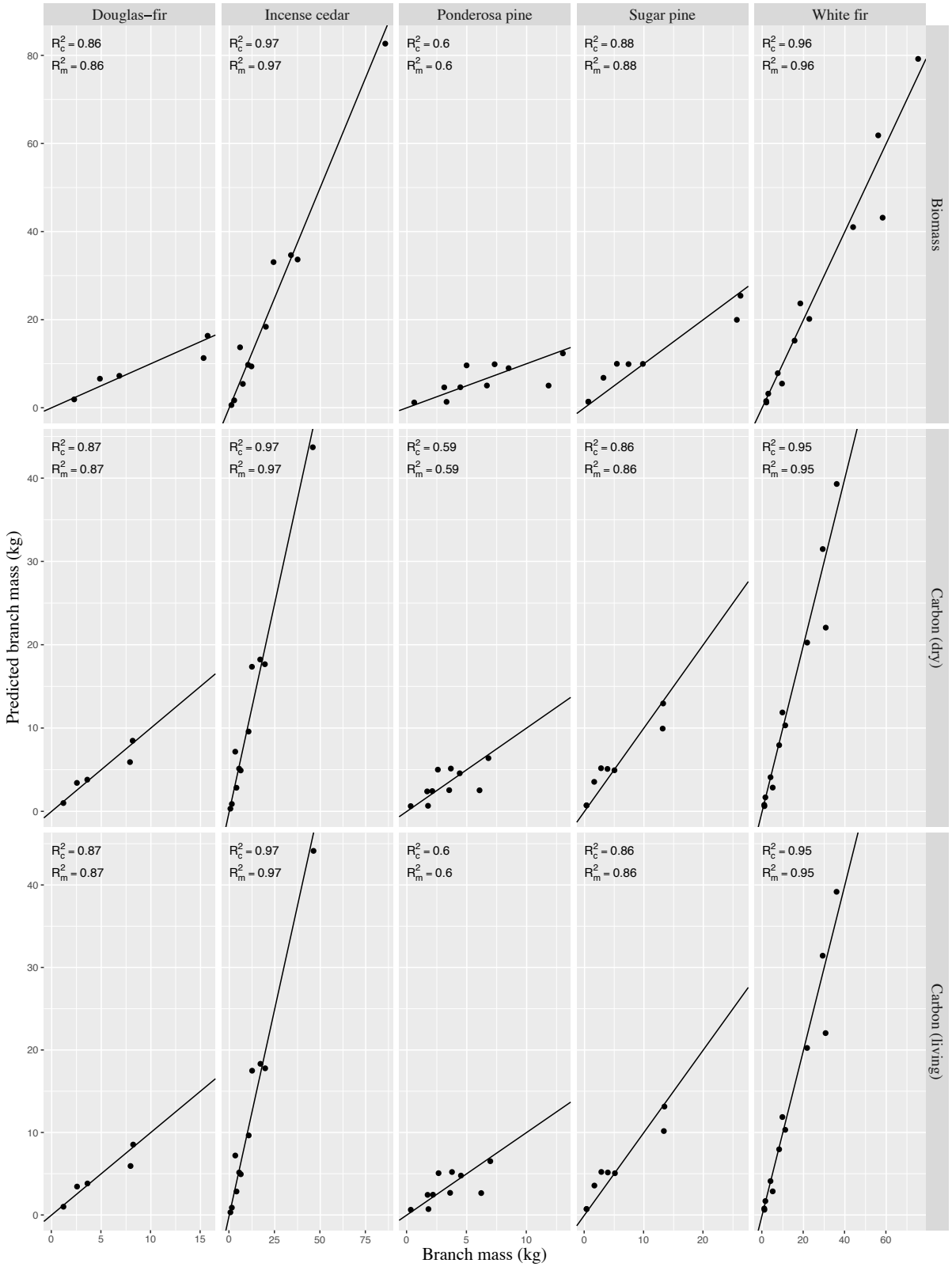

Figure 10. Predicted tree total branch masses vs. the observed. The solid line represents a one to one relationship between the values. R_m^2 is the proportion of variance in the data explained by the fixed effects of the model alone, while R_c^2 is the proportion of variance explained by the entire model.

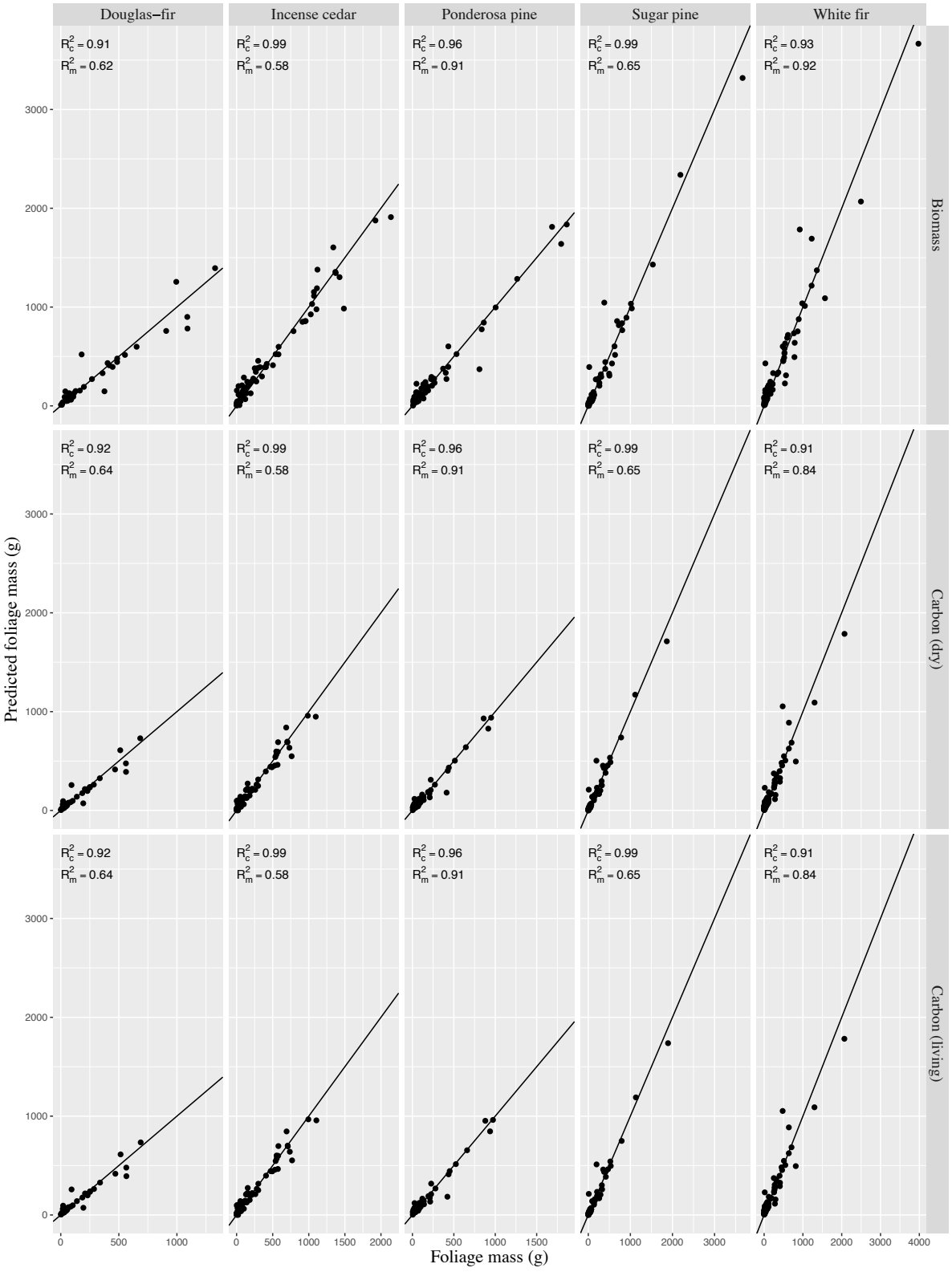

Figure 11. Predicted individual branch foliage masses vs. observed. The solid line represents a one to one relationship between the values. R_m^2 is the proportion of variance in the data explained by the fixed effects of the model alone, while R_c^2 is the proportion of variance explained by the entire model.

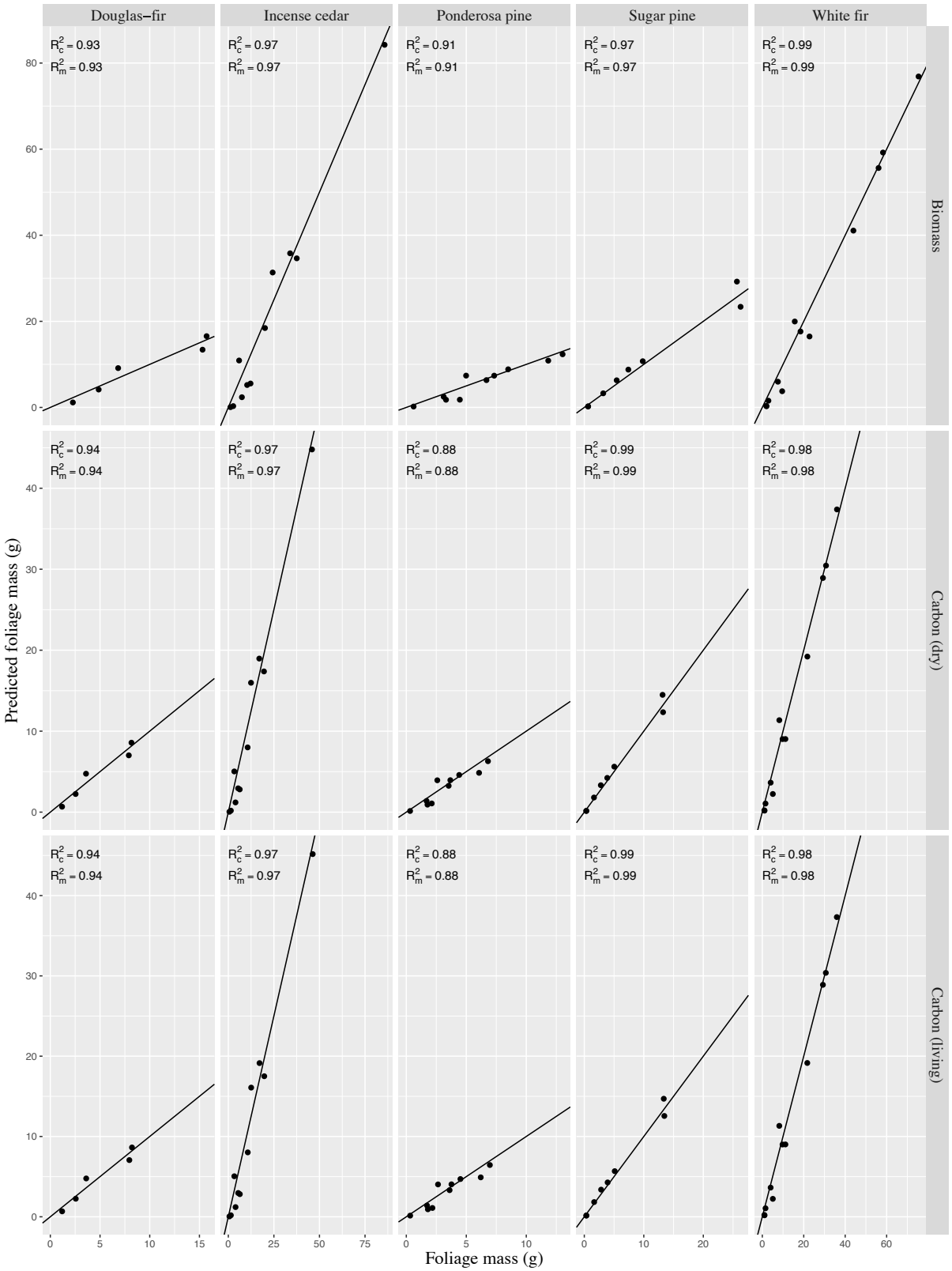

Figure 12. Predicted tree total foliage masses vs. observed. The solid line represents a one to one relationship between the values. R_m^2 is the proportion of variance in the data explained by the fixed effects of the model alone, while R_c^2 is the proportion of variance explained by the entire model.

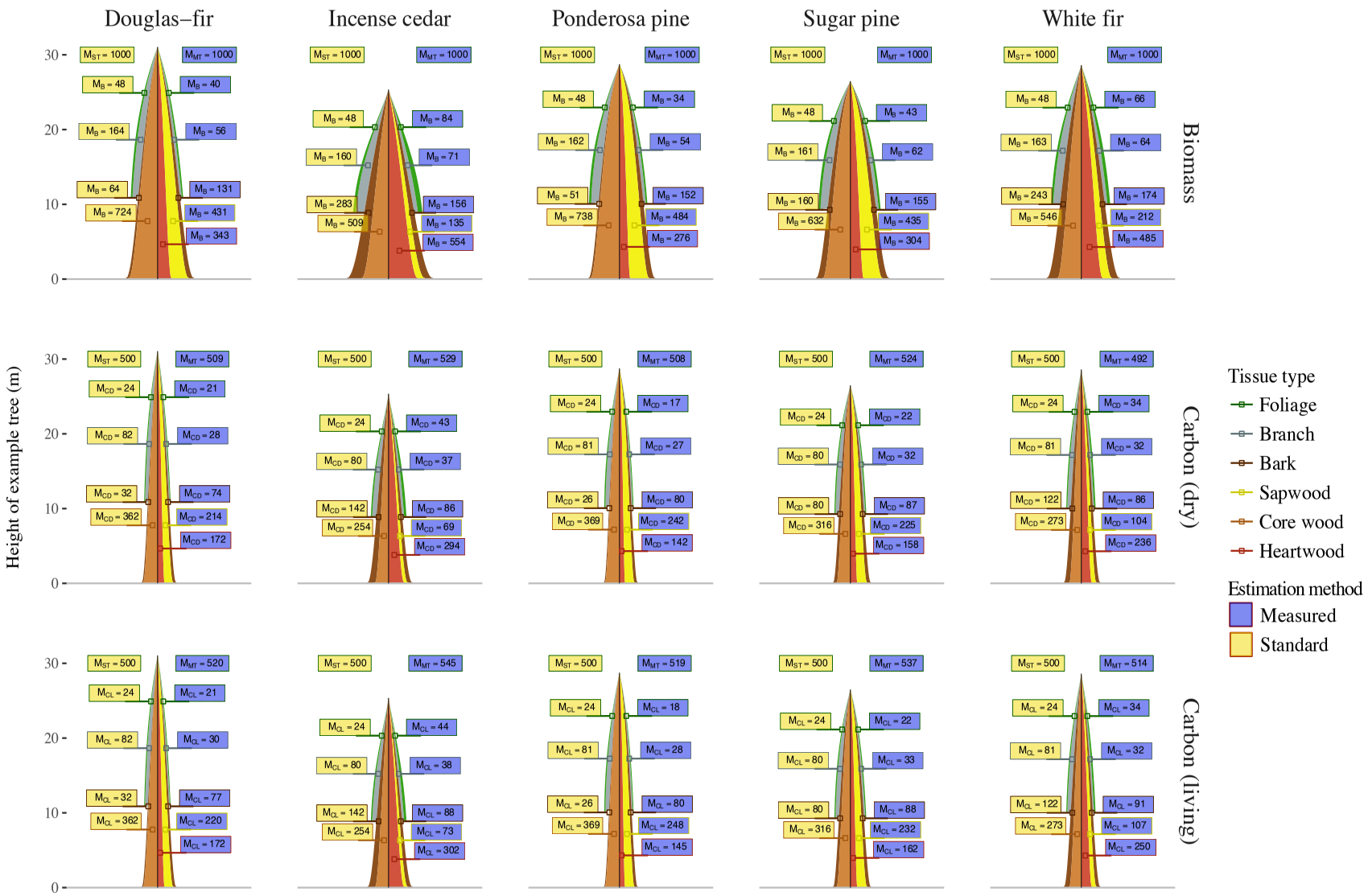

Figure 13. Species masses by mass types: biomass, living carbon mass, and oven-dry carbon mass. Masses estimated using standard approaches are shown in yellow boxes, while masses using models from this study are shown in blue boxes.

Table 13 Sample summary data for wood density, carbon fraction, tree cores, and tree discs

	Tree disc data				Tree core data		Wood density			Carbon fraction			Sample
Species	DBH (cm)	Height (m)	n - tree	n - disc	DBH (cm)	Height (cm)	n - trees	n - cores	n - samples	n - trees	n - cores	n - samples	locations
DF	15.9 (7.0)	11.9 (5.7)	5	24	61.2 (31.7)	35.1 (9.6)	14	47	565	4	6	24	1 & 2
IC	14.2 (8.2)	7.2 (3.6)	6	17	48.1 (32.0)	22.26 (11.8)	15	51	759	7	9	24	1, 2, & 3
PP	18.1 (3.9)	12.8 (5.0)	6	25	71.8 (37.6)	35.4 (13.6)	16	47	950	6	8	40	1, 2, & 3
SP	18.4 (11.1)	11.6 (6.8)	7	39	95.5 (47.4)	40.0 (11.6)	14	55	891	6	8	23	1, 2, & 3
WF	15.8 (10.4)	10.6 (6.7)	7	36	57.7 (26.8)	31.4 (9.3)	27	76	1009	5	10	32	1, 2, & 3

Values in parenthesis follow their respective mean values for a given category. Sample size (n) is shown for each species and given for each studied characteristic. See methods for descriptions of sample locations.

Table 14 Mean carbon fraction data

Carbon type	Species	Bark C	HW C	SW C	Foliage C
Oven-dry	DF	0.569 (0.009)	0.501 (0.005)	0.498 (0.001)	0.515 (0.004)
	IC	0.553 (0.03)	0.531 (0.009)	0.509 (0.008)	0.513 (0.004)
	PP	0.523 (0.008)	0.514 (0.009)	0.499 (0.009)	0.510 (0.005)
	SP	0.563 (0.007)	0.521 (0.005)	0.516 (0.002)	0.509 (0.002)
	WF	0.493 (0.002)	0.488 (0.002)	0.494 (0.002)	0.521 (0.003)
Living	DF	0.588 (0.009)	0.503 (0.01)	0.51 (0.009)	0.518 (0.006)
	IC	0.567 (0.015)	0.545 (0.009)	0.541 (0.008)	0.517 (0.007)
	PP	0.528 (0.008)	0.527 (0.008)	0.512 (0.005)	0.522 (0.006)
	SP	0.57 (0.01)	0.534 (0.005)	0.532 (0.009)	0.517 (0.002)
	WF	0.525 (0.01)	0.517 (0.004)	0.507 (0.009)	0.52 (0.001)

Mean carbon fractions for four tissue types from five conifer species shown. Standard deviations are shown in parenthesis next to the mean value for each category. Data derived from work performed by Jones and O'Hara (2016).

Table 15 Symbols and descriptions of covariates found in final LME models.

Symbol	Covariate description
B_{bk}	Biomass of bark
B_{disc}	Biomass of tree disc
B_{mi}	Biomass of individual component
B_{mt}	Biomass of tree total component
BRA	Branch cross sectional area immediately above the branch collar
D_a	Area density
DBH	Diameter of tree bole at 1.37 m from the base of the tree
D_l	Linear density
HFB	Height from the base of the tree
HFT	Distance from the top of the tree
HLC	Height to base of tree live crown
HLDR	Height to live crown divided by diameter of tree bole at 1.37 m
HT	Tree height
LCR	Live crown length divided by tree height
r	Radius from the pith of the tree to the center of a core segment
RDC	Height from tree top divided by crown length
RH	Height to a point on the tree divided by total tree height

Table 16 Model forms for density, and mass models for associated tree components

Tree portion	Modeled tree characteristic	Model #	Model form
Bole	Area density	19	$D_a = (\alpha_0+\alpha_{ij}) * r * \exp(-\exp(-(HFT^{(\beta_0 + \beta_{ij})} / (HLC)))) + \phi_{ij}$
		20	$D_a = (\alpha_0+\alpha_{ij}) * r * \exp(-\exp(-(HFT^{(\beta_0 + \beta_{ij})} / (HT)))) + \phi_{ij}$
		21	$D_a = (\alpha_0+\alpha_{ij}) * r * (1-\exp(-(\beta_0 + \beta_{ij}) * (HFT^{(\theta_0 + \theta_{ij})}/HLC))) + \phi_{ij}$
		22	$D_a = (\alpha_0+\alpha_{ij}) * r * (1-\exp(-(\beta_0 + \beta_{ij}) * (HFT^{(\theta_0 + \theta_{ij})}/HT))) + \phi_{ij}$
		23	$D_a = (\alpha_0 + \alpha_{ij}) * r * \exp((\beta_0 + \beta_{ij})*HFT/HLC)*\exp((-(\theta_0+\theta_{ij})/(\beta_0 + \beta_{ij}))*(\exp((\beta_0 + \beta_{ij})*HFT/HLC)-1)) + \phi_{ij}$
		24	$D_a = (\alpha_0 + \alpha_{ij}) * r + \phi_{ij}$
		25	$D_a = \alpha_0 * 2 * \pi * r$
	Linear density	26	$D_l = \pi * (DBH*(\alpha+\beta*\log(1-(1-\exp(-\alpha/\beta))*(HFB/HT)^{(1/3)})))^2$
		27	$D_l = \alpha_0 * 2 * \pi * (IBR)^2$
Branch	Individual biomass	28	$B_{mi} = ((\alpha_0 + \alpha_j) *BRA * ((RDC)^{((\beta_0 + \beta_{j)} - 1))} * \exp(-(RDC)^{(\beta_0 + \beta_j)})) + \phi_j$
	Total biomass	29	$B_{mt} = \alpha *(DBH)^{\beta}*\exp(\theta*HLC)$
Bark	Biomass of segment	30	$B_{bk} = \alpha*B_{disc}$
Foliage	Branch foliage	31	$B_{mi} = ((\alpha_0 +\alpha_j) *BRA * ((RDC)^{((\beta_0 + \beta_j) - 1))} * \exp(-(RDC)^{(\beta_0 + \beta_j)})) + \phi_j$
	All foliage	32	$B_{mt} = \alpha *(DBH)^{\beta}*\exp(\theta*HLC)$

Models fit to data for the respective tree portion. For mixed effects models the random effects are assumed to be normally distributed with a mean of 0. Models 19 through 24 were compared directly for performance in predicting bole area densities and the best fit model was determined using log-likelihood ratio testing.

Table 17 Model comparisons for area density and linear density

Density type	Model #	AIC	BIC	Log-likelihood	Test	p-value	R^2
Area density	Final: 23*	20724.49	20876.57	-10338.24			0.982
	23	23300.29	23338.31	-11644.15	Final vs. 23	< 0.001	0.995
	20	23348.75	23380.43	-11669.37	23 vs. 20	< 0.001	0.995
	22	23372.41	23410.43	-11680.20	20 vs. 22	< 0.001	0.993
	21	23379.60	23417.62	-11683.80			0.992
	24	23377.73	23403.08	-11684.86	21 vs. 24	0.346	0.983
	19	23446.03	23477.71	-11718.01	24 vs. 19	< 0.001	0.996
	25	27929.10	27967.12	-13958.55	19 vs. 25	< 0.001	0.956
Linear density	26	3751.52	3794.95	-1863.76			0.992
	27	4421.87	4400.15	-2194.08	26 vs. 27	<0.001	0.465

Models shown were fit to area density data, or linear density data from cores. Tests were for log-likelihood ratio tests of the models specified in the test column. The final model was model 23 fit with additional covariates shown in Table 18 for area density, and model 26 for linear density with parameter estimates shown in Table 19.

Table 18 Parameter estimates for the area density model fit to core segment data

		fixed effect parameter estimates (SD)			random effect SD	
Area density type	Species	α	β	θ	α_{ij} - tree	α_{ij} – core within tree
Biomass	DF	2.12 (0.053)	LCR * (0.141 (0.039))	HLDR * (-0.790 (0.190))	0.092	0.131
	IC	1.876 (0.048)	LCR * (0.141 (0.039))	HLDR * (-0.325 (0.205))	0.092	0.131
	PP	1.866 (0.055)	LCR * (0.141 (0.039))	HLDR * (-1.064 (0.237))	0.092	0.131
	SP	2.242 (0.046)	LCR * (0.141 (0.039))	HLDR * (0.004 (0.207))	0.092	0.131
	WF	1.842 (0.042)	LCR * (0.141 (0.039))	HLDR * (-0.684 0.145))	0.092	0.131
Oven-dry carbon	DF	1.035 (0.035)	LCR * (0.213 (0.035))	HLDR * (-0.779 (0.166))	0.072	0.061
	IC	0.955 (0.032)	LCR * (0.213 (0.035))	HLDR * (-0.242 (0.186))	0.072	0.061
	PP	0.923 (0.034)	LCR * (0.213 (0.035))	HLDR * (-0.925 (0.2))	0.072	0.061
	SP	1.144 (0.031)	LCR * (0.213 (0.035))	HLDR * (0.164 (0.153))	0.072	0.061
	WF	0.873 (0.027)	LCR * (0.213 (0.035))	HLDR * (-0.719 (0.135))	0.072	0.061
Living carbon	DF	1.042 (0.037)	LCR * (0.219 (0.036))	HLDR * (-0.832 (0.172))	0.076	0.063
	IC	0.994 (0.033)	LCR * (0.219 (0.036))	HLDR * (-0.244 (0.182))	0.076	0.063
	PP	0.935 (0.037)	LCR * (0.219 (0.036))	HLDR * (-0.978 (0.208))	0.076	0.063
	SP	1.195 (0.032)	LCR * (0.219 (0.036))	HLDR * (0.293 (0.152))	0.076	0.063
	WF	0.887 (0.028)	LCR * (0.219 (0.036))	HLDR * (-0.781 (0.139))	0.076	0.063

Area density parameter estimates for model 5. Live crown ratio (LCR), and height to live crown divided by diameter at breast height (HLDR), both significantly improved the final model. Random effect standard deviations are given for their respective parameter and level of effect.

Table 19 Parameter estimates for the linear density model fit to core data.

Linear density type	Species	α	β
Biomass	DF	0.363 (0.01)	0.15 (0.014)
	IC	0.309 (0.01)	0.119 (0.012)
	PP	0.356 (0.01)	0.149 (0.018)
	SP	0.331 (0.006)	0.114 (0.007)
	WF	0.327 (0.007)	0.122 (0.011)
Oven-dry carbon	DF	0.256 (0.007)	0.106 (0.01)
	IC	0.219 (0.007)	0.081 (0.008)
	PP	0.252 (0.007)	0.104 (0.013)
	SP	0.238 (0.004)	0.082 (0.005)
	WF	0.229 (0.005)	0.085 (0.008)
Living carbon	DF	0.259 (0.007)	0.107 (0.01)
	IC	0.228 (0.007)	0.087 (0.009)
	PP	0.256 (0.007)	0.107 (0.013)
	SP	0.242 (0.004)	0.084 (0.005)
	WF	0.234 (0.005)	0.087 (0.008)

Mean parameter estimate are shown with standard deviation of the estimate shown in parenthesis for biomass, oven-dry carbon, and living carbon linear density for five species.

Table 20 Parameter estimates for individual branch mass, and tree total branch mass models

		Individual branches		Tree total branch mass		
Mass type	Species	α	β	α	β	θ
Biomass	DF	146.699 (31.477)	0.458 (0.945) + RH*(1.192 (1.178))	54.637 (22.431)	1.425 (0.201) + LCR*(0.614 (0.138))	HLC*(-0.0036 (0.0041)
	IC	138.965 (22.422)	-1.734 (1.678) + RH*(4.775 (2.139))	54.637 (22.431)	1.425 (0.201) + LCR*(0.614 (0.138))	HLC*(0.0045 (0.0021)
	PP	89.035 (22.476)	-12.161 (1.071) + RH*(18.484 (1.487))	54.637 (22.431)	1.425 (0.201) + LCR*(0.614 (0.138))	HLC*(-0.0173 (0.0062)
	SP	174.375 (27.842)	5.851 (0.699) + RH*(-5.009 (0.822))	54.637 (22.431)	1.425 (0.201) + LCR*(0.614 (0.138))	HLC*(-0.0096 (0.0041)
	WF	256.387 (27.577)	-3.432 (0.327) + RH*(2.822 (0.391))	54.637 (22.431)	1.425 (0.201) + LCR*(0.614 (0.138))	HLC*(0.0046 (0.0023)
Oven-dry carbon	DF	76.273 (15.342)	-1.445 (0.511) + RH*(0.673 (0.644))	28.709 (11.838)	1.417 (0.204) + LCR*(0.623 (0.144))	HLC*(-0.0036 (0.0042)
	IC	64.956 (10.609)	-3.644 (1.469) + RH*(6.957 (1.907))	28.709 (11.838)	1.417 (0.204) + LCR*(0.623 (0.144))	HLC*(0.0046 (0.0021)
	PP	42.989 (11.034)	-11.729 (1.169) + RH*(17.479 (1.562))	28.709 (11.838)	1.417 (0.204) + LCR*(0.623 (0.144))	HLC*(-0.0178 (0.0065)
	SP	87.365 (13.186)	5.9 (0.628) + RH*(-5.247 (0.726))	28.709 (11.838)	1.417 (0.204) + LCR*(0.623 (0.144))	HLC*(-0.0103 (0.0043)
	WF	147.358 (14.224)	5.577 (0.621) + RH*(-4.251 (0.823))	28.709 (11.838)	1.417 (0.204) + LCR*(0.623 (0.144))	HLC*(0.004 (0.0024)
Living carbon	DF	79.38 (15.677)	-1.426 (0.522) + RH*(0.65 (0.658))	28.906 (11.845)	1.418 (0.203) + LCR*(0.62 (0.143))	HLC*(-0.0036 (0.0042)
	IC	66.143 (10.816)	-3.615 (1.521) + RH*(6.913 (1.973))	28.906 (11.845)	1.418 (0.203) + LCR*(0.62 (0.143))	HLC*(0.0046 (0.0021)
	PP	43.506 (11.257)	-11.695 (1.218) + RH*(17.434 (1.628))	28.906 (11.845)	1.418 (0.203) + LCR*(0.62 (0.143))	HLC*(-0.0171 (0.0063)
	SP	92.245 (13.436)	5.889 (0.626) + RH*(-5.234 (0.723))	28.906 (11.845)	1.418 (0.203) + LCR*(0.62 (0.143))	HLC*(-0.01 (0.0042)
	WF	139.707 (13.499)	-3.822 (0.206) + RH*(3.318 (0.268))	28.906 (11.845)	1.418 (0.203) + LCR*(0.62 (0.143))	HLC*(0.0039 (0.0023)

Parameter estimates for model 28 for individual branch estimates and model 29 for tree total branch mass estimates. Additional covariates that significantly improved model performance when added to a given parameter are shown. Estimate standard deviations are shown next to the mean parameter estimate for the intercept and any additional covariate present.

Table 21 Parameter estimates for individual branch foliage mass, and tree total foliage mass models

		Individual branch foliage		Tree total foliage	
Leaf mass type	Species	α	β	α	β
Biomass	DF	RH*(189.118 (34.313)) + 29.367 (23.911)	RDC*(2.675 (0.406)) + RH*(29.367 (23.911))	2.324 (0.061) + LCR*(2 (0.272))	-0.231 (0.057)
	IC	RH*(189.118 (34.313)) + 45.071 (20.64)	RDC*(2.675 (0.406)) + RH*(45.071 (20.64))	2.324 (0.061) + LCR*(0.669 (0.154))	0.046 (0.03)
	PP	RH*(189.118 (34.313)) + -31.095 (21.828)	RDC*(2.675 (0.406)) + RH*(-31.095 (21.828))	2.324 (0.061) + LCR*(1.138 (0.273))	-0.128 (0.049)
	SP	RH*(189.118 (34.313)) + -35.802 (23.22)	RDC*(2.675 (0.406)) + RH*(-35.802 (23.22))	2.324 (0.061) + LCR*(1.053 (0.442))	-0.098 (0.083)
	WF	RH*(189.118 (34.313)) + 53.451 (19.732)	RDC*(2.675 (0.406)) + RH*(53.451 (19.732))	2.324 (0.061) + LCR*(1.513 (0.112))	-0.121 (0.01)
Oven-dry carbon	DF	RH*(90.329 (13.776)) + 17.783 (11.544)	RDC*(-2.349 (0.142)) + RH*(17.783 (11.544))	2.324 (0.061) + LCR*(2 (0.272))	-0.231 (0.057)
	IC	RH*(90.329 (13.776)) + 25.606 (9.622)	RDC*(-2.349 (0.142)) + RH*(25.606 (9.622))	2.324 (0.061) + LCR*(0.669 (0.154))	0.046 (0.03)
	PP	RH*(90.329 (13.776)) + -13.211 (9.965)	RDC*(-2.349 (0.142)) + RH*(-13.211 (9.965))	2.324 (0.061) + LCR*(1.138 (0.273))	-0.128 (0.049)
	SP	RH*(90.329 (13.776)) + -15.008 (10.63)	RDC*(-2.349 (0.142)) + RH*(-15.008 (10.63))	2.324 (0.061) + LCR*(1.053 (0.442))	-0.098 (0.083)
	WF	RH*(90.329 (13.776)) + 32.012 (9.435)	RDC*(-2.349 (0.142)) + RH*(32.012 (9.435))	2.324 (0.061) + LCR*(1.513 (0.112))	-0.121 (0.01)
Living carbon	DF	RH*(91.689 (13.892)) + 17.529 (11.654)	RDC*(-2.353 (0.142)) + RH*(17.529 (11.654))	2.324 (0.061) + LCR*(2 (0.272))	-0.231 (0.057)
	IC	RH*(91.689 (13.892)) + 25.491 (9.71)	RDC*(-2.353 (0.142)) + RH*(25.491 (9.71))	2.324 (0.061) + LCR*(0.669 (0.154))	0.046 (0.03)
	PP	RH*(91.689 (13.892)) + -13.062 (10.047)	RDC*(-2.353 (0.142)) + RH*(-13.062 (10.047))	2.324 (0.061) + LCR*(1.138 (0.273))	-0.128 (0.049)
	SP	RH*(91.689 (13.892)) + -15.152 (10.726)	RDC*(-2.353 (0.142)) + RH*(-15.152 (10.726))	2.324 (0.061) + LCR*(1.053 (0.442))	-0.098 (0.083)
	WF	RH*(91.689 (13.892)) + 31.193 (9.531)	RDC*(-2.353 (0.142)) + RH*(31.193 (9.531))	2.324 (0.061) + LCR*(1.513 (0.112))	-0.121 (0.01)

Parameter estimates for model 31 for individual branch foliage estimates and model 32 for tree total foliage mass estimates. Additional covariates that significantly improved model performance when added to a given parameter are shown. Estimate standard deviations are shown next to the mean parameter estimate for the intercept and any additional covariate present.

References

Abascal K, Ganora L, Yarnell E (2005) The effect of freeze-drying and its implications for botanical medicine: A review. Phyther Res 19:655–660.

Akaike H (1974) A new look at the statistical model identification. IEEE Trans Automat Contr 19:716–723.

de Aza CH, Turrión MB, Pando V, Bravo F (2011) Carbon in heartwood, sapwood and bark along the stem profile in three Mediterranean Pinus species. Ann For Sci 68:1067–1076.

Becker GS, Braun D, Gliniars R, Dalitz H (2012) Relations between wood variables and how they relate to tree size variables of tropical African tree species. Trees 26:1101–1112.

Bert D, Danjon F (2006) Carbon concentration variations in the roots, stem and crown of mature Pinus pinaster (Ait.). For Ecol Manage 222:279–295.

Biging GS (1984) Taper Equations for Second-Growth Mixed Conifers of Northern California. For Sci 30:1103–1117.

Brown S (2002) Measuring carbon in forests: current status and future challenges. Environ Pollut 116:363–72.

Calcagno V (2013) glmulti: Model selection and multimodel inference made easy. http://cran.r-project.org/package=glmulti

Castaño-Santamaría J, Bravo F (2012) Variation in carbon concentration and basic density along stems of sessile oak (Quercus petraea (Matt.) Liebl.) and Pyrenean oak (Quercus pyrenaica Willd.) in the Cantabrian Range (NW Spain). Ann For Sci 69:663–672.

Chave J, Andalo C, Brown S, Cairns MA, Chambers JQ, Eamus D, Fölster H, Fromard F, Higuchi N, Kira T (2005) Tree Allometry and Improved Estimation of Carbon Stocks and Balance in Tropical Forests. Oecologia 145:87–99.

Chave J, Coomes D, Jansen S, Lewis SL, Swenson NG, Zanne AE (2009) Towards a worldwide wood economics spectrum. Ecol Lett 12:351–66.

Chojnacky DC, Heath LS, Jenkins JC (2014) Updated generalized biomass equations for North American tree species. Forestry 87:129–151.

Cohen WB, Harmon ME, Wallin DO, Fiorella M (1996) Two Decades of Carbon Flux from Forests of the Pacific Northwest. Bioscience 46:836–844. http://www.jstor.org/stable/1312969 (1 April 2011, date last accessed).

Correia AC, Tomé M, Carlos P, Sónia F (2010) Biomass allometry and carbon factors for a Mediterranean pine (Pinus pinea L .) in Portugal. For Syst 19:418–433.

Cousins SJM, Battles JJ, Sanders JE, York R a. (2015) Decay patterns and carbon density of standing dead trees in California mixed conifer forests. For Ecol Manage. http://linkinghub.elsevier.com/retrieve/pii/S0378112715002996

Van Deusen P, Roesch FA (2011) Sampling a tree for Total Volume, Biomass, and Carbon. J For 109:131–135. http://www.ingentaconnect.com/content/saf/jof/2011/00000109/00000003/art00004 (17 August 2011, date last accessed).

Dewar RC, Cannell MGR (1992) Carbon sequestration in the trees, products and soils of forest plantations - an analysis using UK examples. Tree Physiol 11:49–71.

Díaz MC, Pérez-Coello MS, Cabezudo MD (2002) Effect of drying method on the volatiles in bay leaf (Laurus nobilis L.). J Agric Food Chem 50:4520–4524.

Dixon RK, Brown S, Houghton RA, Solomon AM, Trexier M. C, Wisniewski J (1994) Carbon

pools and flux of global forest ecosystems. Science 263:185–90.
Elias M, Potvin C (2003) Assessing inter-and intra-specific variation in trunk carbon concentration for 32 neotropical tree species. Can J For Res 33:1039–1045.
Fahey TJ, Woodbury PB, Battles JJ, Goodale CL, Hamburg S, Ollinger S, Woodall CW (2009) Forest carbon storage: ecology, management, and policy. Front Ecol Environ
Fogel R, Cromack K (1977) Effect of habitat and substrate quality on Douglas-fir litter decomposition in Western Oregon. Can J Bot 55:1632–1640. <Go to ISI>://A1977DL37400007
Van Geffen KG, Poorter L, Sass-Klaassen U, van Logtestijn RSP, Cornelissen JHC (2010) The trait contribution to wood decomposition rates of 15 Neotropical tree species. Ecology 91:3686–97.
Goodale CL, Apps MJ, Birdsey RA, Field CB, Heath LS, Houghton RA, Jenkins JC, Kohlmaier GH, Kurz W, Liu S, Nabuurs G-J, Nilsson S, Shvidenko AZ (2002) Forest Carbon Sinks in the Northern Hemisphere. Ecol Appl 12:891–899.
Guo H, Murray F (2000) Modelling of emissions of total volatile organic compounds in an Australian house. Indoor Built Environ 9:171–181.
Harkin JM, Rowe JW (1971) Bark and its possible uses. U.S. Department of Agriculture.
Harmon ME, Ferrell WK, Franklin JF (1990) Effects on Carbon Storage of Conversion of Old-Growth Forests to Young Forests. Science (80-) 247:699–702. http://www.sciencemag.org/content/247/4943/699.short (1 April 2011, date last accessed).
Hollinger DYY, MacLaren JPP, Beets PNN, Turland J (1993) Carbon sequestration by New Zealand's plantation forests. New Zeal J For Sci 23:194–208. http://scholar.google.com/scholar?hl=en&btnG=Search&q=intitle:Carbon+sequestration+by+new+zealand's+plantation+forests#0 (16 June 2011, date last accessed).
Hoover C, Stout S (2007) The Carbon Consequences of Thinning Techniques : Stand Structure Makes a Difference. J For 105:266–270. http://www.ingentaconnect.com/content/saf/jof/2007/00000105/00000005/art00013 (1 April 2011, date last accessed).
Houghton RA (2005) Aboveground Forest Biomass and the Global Carbon Balance. Glob Chang Biol 11:945–958. http://www.blackwell-synergy.com/doi/abs/10.1111/j.1365-2486.2005.00955.x (17 July 2010, date last accessed).
Hynynen J, Ahtikoski A, Siitonen J, Sievanen R, Liski J (2005) Applying the MOTTI simulator to analyse the effects of alternative management schedules on timber and non-timber production. For Ecol Manage 207:5–18.
Ikonen V-P, Peltola H, Wilhelmsson L, Kilpelainen A, Vaisanen H, Nuutinen T, Kellomaki S, Kilpeläinen A, Väisänen H, Kellomäki S (2008) Modelling the distribution of wood properties along the stems of Scots pine (Pinus sylvestris L.) and Norway spruce (Picea abies (L.) Karst.) as affected by silvicultural management. For Ecol Manage 256:1356–1371. http://linkinghub.elsevier.com/retrieve/pii/S0378112708005392 (20 August 2010, date last accessed).
Jenkins JC, Chojnacky DC, Heath LS, Birdsey RA (2003) National-Scale Biomass Estimators for United States Tree Species. For Sci 49
Johansson M-B, Berg B, Meentemeyer V (1995) Litter mass-loss rates in late stages of decomposition in a climatic transect of pine forests. Long-term decomposition in a Scots pine forest. IX. Can J Bot 73:1509–1521.
Jones DA, O'Hara KL (2012) Carbon density in managed coast redwood stands: implications for

forest carbon estimation. Forestry 85:99–110. http://forestry.oxfordjournals.org/cgi/doi/10.1093/forestry/cpr063 (24 September 2014, date last accessed).
Jones DA, O'Hara KL (2016) The influence of preparation method on measured carbon fractions in tree tissues. Tree Physiol:tpw051. http://treephys.oxfordjournals.org/lookup/doi/10.1093/treephys/tpw051
Jones DA, O'Hara KL, Battles JJ, Gersonde RF (2015) Leaf Area Prediction Using Three Alternative Sampling Methods for Seven Sierra Nevada Conifer Species. Forests 6:2631–2654. http://www.mdpi.com/1999-4907/6/8/2631/
Jordan L, Souter R, Parresol B, Daniels RF (2006) Application of the Algebraic Difference Approach for Developing Self-Referenc ... For Sci 52:81–92.
Kaar WE, Brink DL (1991) Summative Analysis of Nine Common North American Woods. J Wood Chem Technol 11:479–494.
Karchesy J, Koch P (1979) Energy Production from Hardwoods Growing on Southern Pine Sites. http://www.srs.fs.usda.gov/pubs/viewpub.php?index=2383 (15 April 2014, date last accessed).
Laiho R, Laine J (1997) Tree stand biomass and carbon content in an age sequence of drained pine mires in southern Finland. For Ecol Manage 93:161–169.
Lamlom SH, Savidge RA (2003) A reassessment of carbon content in wood: variation within and between 41 North American species. Biomass and Bioenergy 25:381–388.
Lamlom SH, Savidge RA (2006) Carbon content variation in boles of mature sugar maple and giant sequoia. Tree Physiol 26:459–68.
Langum CE, Yadama V, Lowell EC (2009) Physical and Mechanical Properties of Young-Growth Douglas-Fir and Western Hemlock from Western Washington. For Prod J 59:37–47.
Litton CM, Raich JW, Ryan MG (2007) Carbon allocation in forest ecosystems. Glob Chang Biol 13:2089–2109. http://www.blackwell-synergy.com/doi/abs/10.1111/j.1365-2486.2007.01420.x
Malmsheimer RW, Bowyer JL, Fried JS, Gee E, Izlar RL, Miner RA, Munn IA, Oneil E, Stewart WC (2011) Managing Forests because Carbon Matters: Integrating Energy, Products, and Land Management Policy. J For 109
Martin AR, Gezahegn S, Thomas SC (2015) Variation in carbon and nitrogen concentration among major woody tissue types in temperate trees. Can J For Res 45:744–757. http://www.nrcresearchpress.com/doi/full/10.1139/cjfr-2015-0024#.VmhUXPmDGko
Martin AR, Thomas SC (2011) A Reassessment of Carbon Content in Tropical Trees. PLoS One 6:1–9.
Matthews G (1993) The carbon content of trees. Forestry Commission Technical Paper 4, Forestry Commission, Edinburgh, Scotland.
McKinley DC, Ryan MG, Birdsey RA, Giardina CP, Harmon ME, Heath LS, Houghton RA, Jackson RB, Morrison JF, Murray BC, Pataki DE, Skog KE (2011) A synthesis of current knowledge on forests and carbon storage in the United States. Ecol Appl 21:1902–1924.
Means JE, Hansen HA, Koerper GJ, Alaback PB, Klopsch MW (1994): Software for Computing Plant Biomass-BIOPAK Users Guide Portland: USDA Forest Service Pacific Northwest Research Station; Gen Tech Rep PNW-GTR-340.
Melson S, Harmon M (2011) Estimates of live-tree carbon stores in the Pacific Northwest are sensitive to model selection. Carbon Balance Manag 6:2.

Miles PD, Smith WB (2009) Specic Gravity and Other Properties of Wood and Bark for 156 Tree Species Found in North America.

Nakagawa S, Schielzeth H (2013) A general and simple method for obtaining R2 from generalized linear mixed-effects models. Methods Ecol Evol 4:133–142.

Neilson ET, MacLean DA, Arp PA, Meng F-R, Bhatti JS (2006) Modeling carbon sequestration with CO2 Fix and a timber supply model for use in forest management planning. Can J Soil Sci 86:219–233.

Nogueira EM, Fearnside PM, Nelson BW, Barbosa RI, Keizer EWH (2008) Estimates of forest biomass in the Brazilian Amazon: New allometric equations and adjustments to biomass from wood-volume inventories. For Ecol Manage 256:1853–1867.

Nogueira EM, Fearnside PM, Nelson BW, Franca MB (2007) Wood density in forests of Brazil's 'arc of deforestation': Implications for biomass and flux of carbon from land-use change in Amazonia. For Ecol Manage 248:119–135. http://linkinghub.elsevier.com/retrieve/pii/S0378112707003672 (16 August 2010, date last accessed).

Pacala SW, Hurtt GC, Baker D, Peylin P, Houghton RA, Birdsey RA, Heath L, Sundquist ET, Stallard RF, Ciais P, Moorcroft P, Caspersen JP, Shevliakova E, Moore B, Kohlmaier G, Holland E, Gloor M, Harmon ME, Fan SM, Sarmiento JL, Goodale CL, Schimel D, Field CB (2001) Consistent land- and atmosphere-based U.S. carbon sink estimates. Science 292:2316–20. http://www.ncbi.nlm.nih.gov/pubmed/11423659 (15 March 2011, date last accessed).

Parresol BR, Thomas CE (1989) A density-integral approach to estimating stem biomass. For Ecol Manage 26:285–297.

Peng M, Stewart J (2013) Development, validation, and application of a model of intra-and inter-tree variability of wood density for lodgepole pine in western Canada. Can J For Res 43:1172–1180. http://www.nrcresearchpress.com/doi/abs/10.1139/cjfr-2013-0208#.UtcEqnlIhg0 (15 April 2014, date last accessed).

Pérez-Harguindeguy N, Díaz S, Lavorel S, Poorter H, Jaureguiberry P, Bret-Harte MS, Cornwell WK, Craine JM, Gurvich DE, Urcelay C, Veneklaas EJ, Reich PB, Poorter L, Wright IJ, Ray P, Enrico L, Pausas JG, Vos AC de, Buchmann N, Funes G, Quétier F, Hodgson JG, Thompson K, Morgan HD, Steege H ter, Heijden MGA van der, Sack L, Blonder B, Poschlod P, Vaieretti M V., Conti G, Staver AC, Aquino S, Cornelissen JHC (2013) New Handbook for standardized measurment of plant functional traits worldwide. Aust J Bot 23:167–234. http://www.uv.es/jgpausas/papers/PerezHarguindeguy-2013-AJB_traits-handbook2.pdf

Peri PL, Gargaglione V, Martínez Pastur G, Lencinas MV (2010) Carbon accumulation along a stand development sequence of Nothofagus antarctica forests across a gradient in site quality in Southern Patagonia. For Ecol Manage 260:229–237.

Pinheiro JC, Bates DM (2000) Mixed-Effects Models in S and S-Plus Chambers J, Eddy W, Härdle W, Sheather S, Tierney L (eds). Springer-Verlag New York, Inc., New York. http://books.google.com/books?hl=en&lr=&id=RFDe_BKxvRIC&oi=fnd&pg=PR7&dq=Mixed-Effects+Models+in+S+and+S-Plus&ots=mOs4EAZUH0&sig=4wU0_ouUVCvyHSoUUla4zXs6vDs (19 August 2014, date last accessed).

Pinheiro J, Bates D, Saikat DebRoy, Sarkar D, Team RC (2015) nlme: Linear and Nonlinear Mixed Effects Models. http://cran.r-project.org/package=nlme

Ver Planck NR, MacFarlane DW (2014) A vertically integrated whole-tree biomass model. Trees 29:449–460. http://link.springer.com/10.1007/s00468-014-1123-x
Poorter L, Mcneil A, Hurtado VH, Prins HHT, Putz FE (2014) Bark traits and life-history strategies of tropical dry- and moist forest trees. Funct Ecol 28:232–242.
R Development Core Team (2015) R: A Language and Environment for Statistical Computing. http://www.r-project.org
Rueda R, Williamson GB (1992) Radial and vertical wod specific-gravity in Ochroma pyramidale (Cav ex Lam) Urb (Bombacaceae). Biotropica 24:512–518.
Savidge RA, Barnett JR, Napier R (2000) Biochemistry of seasonal cambial growth and wood formation-an overview of the challenges. In: Savidge RA, Barnett JR, Napier R (eds) Cell and Molecular Biology of Wood Formation. BIOS Scientific Publishers Limited, 2000
Schweingruber FH, Börner A, Schulze E-D (2008) Atlas of Woody Plant Stems Czeschlik D, Schlitzberger A (eds). Springer-Verlag, Heidelberg, Germany.
Skog KE (2008) Sequestration of carbon in harvested wood products for the United States. For Prod J 58:56–72.
Stamm AJ (1928) Density of wood substance, adsorption by wood, and permeability of wood. J Phys Chem 33:398–414. http://pubs.acs.org/doi/abs/10.1021/j150297a008 (1 April 2011, date last accessed).
Teskey RO, Saveyn A, Steppe K, McGuire MA (2008) Origin, fate and significance of CO2 in tree stems. New Phytol 177:17–32. http://www.ncbi.nlm.nih.gov/pubmed/18028298
Thomas SC, Malczewski G (2007) Wood carbon content of tree species in Eastern China: interspecific variability and the importance of the volatile fraction. J Environ Manage 85:659–62.
Thomas SC, Martin AR (2012a) Data from: Carbon content of tree tissues: a synthesis. Forests. http://dx.doi.org/10.5061/dryad.69sg2
Thomas SC, Martin AR (2012b) Carbon Content of Tree Tissues: A Synthesis. Forests 3:332–352.
Thuille A, Buchmann N, Schulze E-D (2000) Carbon stocks and soil respiration rates during deforestation, grassland use and subsequent Norway spruce afforestation in the Southern Alps, Italy. Tree Physiol 20:849–57. http://www.ncbi.nlm.nih.gov/pubmed/11303575
Tolunay D (2009) Carbon concentrations of tree components, forest floor and understorey in young Pinus sylvestris stands in north-western Turkey. Scand J For Res 24:394–402.
Wiemann MC, Williamson GB (1989) Radial Gradients in the Specific Gravity of Wood in Some Tropical and Temperate Trees. For Sci 35:197–210. http://www.ingentaconnect.com/content/saf/fs/1989/00000035/00000001/art00017 (1 May 2011, date last accessed).
Williamson GB, Wiemann MC (2010) Measuring wood specific gravity...correctly. Am J Bot 97:519–524.
Woodall CW, Heath LS, Domke GM, Nichols MC (2010) Methods and Equations for Estimating Aboveground Volume , Biomass , and Carbon for Trees in the U . S . Forest Inventory. Newtown Square, PA.
Woodbury PB, Smith JE, Heath LS (2007) Carbon sequestration in the U.S. forest sector from 1990 to 2010. For Ecol Manage 241:14–27.
Woodcock DW, Shier AD (2002) Wood specific gravity and its radial variations: the many ways to make a tree. Trees 16:437–443. http://link.springer.de/link/service/journals/00468/bibs/2016006/20160437.htm (12

September 2011, date last accessed).
Zakrzewski WT, Duchesne I (2012) Stem biomass model for jack pine (Pinus banksiana Lamb.) in Ontario. For Ecol Manage 279:112–120. http://dx.doi.org/10.1016/j.foreco.2012.05.012
Zhang Q, Wang C, Wang X, Quan X (2009) Carbon concentration variability of 10 Chinese temperate tree species. For Ecol Manage 258:722–727.